RENEWABLE ENERGY MANAGEMENT FOR NON-DEFERRABLE LOADS WITH DYNAMIC ELECTRICITY PRICING

JOHANN LEITHON-MELO
(B.Sc.) National University of Colombia, Bogotá, Colombia
(M.Eng.) Huazhong University of Science and Technology, Wuhan, China

A THESIS SUBMITTED FOR THE DEGREE OF DOCTOR OF PHILOSOPHY
DEPARTMENT OF ELECTRICAL AND COMPUTER ENGINEERING
NATIONAL UNIVERSITY OF SINGAPORE
2016

Supervisors:
Dr. Sumei Sun, Main Supervisor
Professor Teng Joon Lim, Co-Supervisor

Examiners:
Associate Professor Mehul Motani
Associate Professor Biplab Sikdar
Professor Vincent Wong, University of British Columbia

DECLARATION

I hereby declare that this thesis is my original work and it has been written by me in its entirety. I have duly acknowledged all the sources of information which have been used in the thesis.

This thesis has also not been submitted for any degree in any university previously.

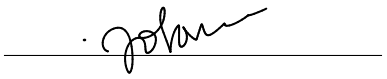

Johann Leithon-Melo

8th August 2016

ACKNOWLEDGEMENTS

I want to thank my supervisors Dr. Sumei Sun and Prof. Teng Joon Lim for their guidance, feedback, support, and encouragement. My sincere gratitude goes to Dr. Sun for welcoming me at the Institute for Infocomm Research (I^2R) in early 2011, and giving me the opportunity to start my research career in Singapore. My appreciation also goes to Prof. Lim for the fruitful discussions, the encouragement, and the valuable advice.

I want to thank my thesis advisers Dr. Liang Ying Chang and Prof. Mehul Motani for their feedback and recommendations during our various committee meetings. My appreciation also goes to the A*STAR Graduate Academy for sponsoring my research, and looking after my progress and well-being during these four years.

My earnest gratitude goes to all the inspiring professors at the National University of Singapore (NUS), especially Prof. Pooi-Yuen Kam, Prof. Zhang Rui, Prof. Vincent Tan, Prof. Bharadwaj Veeravalli, Prof. Kay Chen Tan, Prof. Dipti Srinivasan, Randall Y.C. Sie, and Luda Kopeikina, who exerted a direct influence in my formation through their teaching and sharing of experiences.

My appreciation goes to Mr. Masami Ueda, Mr. Akihiro Sakurai, Mr. Eiji Tomimura, Mr. Jun-Ichi Shirasu, and other engineers at Sumitomo Electric Industries who hosted me in Japan during the summer of 2014. In this internship I was able to understand the practical dimensions of my research problem.

I want to thank Prof. Yuen Chau for introducing me to I^2R in 2011, and hosting me at Singapore University of Technology and Design in 2012. My appreciation also goes to my friends in I^2R for their help and kindness, especially Chin Keong Ho, Peng Hui Tan, Xiaojuan Zhang, Jingon Joung, and Koichi Adachi. Many thanks also to my laboratory mates for the good conversations and their assistance: Zhang Peng, Mohammad Heggo, Linhao Dong, Shanlin, Yang Gang, Elnaz, Zhongxiang, David Martin, and the researchers who visited us since 2012.

My gratitude goes to all my friends in NUS with whom I shared enjoyable moments during these four years. Special thanks to Prasad, Anshoo, Amna, Utku, Chenlong, Wang Qian, and Ying Hao. My earnest appreciation also goes to Zeng You, Juliana Forero, Natalia López, Carlos Rivera, Naya Revelo, Luis Díaz, Luis Suárez, Diego Espitia, and Rachel Tang, for their unlimited friendship and support.

Last but not least, I want to thank my family for their unconditional loving support and confidence.

Contents

Summary

Assuming dynamic electricity prices, in this thesis we propose strategies to minimize the energy cost incurred by a non-deferrable load over a finite planning horizon. A non-deferrable load can be a valid model for facilities such as cellular base stations or office buildings, which have insufficient flexibility to schedule their power consumption. To propose our strategies we assume that the facility is equipped with a renewable energy harvester and a storage device. Moreover, we take into account the non-linear properties of the discharging operation, and the stochastic nature of the renewable energy arrivals.

We start by designing strategies that assume exact knowledge of future renewable energy arrivals, and which can be used to determine performance bounds. The proposed strategies are obtained by solving a constrained optimization problem through techniques such as linear programming, evolutionary algorithms, or calculus of variations. The strategies based on linear programming and evolutionary algorithms can be tuned to incur different computational costs, and thus provide precision-adjustable solutions. The strategy based on calculus of variations is shown to be simpler, more insightful, and leading to an acceptable performance.

We then propose an energy management algorithm, which does not require exact knowledge of future renewable energy arrivals, but relies on forecasting techniques such as a first-order linear predictor, or a time series model. We also introduce a forecasting technique based on time-inhomogeneous Markov chains, which has some advantages over existing techniques, e.g. it is simpler, uses bounded random variables, and can be continuously improved with new observations. In addition, we propose a strategy that does not require estimates of future renewable energy arrivals, and is simpler than existing proposals.

Thereafter, we investigate cooperative strategies, in which participants share renewable energy to minimize their collective expenditure. We consider both centralized and distributed renewable energy generation and storage. In the distributed arrangement, the facilities are equipped with their own generators, and are enabled to share renewable power through the smart grid at a transfer fee. In the centralized arrangement, all the facilities share access to a single energy farm, from which renewable power can be drawn at no cost. We investigate the conditions under which these two arrangements lead to a similar performance, and discuss their advantages and drawbacks.

Assuming non-linear electricity pricing, we finally propose storage management strategies to minimize the expenditure incurred by a non-deferrable load over a finite planning horizon. We specifically consider continuous-time block pricing, which imposes extra charges on users who breach pre-defined power consumption thresholds. We then derive optimization strategies through linearisation and calculus of variations. We also investigate the relationship between their achievable performance and the storage capacity.

For each of the proposed strategies we provide relevant numerical results, which allow us to verify our analysis and obtain further insights. We also provide formal proofs of the most important results across chapters.

List of Tables

List of Figures

List of Symbols

$\preceq$	element-wise $\leq$
$\approx$	approximately equal to
$\sim$	distributed as
$\mathscr{U}(a,b)$	uniformly distributed between a and b
$\mathscr{N}(\mu,\sigma^2)$	normally distributed with mean μ and variance σ^2
$\mathbf{a}^T$	the transpose of vector $\mathbf{a}$
$a(i)$	the ith element of vector $\mathbf{a}$
$\mathcal{I}_i$	indicator function for the ith item
$\mathbf{I}$	identity matrix
$\mathbf{1}$	column vector of ones
$\mathbf{0}$	matrix of zeroes
$\mathbf{A}$	lower triangular matrix of ones
$A(i,j)$	the element at the ith row and jth column of matrix $\mathbf{A}$
$\mathbb{E}[\cdot]$	the expectation operator
$\mathbb{E}_{t,J}[\cdot]$	expectation with knowledge of the process $J(t)$ up to time t
$\mathcal{S}$	a state space
Ω	a sample space
$\delta_{i,j}$	Kronecker delta, i.e. $\delta_{i,j}=1$ if $i=j$, and $\delta_{i,j}=0$ if $i\neq j$
$\{\ldots\}$	elements in a set
$\lvert\mathscr{A}\rvert$	cardinality of $\mathscr{A}$
A^C	the complement of set A
$\emptyset$	the empty set
$\mathbb{N}$	natural numbers
$\mathbb{R}$	real numbers
$\mathbb{R}^N$	vector of N real numbers
$\mathbb{R}^{M\times N}$	matrix of real numbers whose size is $M\times N$
$\mathbb{R}_+^N$	vector of N positive real numbers
s.t.	subject to
max.	maximize
min.	minimize
$f(x), \quad f[x]$	a function $f(\cdot)$ of variable x
$C^2([0,\infty)\times\mathbb{R})$	twice continuously differentiable on $([0,\infty)\times\mathbb{R})$
$f(t,x)\in C^{1,2}$	$f(t,x)$ is continuously differentiable on t and twice continuously differentiable on x
$\exp(x)$	e^x where e is Euler's number
$\log(x)$	natural logarithm of x
$f'(x)$	the first derivative of $f(x)$ with respect to x
$\frac{\partial}{\partial x}f$	the first-order partial derivative of $f(\cdot)$ with respect to x
$\frac{\partial^2}{\partial x^2}f$	the second-order partial derivative of $f(\cdot)$ with respect to x
$(x)^+ \quad [x]_+$	x if $x>0$, else 0

Chapter 1

Introduction

1.1 Motivation

The world's final consumption[1] of electricity has been steadily increasing in the past twenty years [1]. At the same time, renewable energy has become cheaper, especially the production of solar energy, which has seen considerable growth in many countries worldwide [2].

The penetration of renewable energy is expected to continue growing as global concerted strategies to reduce CO_2 emissions start to take effect [3]. It is well known, however, that the integration of renewable energy poses several challenges [4], e.g. how to deal with its variability, store it efficiently, etc.

Energy storage devices can be used to tackle renewable energy intermittency, and enhance its utility. Among the storage solutions available in the market, the ones based on lead-acid batteries are the cheapest alternative, and the most popular in the energy management industry [5]. They, however, exhibit non-linear characteristics such as the relationship between the discharging rate and the remaining charge [6]. As a result, the design of battery-aided strategies for renewable energy management is challenging, not only because of the random nature of the harvesting operation, but also because of the non-linear characteristics of the storage device.

In this thesis we propose cost-aware energy management strategies for facilities

[1] Final consumption refers to "goods or services used up by individual households or the community." Organisation for Economic Cooperation and Development (OECD), Glossary of Statistical Terms.

with non-deferrable loads, and renewable energy harvesting and storage capabilities. We also investigate cooperative strategies, in which a group of facilities share renewable energy to minimize their collective expenditure. Finally, we propose strategies that account for non-linear electricity pricing schemes such as consumption-based block pricing.

1.2 Background

In this section we provide a brief introduction to some optimization techniques and concepts that are used throughout this thesis.

1.2.1 Retail Electricity Pricing, Demand Response, and Net Metering

Retail Electricity Pricing

Retail electricity pricing refers to the energy tariffs that utilities design to maximize their profit, remain competitive, and influence the aggregate electricity demand [7]. The last objective can be achieved through pricing programs that are designed to influence the users' power consumption behaviour [8]. Some electricity pricing schemes are part of programs targeted at specific customers. For example, in Fig. 1.1 we have plotted the energy rates offered by Southern California Edison to its medium-size customers who also satisfy other eligibility criteria. As observed, rates vary throughout a 24-hour period, and are seasonally adjusted too. The data shown were taken from [9].

Electricity pricing schemes are linear when the cost of consuming a given amount of power is directly proportional to the quantity consumed. Consumption-based block pricing is a non-linear electricity pricing scheme which has been implemented in various jurisdictions worldwide [10], [11]. In most cases, the block tariffs are increasing, i.e. the higher the consumption, the more expensive the additional kilowatt hour, and this is meant to discourage excessive consumption. Fig. 1.2, taken from [12], illustrates the

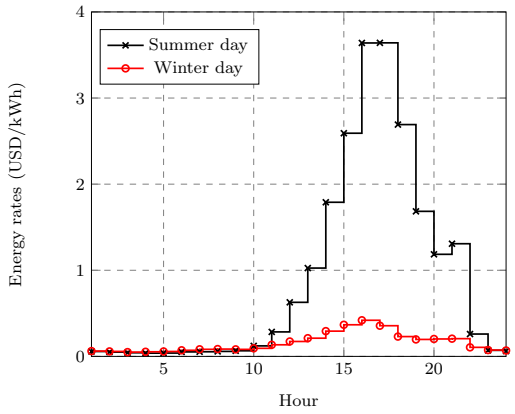

Figure 1.1: Energy rates offered by Southern California Edison to medium-size customers under its real-time pricing program.

concept of increasing block tariffs.

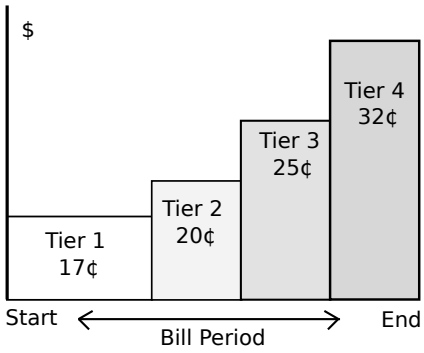

Figure 1.2: Increasing block rates from Pacific Gas and Electric Company, base tiered plan.

Demand Response

The United States Department of Energy and the Federal Energy Regulatory Commission define Demand Response as "[c]hanges in electric usage by end-use customers from their normal consumption patterns in response to changes in the price of electricity over time, or to incentive payments designed to induce lower electricity use at times of high wholesale market prices or when system reliability is jeopardized" [13], [14]. Demand response programs include time-varying energy rates which are designed to encourage users to shift their power consumption to non-peak hours and thus make the

distribution networks more efficient and the whole system more cost effective [15].

Net Metering Policy

In the Energy Policy Act of 2005, the government of the United States define net metering as a "service to an electric consumer under which electric energy generated by that electric consumer from an eligible on-site generating facility and delivered to the local distribution facilities may be used to offset electric energy provided by the electric utility to the electric consumer during the applicable billing period" [16].

According to the Solar Energy Industries Association [17], net metering allows the households to inject their excess renewable energy into the grid and obtain credits in return. In some jurisdictions, the credits obtained correspond to the retail value of the energy injected into the grid. In other jurisdictions, the compensation is lower, e.g. based on wholesale electricity prices [18].

As shown in Fig. 1.3, the number of residential net metering subscribers has been increasing in the past years at a very fast pace, the data are from [19]. A similar policy to stimulate the deployment of distributed renewable energy generators is the adoption of Feed-in Tariffs [20], [21], which are contracts that guarantee the purchase of the renewable energy harvested over long periods of time. The hardware arrangement required to implement feed-in policies is shown in Fig. 1.4, a schematic taken from [22].

1.2.2 Peukert's Law

In this thesis we propose strategies to minimize the energy bill incurred by non-deferrable loads over a finite planning horizon. The proposed strategies are targeted at facilities equipped with renewable energy harvesters and storage devices. Throughout the thesis we use a general model to describe the dynamics of the storage device. However, we also consider a simplified model based on Peukert's Law to obtain more

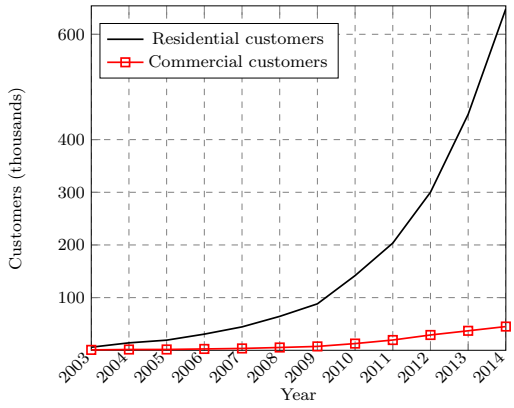

Figure 1.3: Net metering growth in the United States.

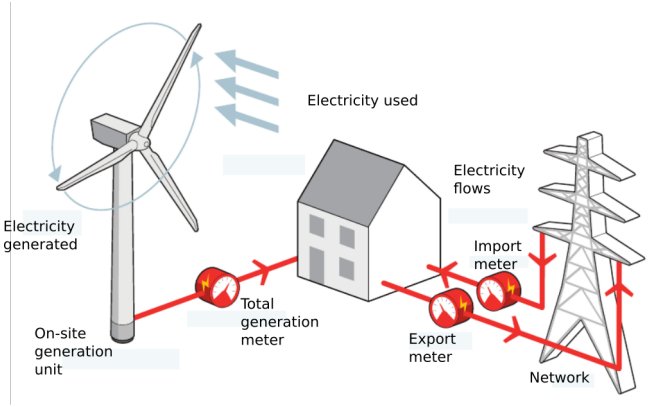

Figure 1.4: System arrangement for feed-in schemes.

insightful closed-form analytical results. Hence, in this section we describe Peukert's Law and its limitations.

Let $I_{\mathrm{No}} > 0$ be the nominal current for which the nominal storage capacity has been indicated by the battery manufacturers. If the battery is connected to a load $I_{\mathrm{D}}(t) > I_{\mathrm{No}}$, then Peukert's Law states that the current drained from the storage device to effectively deliver $I_{\mathrm{D}}(t)$ is:

$$\tilde{I}_{\mathrm{D}}(t) = I_{\mathrm{D}}(t) \left(\frac{I_{\mathrm{D}}(t)}{I_{\mathrm{No}}} \right)^{\kappa - 1}, \tag{1.1}$$

where $\kappa > 1$ is Peukert's exponent, which depends on the battery type. Assuming a

constant output voltage $V_{\mathrm{No}} > 0$, the power intentionally drained at time t is thus:

$$\tilde{D}(t) = I_{\mathrm{D}}(t) \left(\frac{I_{\mathrm{D}}(t)}{I_{\mathrm{No}}} \right)^{\kappa - 1} V_{\mathrm{No}}. \tag{1.2}$$

And the power effectively delivered to the load is:

$$D(t) = I_{\mathrm{D}}(t) V_{\mathrm{No}}. \tag{1.3}$$

As observed, there is a power loss incurred when $D(t) > V_{\mathrm{No}} I_{\mathrm{No}}$. This phenomenon is known as Peukert's effect [6], and affects lead-acid batteries in particular. Since Peukert's effect only occurs when $D(t) > V_{\mathrm{No}} I_{\mathrm{No}}$, the following relationship, obtained from (1.2) and (1.3), can be assumed between $D(t)$ and $\tilde{D}(t)$:

$$\tilde{D}(t) = \begin{cases} V_{\mathrm{No}} I_{\mathrm{No}} \left[\frac{D(t)}{V_{\mathrm{No}} I_{\mathrm{No}}} \right]^{\kappa}, & D(t) > V_{\mathrm{No}} I_{\mathrm{No}} \\ D(t), & D(t) \leq V_{\mathrm{No}} I_{\mathrm{No}} \end{cases}. \tag{1.4}$$

Eq. (1.4) can be alternatively written as follows:

$$\tilde{D}(t) = \max \left\{ Q_{\mathrm{No}} \left[\frac{D(t)}{Q_{\mathrm{No}}} \right]^{\kappa}, D(t) \right\}, \tag{1.5}$$

where $Q_{\mathrm{No}} \triangleq V_{\mathrm{No}} I_{\mathrm{No}}$. Similarly, $D(t)$ can be written in terms of $\tilde{D}(t)$ as follows:

$$D(t) = \min \left\{ Q_{\mathrm{No}} \left[\frac{\tilde{D}(t)}{Q_{\mathrm{No}}} \right]^{\frac{1}{\kappa}}, \tilde{D}(t) \right\}. \tag{1.6}$$

Peukert's Law can be used to estimate the remaining charge in lead-acid batteries, when the temperature and discharging rate do not change over time. When Peukert's Law is used to model batteries subject to time-varying discharging rates or temperatures, it underestimates the remaining charge [23].

The discharging model based on Peukert's Law is used in this thesis to illustrate the performance of the proposed strategies, and obtain concrete results at the last stage of the analysis. Although this model may lead to an underestimation of the energy remain-

ing in the storage device, it has some advantages over the linear models. Specifically, this model can be tuned to represent different storage devices because its parameters can be chosen to resemble empirical characteristics of any particular lead-acid battery. Moreover, given its simplicity, this model allows us to obtain analytic results in closed form, which are more insightful than algorithmic solutions.

1.2.3 Optimization Techniques

In this section we briefly describe the main aspects of the optimization techniques used in this thesis.

Continuous-Time Optimization

In a continuous-time unidimensional optimization problem the decision variable is a trajectory that maximizes or minimizes a functional, known as the objective. A functional is a mapping from the function space onto the real line, e.g. the mapping of a smooth trajectory $u(t)$ in a closed interval $[a,b]$ to its length can be written as:

$$\mathsf{length}(u) = \int_a^b \sqrt[2]{1+u'(t)}dt, \tag{1.7}$$

where $u'(t) = \frac{d}{dt}u(t)$.

- Calculus of variations: In this thesis we use the theory of calculus of variations to solve optimization problems of the following nature:

$$\text{P1.0:} \quad \min_{u(t)}./\max. \quad \int_a^b \mathscr{G}\left[t,u(t)\right]dt$$

s.t.

$$\int_a^b \mathcal{J}\left[u(t)\right]dt = K,$$

where $K \in \mathbb{R}$. P1.0 is a calculus of variations problem with a single equality constraint in integral form. To solve P1.0 we use the Lagrange multipliers rule for calculus of

variations [24]. We thus start by writing the following Lagrangian:

$$\mathscr{L}(u,\lambda) = \int_a^b \mathscr{G}\left[t,u(t)\right] dt + \lambda \left[\int_a^b \mathscr{J}\left[u(t)\right] dt - K\right].$$

The condition for optimality, also known as Euler-Lagrange equation, states $\frac{\partial}{\partial u}\mathscr{L}(u,\lambda) = 0$. Solving this equation leads to a candidate solution in terms of λ, a constant that can be then chosen to satisfy the integral constraint.

- Optimal control in continuous time: We describe the most important principles in the optimal control theory of continuous-time systems. We use these concepts in Chapter 3, where we propose an online optimization strategy based on optimal control. The following development and further details can be found in [25]. Let $x(t) \in \mathbb{R}$ represent the state of a dynamic system which evolves according to the following equation:

$$\frac{d}{dt}x(t) = f(x,u,t), \quad x(0) = x_0, \tag{1.8}$$

where $f : \mathbb{R}^3 \to \mathbb{R}$ is a function which models the evolution of the system in terms of its current state $x(t)$ and the control signal $u(t)$. The state variable $x(t)$ represents physical quantities such as population size in a bacterial colony, the concentration of a chemical in a solution, or the amount of radioactive material in a sample. The control signal $u(t)$ represents variables such as the amount of food present in the bacterial colony, or the rate at which a chemical is added to a solution. In our optimization problem, the state variable represents the amount of renewable energy stored at any point in time, and the control signal is the amount of power that we draw from the storage device over time.

  We are interested in designing the control signal $u(t)$ so that the performance of the system is optimized. The performance metric is a functional which depends on the trajectory taken by the state $x(t)$ and the control signal $u(t)$ over the planning horizon

$[0,H]$. In general, we can assume that the performance metric is

$$\chi = \int_0^H \mathscr{G}(x,u,t)dt + \mathsf{B}(x(H),H), \tag{1.9}$$

where $\mathscr{G} : \mathbb{R}^3 \to \mathbb{R}$ is a well-defined function in $[0,H]$, and $\mathsf{B} : \mathbb{R}^2 \to \mathbb{R}$ is a bequest function, which expresses a given intention for the system state $x(t)$ at the end of the planning horizon, i.e. when $t = H$. Examples of bequest functions are:

$$\mathsf{B}(x(H),H) = -\left(x(H) - x_D\right)^2,$$

or

$$\mathsf{B}(x(H),H) = \mathsf{w} \cdot x(H).$$

In the first case, the bequest function *penalizes* deviations from a desired end state x_D. In the second case, the bequest function assigns a weight w to the state at $t = H$. The quantity $\mathsf{w} \cdot x(H)$ can be thought of as a cost or an asset, depending on whether the objective is to maximize or minimize (1.9).

The optimal control problem is to find the $u(t)$, which will optimize the performance metric by driving the system state along the optimal trajectory [26].

In the following we enunciate Pontryagin's Maximum Principle, which is a set of necessary conditions for $u(t)$ to maximize the performance metric. First, we define the following function, known as the Hamiltonian of the system:

$$\mathscr{H}(x,u,\lambda,t) = \mathscr{G}(x,u,t) + \lambda(t) f(x,u,t). \tag{1.10}$$

From its definition, we see that:

$$\frac{\partial}{\partial \lambda}\mathscr{H}(x,u,\lambda,t) = f(x,u,t) = \frac{d}{dt}x(t).$$

Let $u^*(t)$ and $x^*(t)$ denote respectively the optimal control signal and optimal system

state trajectory with boundary condition $x(0) = x_0$, then $u^*(t)$ and $x^*(t)$ satisfy [25]:

$$\mathscr{H}(x^*, u^*, \lambda, t) \geq \mathscr{H}(x, u, \lambda, t), \ \forall\, x,\ u. \tag{1.11}$$

$$\frac{d}{dt}x^*(t) = f(x^*, u^*, t), \ \ x^*(0) = x_0. \tag{1.12}$$

$$\frac{d}{dt}\lambda = -\frac{\partial}{\partial x}\mathscr{H}(x, u, \lambda, t), \quad \lambda(H) = \frac{\partial}{\partial x}\mathsf{B}(x(t), t)\bigg|_{t=H} \tag{1.13}$$

The condition (1.11) ensures that $u^*(t)$ maximizes the Hamiltonian $\mathscr{H}(x, u, \lambda, t)$. If $\mathscr{H}(x, u, \lambda, t)$ is concave in u, this condition reduces to:

$$\frac{\partial}{\partial u}\mathscr{H}(x, u, \lambda, t)\bigg|_{u(t)=u^*(t)\ \forall\ t} = 0. \tag{1.14}$$

The condition (1.12) ensures that the optimal trajectory satisfies the model stated in the differential equation (1.8). The condition (1.13) is known as the costate equation, and establishes the optimality conditions for the Lagrange multipliers $\lambda(t)$.

- Continuous-time stochastic dynamic programming: We use this technique to solve a stochastic control problem. In a continuous-time stochastic control problem, the state variable is subject to uncertainty, and the objective is to optimize the expected value of a functional which depends on both the state variable and the control signal. We consider the following stochastic control problem:

$$\text{P1.1:} \quad \max_{u(t)} \quad \mathbb{E}\left[\int_0^H \mathscr{G}(\tau, x, u)d\tau + \mathsf{B}(x(H), H)\right]$$

where the decision variable is $u(t)$, and the expected value is taken over realisations of the stochastic process $x(t)$, which evolves according to the following equation:

$$dx = f(x, u, t)dt + \mathsf{noise}, \tag{1.15}$$

where noise is a random variable whose distribution can be chosen to satisfy statistical properties of the system.

The value[2] function associated to P1.1 is

$$V(t,x) = \max_{u} \quad \mathbb{E}_{t,x}\left[\int_t^H \mathscr{G}(\tau,x,u)d\tau + \mathsf{B}(x(H),H)\right], \tag{1.16}$$

where $\mathbb{E}_{t,x}[\cdot]$ denotes expectation with perfect knowledge of the stochastic process $x(t)$ up to time t. From its definition, the value function satisfies this boundary condition:

$$V(H,x) = \mathsf{B}(x(H),H). \tag{1.17}$$

Next, we apply Bellman's principle to the value function $V(t,x)$. Bellman's principle establishes that [25]: "An optimal policy has the property that, whatever the initial state and initial decision are, the remaining decision must constitute an optimal policy with regard to the outcome resulting from the first decision." Let $u^*(t)$ and $x^*(t)$ denote respectively the optimal control and state trajectory. Then, by Bellman's principle, $u^*(t)$ and $x^*(t)$ must be such that the value function (1.16) satisfies:

$$V(t,x^*) = \mathbb{E}_{t,x}\left[\int_t^{t+\Delta t} \mathscr{G}(\tau,x^*,u^*)d\tau\right] + V(t+\Delta t, x^*+\Delta x^*), \tag{1.18}$$

where

$$\begin{aligned}&\mathbb{E}_{t,x}\left[\int_t^{t+\Delta t} \mathscr{G}(\tau,x^*,u^*)d\tau\right] + V(t+\Delta t,x^*+\Delta x^*)\\ &= \max_{u} \quad \mathbb{E}_{t,x}\left[\int_t^{t+\Delta t} \mathscr{G}(\tau,x,u)d\tau + V(t+\Delta t,x+\Delta x)\right].\end{aligned}$$

For small Δt, we can approximate $V(t+\Delta t,x^*+\Delta x^*)$ using Taylor's series:

$$V(t+\Delta t,x^*+\Delta x^*) \approx V(t,x^*) + \Delta t\frac{\partial}{\partial t}V(t,x^*) + \Delta x^*\frac{\partial}{\partial x^*}V(t,x^*) + (\Delta x^*)^2\frac{1}{2}\frac{\partial^2}{\partial (x^*)^2}V(t,x^*),$$

where we have only included three terms because the rest of the terms scale up with $(\Delta t)^2$, which is significantly[3] smaller. After replacing Taylor's approximation into

[2] Also known as the cost-to-go function in the dynamic programming literature.

[3] For stochastic $x(t)$, the quantity $(\Delta x)^2$ cannot be disregarded. For example, if $x(t)$ is the Wiener process, see definition in Sec. 1.2.4, then $\mathbb{E}[(\Delta x)^2] = \Delta t$.

(1.18) we obtain the following partial differential equation, known as the Hamilton-Jacobi-Bellman equation [25]:

$$\Delta t \frac{\partial}{\partial t} V(t,x^*) + \Delta x^* \frac{\partial}{\partial x^*} V(t,x^*) + (\Delta x^*)^2 \frac{1}{2} \frac{\partial^2}{\partial (x^*)^2} V(t,x^*) = -\mathbb{E}_{t,x} \left[\int_t^{t+\Delta t} \mathscr{G}(\tau, x^*, u^*) d\tau \right],$$

which can be used to determine candidate solutions to P1.1.

Discrete-Time Optimization

- Linear programming: A linear programming problem is a convex optimization problem in which the objective and the constraints are all linear. A general linear program can be expressed as [27]:

$$\text{LP1: } \min. \ \mathbf{c}^T \mathbf{x}$$

subject to:

$$\mathbf{G}\mathbf{x} \preceq \mathbf{h} \tag{1.19a}$$

$$\mathbf{M}\mathbf{x} = \mathbf{b}. \tag{1.19b}$$

In LP1, $\mathbf{G} \in \mathbb{R}^{M \times N}$, $\mathbf{h} \in \mathbb{R}^M$, $\mathbf{M} \in \mathbb{R}^{P \times N}$, $\mathbf{b} \in \mathbb{R}^P$, and the design variable is $\mathbf{x} \in \mathbb{R}^N$. There are several methods to solve linear programming problems, e.g. the simplex method, or interior point methods such as the Karmarkar algorithm [28]. These algorithms are implemented in most numerical software platforms.

- Evolutionary algorithms: They are strategies inspired by natural selection, which are used to search for optimal solutions in a given feasible space by using evolutionary operators such as crossover and mutation. Candidate solutions undergo random mutations and recombine to generate new candidates. Selection criteria are implemented to keep the best individuals across the different iterations. The algorithm stops when a condition is met, e.g. a threshold is passed, an acceptable solution is found, or a

limited number of iterations is reached. The evolutionary algorithms are useful to attack complex problems that may be intractable analytically. Their main disadvantage is that the obtained solution is not necessarily optimal, and since the search is randomized, different results are possibly obtained in each run. For a more detailed discussion on the topic, readers are referred to [29]. In this thesis, we use a specific type of evolutionary algorithm known as *evolutionary strategy*. Unlike genetic algorithms, evolutionary strategies do not require binary coding, and hence the decision variables can be optimized directly through mutation and recombination.

1.2.4 Continuous-Time Stochastic Modelling

In Chapter 4 we use the concept of stochastic differential equation to model the evolution of renewable energy reserves over time. In the following we describe some useful concepts to understand such models:

- Wiener process: The Wiener process $\mathscr{W}(t)$ is the standard Brownian motion and has the following properties [30]:
  - $\mathscr{W}(t_1) - \mathscr{W}(t_0) \sim \mathscr{N}(0, t_1 - t_0)$ for $t_1 > t_0$.
  - $\mathscr{W}(t)$ has continuous sample paths.
  - $\mathscr{W}(t)$ has independent increments, i.e. if $t_0 < t_1 < \ldots < t_n$, then $\mathscr{W}(t_0)$, $\mathscr{W}(t_1) - \mathscr{W}(t_0), \ldots, \mathscr{W}(t_n) - \mathscr{W}(t_{n-1})$ are statistically independent.
- Sample space: The set containing all the possible outcomes of a random experiment.
- Sigma-algebra: Consider a random experiment whose sample space is denoted by Ω. Then, a collection of subsets of Ω is a σ-algebra $\mathscr{D}$ if it has the following properties [31]:
  - $\Omega \in \mathscr{D}$, and $\emptyset \in \mathscr{D}$

  - If $A \in \mathscr{D}$, then $A^C \in \mathscr{D}$
  - If $A_1, A_2, \ldots \in \mathscr{D}$, then $\bigcup_{i=1}^{\infty} A_i \in \mathscr{D}$.

- Filtration: Consider the time interval $[0,H]$, and assume that for all $t \in [0,H]$ there is a σ-algebra denoted by $\mathscr{D}(t)$. If for all $s,\ t \in [0,H]$ such that $s \leq t$, we have $\mathscr{D}(s) \subseteq \mathscr{D}(t)$, then the collection of σ-algebras $\mathscr{D}(t),\ t \in [0,H]$ is called a filtration.

- Borel σ algebra in $[a,b]$: Assume that the sample space of a random experiment is the closed interval $[a,b]$, then to construct a Borel σ-algebra we start with a closed interval in $[a,b]$ and add *everything necessary* to form a σ-algebra [32]. The sets that are part of a Borel σ-algebra are called Borel sets.

- Measurable random variable: Let $\mathcal{B}$ denote a Borel subset of $\mathbb{R}$, and X be a random variable in a sample space Ω. We say that X is $\mathscr{D}(t)$-measurable if every collection of subsets of the form $X \in \mathcal{B}$ is also in $\mathscr{D}(t)$.

- Adapted stochastic process: Consider a sample space Ω and a filtration $\mathscr{D}(t)$, then we say that the stochastic process $X(t)$ is adapted to the filtration $\mathscr{D}(t)$, if for any t, the random variable $X(t)$ is $\mathscr{D}(t)$-measurable.

- Continuous-time Markov process: A continuous-time Markov process $X(t)$ is a stochastic process which has the Markov property, i.e. "the future behaviour of the process $X(t),\ t > t_n$ depends on its past $X(s),\ -\infty < s < t_n$, only through its current state $X(t_n)$" [31].

- Diffusion process: A diffusion process is a continuous-time Markov process with continuous sample paths. Diffusion processes are the solutions to stochastic differential equations, also called diffusion equations [31]. An example of such a process is the Brownian motion.

- Stochastic differential equation: Let $d\mathscr{W} = \mathscr{W}(t+dt) - \mathscr{W}(t)$ for small dt, then the following equation describes a diffusion process $X(t)$:

$$dX(t) = f(X,U,t)dt + g(X,U,t)d\mathscr{W}. \tag{1.20}$$

The functions $f(X,U,t)$ and $g(X,U,t)$ in (1.20) are adapted processes to the filtration generated by X. Moreover, the Ito interpretation of this stochastic differential equation is that $X(t)$ satisfies:

$$X(t) = X(0) + \int_0^t f(X(s),U(s),s)ds + \int_0^t g(X(s),U(s),s)d\mathscr{W}, \tag{1.21}$$

where the second integral is a stochastic integral [33].

- Stochastic integral: In this thesis, we use Ito's integral definition for real-valued deterministic integrands. Let $\mathscr{W}(t)$ denote the standard Wiener process, then under Ito's integral definition, the term

$$\int_0^H g(t)d\mathscr{W},$$

represents a zero-mean normally distributed random variable, whose variance σ^2 is

$$\sigma^2 = \int_0^H g^2(t)dt.$$

As seen, for this stochastic integral to exist, $g(t)$ must be square-integrable in the interval $[0,H]$ [32].

- Ito's lemma: Let X be a diffusion process, i.e.

$$dX(t) = f(X,U,t)dt + g(X,U,t)d\mathscr{W}, \tag{1.22}$$

and let $h(X,t)$ be a twice continuously differentiable function on $([0,\infty)\times\mathbb{R})$ i.e., $h(X,t) \in C^2([0,\infty)\times\mathbb{R})$. Then Ito's lemma says that $Y(t) = h(X,t)$ is also an Ito

process [33], whose diffusion equation is:

$$dY = \frac{\partial}{\partial t}h(X,t)dt + \frac{\partial}{\partial X}h(X,t)dX + \frac{1}{2}\frac{\partial^2}{\partial X^2}h(X,t)\,(dX)^2\,, \tag{1.23}$$

The quantity $(dX)^2 = dXdX$ can be computed from (1.22) as follows:

$$\begin{aligned}(dX)^2 &= [f(X,U,t)dt + g(X,U,t)d\mathscr{W}]^2 \\ &= [f(X,U,t)]^2\,dtdt + 2f(X,U,t)g(X,U,t)dtd\mathscr{W} + [g(X,U,t)]^2\,d\mathscr{W}\,d\mathscr{W}\,.\end{aligned}$$

Moreover, by using the following stochastic calculus rules [33]:

$$(d\mathscr{W})^2 = d\mathscr{W}\,d\mathscr{W} = dt, \quad dtd\mathscr{W} = 0, \quad d\mathscr{W}\,dt = 0, \quad dtdt = 0 \tag{1.24}$$

we obtain:

$$(dX)^2 = [g(X,U,t)]^2\,dt. \tag{1.25}$$

And replacing (1.22) and (1.25) in (1.23) yields:

$$\begin{aligned}dY = &\left[\frac{\partial}{\partial t}h(X,t) + f(X,U,t)\frac{\partial}{\partial X}h(X,t) + \frac{1}{2}\,[g(X,U,t)]^2\,\frac{\partial^2}{\partial X^2}h(X,t)\right]dt \\ &+ g(X,U,t)\frac{\partial}{\partial X}h(X,t)d\mathscr{W},\end{aligned}$$

which is a diffusion process written in differential form.

1.2.5 Statistical Models

We use statistical models to generate random arrivals of renewable energy, and estimate signal values in the future. This helps us to evaluate the performance of the proposed online strategies in Chapter 3, where, among others, we consider the following models:

- Auto-Regressive Integrated Moving Average (ARIMA) Time Series Model: Let $\mathbf{r} \in \mathbb{R}_+^N$ denote a vector of renewable energy arrivals over an N-slot time period, then define the first-order difference process $\mathbf{r}_{[1]}$ as $r_{[1]}(i) := r_{[0]}(i) - r_{[0]}(i-1),\ i \in \{2,\ldots,N\}$, where $r_{[0]}(i) = r(i)\ \forall\ i$. In general, let the nth order difference process be

defined as

$$r_{[n]}(i) := r_{[n-1]}(i) - r_{[n-1]}(i-1),$$

with $n \geq 1$. Then, $\mathbf{r}$ is an ARIMA(m,n,q) process, with $m,\ n,\ q\ \in \mathbb{N}$, if $\mathbf{r}_{[n]}$ is an Auto Regressive Moving Average ARMA(m,q) process, i.e.,

$$r_{[n]}(i) = \eta_0 + \sum_{j=1}^{m} \eta_j r_{[n]}(i-j) + \sum_{j=1}^{q} \theta_j \omega(i-j) + \omega(i), \tag{1.26}$$

where $\eta_j\ \in\ \mathbb{R},\ \theta_j\ \in\ \mathbb{R},\ j \in\ \{0,1,\ldots,q\},\ \omega(i) \sim \mathcal{N}(0,\sigma^2)$, and $\mathbb{E}[\omega(i)\omega(j)] = \delta_{i,j}\sigma^2$. Moreover, the following polynomials do not have common factors:

$$\phi_1(z) = 1 - \eta_1 z - \eta_2 z^2 - \ldots - \eta_m z^m, \tag{1.27}$$

$$\phi_2(z) = 1 + \theta_1 z + \theta_2 z^2 + \ldots + \theta_q z^q. \tag{1.28}$$

By definition, the lower order difference processes also follow ARIMA time series models. Specifically, the jth order difference process, with $1 \leq j \leq n$ follows an ARIMA(m,j,q) time series model.

In an ARMA(m,q) time series, the mean of the current output is obtained as a linear combination of the previous m output samples. Similarly, the stochastic component of the series is correlated up to the qth previous white noise sample. In an ARIMA(m,n,q), the parameter n represents the number of times the process needs to be "differentiated" in order to obtain a stationary ARMA(m,q) time series. ARIMA generalizes autoregressive (AR), moving-average (MA) and ARMA time series, and can be used to model processes that are not[4] stationary [34].

- Time-Inhomogeneous Markov Chain Model: In a time-inhomogeneous Markov chain, the transition probabilities change over time. We use such a model to make intra-day forecasts of renewable energy arrivals. We assume that the probability of

[4] ARMA process are by definition stationary.

transitioning from state A to state B depends on the time of the day. For example, transitioning from a cloudy state to a sunny state is more likely to happen at noon than in the late afternoon, when a transition to a *darker* state is more likely.

1.3 Literature Review and Challenges

1.3.1 Related Works

The concept of energy management encompasses various actors, technologies and purposes. We can therefore classify the works currently available in the literature using different criteria. For the sake of exposition, we will discuss the existing strategies in terms of their beneficiaries (utilities, end consumers, or both), and their assumptions regarding availability of information (genie-aided vs. real-time strategies).

In terms of their beneficiaries, the proposals in the literature can be classified into three categories:

1. Energy management solutions from the perspectives of the consumers: These proposals are targeted at the end users, who may be households, companies or government entities. There is currently a vast literature on home/building energy management. The proposed solutions involve optimizing the operation of household appliances, and the use of locally harvested renewable energy. There are home energy management proposals that aim at reducing on-grid energy consumption such as [35]–[37], other works aim at minimizing operational costs, and hence take into account specific pricing schemes [38]–[68]. Strategies to optimize the integration of renewable energy as a complementary or alternative power source, are described in [69]–[76].

Some works propose strategies to minimize the energy bill through storage management such as [59]–[64]. Other proposals intend to minimize energy costs by schedul-

ing residential appliances over a finite planning horizon [47]–[54]. The appliances considered can be deferrable or non-deferrable. The operation of the former can be shifted to low-price periods, whereas non-deferrable appliances can be controlled by relaxing comfort requirements [45]–[47]. Non-deferrable appliances include air conditioning units, heaters and lighting devices.

Energy management solutions targeted at enterprises depend on the nature of their activities and hence the industries they belong to. In the context of telecommunication companies, energy management is a concept that encompasses solutions with different scopes, among which, the strategies aimed at reducing the power consumption in base stations, have attracted most of the attention.

Traditionally, wireless communication schemes have been designed to provide high performance by considering both bandwidth and energy constraints. In that sense, wireless communication solutions have been energy-aware from the beginning. Modulation schemes, for example, have been chosen to provide the lowest probability of error per available transmission power (signal-to-noise ratio) [77]. Similarly, detection and coding strategies have been designed to enhance reliance at any given signal-to-noise ratio [78].

In recent years, the concept of energy sustainability emerged, and the research focus shifted towards studying the potential of renewable energy in making communication networks more sustainable [79]–[84]. Powering communication networks with renewable energy is thus part of the efforts to reduce their carbon footprint, and operational costs [85], [86]. Substantial research work has been focused on optimizing the operation of wireless communications under energy harvesting constraints. In particular [87]–[106] investigate strategies to optimize the use of renewable energy under

different performance metrics, e.g. quality-of-service, network coverage, throughput, etc. On the other hand, works such as [107]–[110] investigate renewable energy sharing strategies that minimize the on-grid electricity usage, while maintaining a specified energy demand, or a level of quality-of-service.

With the envisioning of an efficient and smart power grid, the research attention began to focus on how these improvements could benefit the operation of communication networks [111], [112]. Then, energy management in communication networks became aware of pricing schemes and billing programs such as demand response and net metering. In works such as [113]–[124] the authors develop strategies to integrate renewable energy in communication networks and minimize their energy bill, or on-grid energy consumption, while maintaining quality-of-service, or a specified power demand.

2. Energy management from the perspectives of the electric company and the grid operator: These proposals intend to optimize the operation of energy retailing companies and grid operators. The utilities aim at maximizing their profit while ensuring the reliability of their systems, and reducing their carbon footprint by leveraging alternative sources of energy.

The grid operators intend to maximize the efficiency of their transportation/distribution networks while maintaining the stability of the system. Common challenges for grid operators include: the stabilization of the grid in the event of load imbalance or power outage, the proper integration of distributed energy generators, the reduction of dissipation losses in their transmission lines, the reduction of the peak-to-average power ratio in their distribution lines, etc.

With the modernization of the power grid, the concept of *microgrid* emerged as an

alternative to cope with the challenges listed above. Microgrids are geographically-defined energy ecosystems with distributed power generation capacity, often from renewable sources, local users, and distribution lines [125]. Microgrids can operate in grid-connected mode or stand-alone mode. In grid-connected mode, the energy management strategies focus on minimizing operational costs, whereas in stand-alone mode, the focus is on meeting the load demand and preventing power outage [126].

Proposals to minimize the operational cost of microgrids, or smart grids, are described in [126]–[146]. The proposed solutions involve storage management strategies [127]–[132], load or generation forecasting [130]–[133], capacity planning (unit commitment and economic dispatch[5]) [129], [137], [143], [144], etc. The existing cost-minimization strategies use optimization techniques such as genetic algorithms [130], the Karush–Kuhn–Tucker conditions [128], [139], Lyapunov optimization [127],[143],[146], mixed-integer linear programming [126],[131],[132],[137],[140], dual decomposition [134], alternating direction method of multipliers [129], linear programming [142], direct search methods [141], etc.

Strategies to facilitate the integration of renewable energy into the power grid are presented in [139],[140],[142],[143],[145]–[149]. The strategies proposed are based on storage management [145]–[147], load management [142], [143], capacity planning [148], [149], or cooperation among distributed generators [139], [140], [146]. Cooperative strategies exploit geographic variations in the load and energy generation in order to minimize operational costs. The energy exchange helps to reduce load curtailment due to unexpected peaks in the energy demand.

[5]The unit commitment problem is formulated to determine the optimal operation times of various energy generators. The economic dispatch problem consist of designing the optimal energy procurement from different generation units. The two optimization problems are solved to minimize operational costs while satisfying the energy demand.

The economic impact of using energy storage devices in power grids is discussed in [150], while profit maximization approaches for utilities and microgrids are studied in [147], [151]–[153]. These works propose strategies to assess the financial benefits of investing in energy storage devices, and provide guidance on how to determine their optimal size and arrangement. Works such as [147] take into consideration the battery cost and its lifetime as well.

3. Energy management for social welfare maximization: These strategies take into account actors involved at all stages including the energy generation, transportation, retailing and consumption. The purpose of these strategies is to maximize the efficiency of the transportation/distribution systems, increase the consumers' satisfaction, and reduce the use of polluting energy sources. Some of these strategies involve designing the pricing schemes in order to achieve a desirable demand response, and some proposals use game-theoretic arguments because consumers and utilities may have different priorities. Social-welfare optimization schemes have been proposed in [154]–[166]. These proposals seek to benefit both the electric utility and the consumers, or establish the trade-off between the interests of the two. Some of these strategies are based on demand response [155]–[162]. In general, existing strategies are designed using a centralized [161]–[163], or a distributed approach [157], [159], [160], [164], [166].

In the following, we categorize prior work into genie-aided solutions and real-time strategies:

- **Genie-aided strategies:** These strategies assume exact knowledge of the variables involved in the problem, including information across the entire optimization horizon. The resulting solutions cannot be implemented in practice, but are used as a

benchmark for strategies that only use causally-available information. Genie-aided strategies are proposed in [90], [100], [103], [119], [129], [137].

- **Online or real-time strategies:** These strategies only use causally-available information. The information unavailable through measurements is estimated by using different forecasting techniques [45], [46], [131], [132], [139], [144], [167]. Often times, prediction errors are taken into account in the optimization, as in [46], [139], in order to design robust strategies. The forecasting methods can be based on auto-regressive models [63], [133], [140], prediction filters [44], neural networks and other machine learning techniques [63], [75], [133], [135], or results obtained from physical models for weather prediction [74], [75], [79]. Approximate solutions available in the literature have been obtained using heuristics [94], [100], [108], [136], or Lyapunov optimization [40], [41], [60], [64], [95], [127], [143], [146]. In most of these strategies, the estimation methods are used to predict renewable energy arrivals and power consumption profiles. In some works, the energy prices are assumed uncertain as well [44], [46], [63]. The existing real-time energy management strategies are based on successive estimations, rolling window optimization, and repeated computations [45], [46], [65], [67], [132], [133], [144], [156]. As a result, current solutions incur a considerable computational cost. To reduce their computational complexity, it has been proposed to decrease the sampling frequency, and augment the time between consecutive decisions, which inevitably results in performance loss.

1.3.2 Challenges

As described in Sec. 1.3.1, there is currently a vast literature on cost-aware energy management. However, as of mid-2012, which marks the beginning of this investigation, there were some challenges that we decided to address in this thesis. In particular, the

following:

- Back in 2012, there was the need for an analytical framework[6] and a system model that could lay the foundation for devising energy management strategies, and facilitate their practical implementation. The required system model needed to characterize the renewable energy harvesting operation, account for relevant pricing and incentives programs, and describe the energy storage dynamics, including the non-linear relationship between the discharging rate and the remaining charge. The challenge was thus to establish the framework to devise energy management strategies, determine performance benchmarks, and draw insights from genie-aided solutions.

- Existing strategies, especially the ones intended for practical[7] implementation, have high computational complexity because they rely on successive calculations and statistical forecasting. The challenge is therefore to reduce the computational complexity by resorting to alternative analytical tools or approaches.

- Existing online strategies rely on forecasting techniques which are mostly based on statistical estimation. These techniques require continuous model revision as observations are recorded on a rolling basis. This revision incurs further computational burden because estimating the model alone requires solving additional optimization problems. Hence, the challenge is to reduce the dependency of current solutions on forecasting techniques.

- As of 2012, there were no energy management strategies for non-deferrable load facilities, which could handle time-varying consumption-based block pricing. Hence, the challenge was to incorporate non-linear pricing models in the optimization, and

[6] Analytical framework refers to the set of assumptions, mathematical relationships, system topology, and mathematical formulation that are introduced to study the energy management problem.

[7] Genie-aided strategies cannot be implemented in practice, but they provide performance upper bounds.

study their implications by drawing insights from analytical results. A related challenge was to minimize the cost of deploying the energy management system by properly assessing the required energy storage capacity. Thus, storage sizing methods needed to be devised.

1.4 Organization, Contributions, and Bibliographical Notes

1.4.1 Organization

Aside from this introductory chapter, this thesis is composed of five chapters. In Chapter 2, we formulate the main optimization problem and devise genie-aided solutions which provide insights and a performance benchmark for the online algorithms that we propose in Chapter 3. In Chapter 4 we propose strategies to minimize the energy cost incurred by a group of facilities over a finite planning horizon. The facilities are equipped with renewable energy harvesters and storage devices, and are enabled to share renewable energy among each other. Assuming a dynamic block pricing scheme, in Chapter 5 we propose strategies to minimize the expenditure incurred by a non-deferrable load over a finite planning horizon. Finally, in Chapter 6 we present conclusions and describe future research directions.

1.4.2 Contributions

The main contributions of this thesis are the following:

- We establish the mathematical framework to design strategies that minimize the energy bill incurred by a non-deferrable load facility over a finite planning horizon. The facility is assumed equipped with a renewable energy harvester and a storage device. Hence, the proposed framework incorporates models for the energy storage device, the renewable energy arrivals, and the pricing and incentives schemes. Earlier works did not take into account all these elements in their modelling, e.g. our works were

among the first to incorporate considerations such as a limited discharging rate, or physical phenomena such as Peukert's effect.

- We propose strategies to overcome the challenges that arise in the formulation and analysis of the mathematical problems formulated to determine optimal energy management policies in different scenarios. These strategies include the use of substitutions and simplifications, decomposition methods, and combination of techniques.

- The proposed energy management strategies can be used to reduce the complexity of existing proposals, as well as their reliance on forecasts. In current solutions, decision variables are updated by solving the same optimization problem multiple times. This approach incurs a number of mathematical operations, which can be reduced by updating the decision variables directly through analytic expressions. Hence, this thesis shows how alternative techniques can be used to solve the relevant optimization problems and obtain analytic results, which can be simpler and more insightful than the algorithmic solutions available in the literature. The thesis also proposes an optimization framework to study the problem of cooperative energy management, which can be used to determine the achievable cost savings in two different scenarios, namely, cooperation with distributed generation and storage, and cooperation with centralized generation and storage.

The following are specific contributions of this thesis:

- We propose three genie-aided strategies which have several advantages over the existing renewable energy management solutions in the literature. The proposed strategies use a general discharging model which can be tuned to depict practical storage systems. The proposed strategies are devised by solving a constrained optimization problem through linear programming, evolutionary algorithms, or calculus of vari-

ations. The strategies based on linear programming or evolutionary algorithms can be fine tuned to deliver results at different levels of accuracy, and incur different computational costs. The strategy obtained through calculus of variations is based on analytical expressions, and hence provides valuable insights, which can be used to reduce the computational complexity of existing online strategies.

- We propose two online renewable energy management strategies. The first strategy is based on forecasting techniques such as a linear predictor, a time series model, or a time-inhomogeneous Markov chain. The second proposed strategy does not require statistical forecasting and is model-independent. Moreover, this strategy is based on analytical results, and has lower computational complexity than existing proposals.[8] To design this strategy we solve a constrained optimization problem by introducing some ingenious substitutions and relaxations.

- We propose two offline strategies to minimize the energy bill incurred by a set of facilities equipped with renewable energy harvesters and storage devices. The facilities are enabled to share renewable energy, either through the smart grid or dedicated power lines, and their loads are assumed to be non-deferrable. To devise the first strategy we assume that each facility is equipped with its own renewable energy harvester and storage device. The second strategy is designed assuming that all the facilities have shared access to a farm where renewable energy is harvested and stored. We then compare the two strategies and draw the relevant conclusions.

  Assuming a set of facilities with shared access to an energy farm, where renewable energy is harvested and stored, we propose an online strategy to minimize their col-

[8] In existing online strategies, an optimization problem is solved every time the decision variables need to be updated. In some cases, the optimization problem is a linear programming problem, which can be solved in polynomial time. In contrast, the proposed strategy uses analytic results, which are able to update the decision variables in linear time.

lective expenditure over a finite planning horizon. The proposed strategy is based on continuous-time dynamic programming, and uses stochastic differential equations to model the random process governing the behaviour over time of the renewable energy available at the farm.

- Assuming dynamic block pricing, we propose two genie-aided strategies to minimize the energy bill incurred by a non-deferrable load over a finite planning horizon. Both strategies are devised by solving the pertinent optimization problem. The first strategy uses linearisation and discretisation in time, and the second strategy is based on calculus of variations. We compare the two strategies and advise on their advantages and disadvantages.

1.4.3 Bibliographical Notes

Parts of this thesis have been published or submitted for publication in different venues:

- The material in Chapter 2 draws from [168], [169], [170], and [171].
- The material in Chapter 3 draws mainly from [172] and [173].
- The material in Chapter 4 draws mainly from [174] and [175].
- The material in Chapter 5 draws mainly from [171] and [176].

Chapter 2

Offline Energy Management Strategies

In this chapter we formulate an optimization problem to minimize the energy expenditure incurred by a non-deferrable load facility, such as a cellular base station,[1] over a finite planning horizon. We assume that the facility is equipped with a renewable energy harvester and a storage device. We then use different optimization techniques to obtain three genie-aided solutions, so named because they use exact knowledge of renewable energy arrivals and load across the entire planning horizon. The first method is based on discretisation in time and linearisation, and provides a solution with different levels of accuracy depending on the sampling frequency and the number of linear inequalities employed. The second method uses an evolutionary algorithm to obtain a high-performing strategy, which is not necessarily optimal. The third method uses calculus of variations (CoV) to obtain an analytical solution. Finally, numerical results are presented for verification and further insight.

2.1 Contributions

The main contributions of this chapter are the following:

- We establish the mathematical framework to design strategies that minimize the energy bill incurred by a non-deferrable load facility over a finite planning horizon. It is assumed that the facility is equipped with a renewable energy harvester and a

[1] A non-deferrable load has insufficient flexibility to shift its power consumption to low-price periods. In the case of a cellular base station, part of its energy consumption depends on requests made externally by mobile users, hence, it has less flexibility to schedule its power-consuming tasks.

storage device. Therefore, the proposed framework incorporates a general model for the storage device, which takes into account the non-linear relationship between the discharging rate and the remaining charge. The proposed framework allows us to formulate a mathematical problem to minimize the energy expenditure incurred by *any* non-deferrable load over a finite planning horizon.

- We propose three genie-aided strategies which are obtained by solving a constrained optimization problem through different methods. In the first method we use linearisation and discretisation in time, which allows us to cast the problem as a linear program, and obtain a precision-adjustable solution. In the second method we use an evolutionary strategy to obtain a solution within the available[2] computational capacity. In the third method we use calculus of variations to obtain a more insightful analytical solution. We finally provide numerical results, from which we draw relevant insights.

2.2 System Model

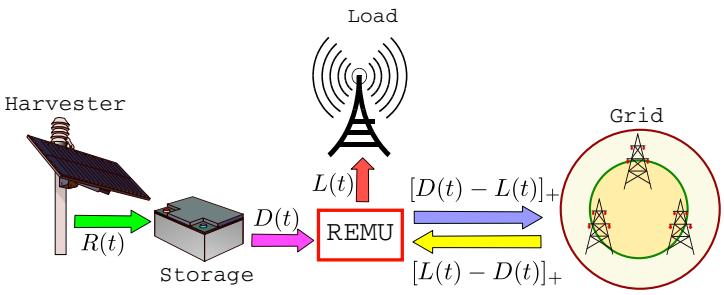

Figure 2.1: System model. The non-deferrable load is represented by a base station, and the storage device by a lead-acid battery. REMU stands for renewable energy management unit.

[2]The computational cost of the proposed strategy can be adjusted by changing the sampling frequency and stopping criterion.

2.2.1 General Setup

Fig. 2.1 shows the principal elements of the system of interest. The first element in the system is the non-deferrable load facility, which is represented by a base station. The facility is equipped with renewable energy harvesting and storage capabilities. As shown, the load is permanently connected to the power grid through the renewable energy management unit (REMU), which controls the bi-directional power flow with the grid, and schedules the discharging operations. As shown in Fig. 2.1, the facility can be powered directly from the grid, and the storage device.

We consider a finite planning horizon of H time units, where H can be made arbitrarily large, as long as the physical properties of the components in the system remain constant in $[0,H]$. The load varies as a function of time $t \in [0,H]$, and is denoted by $L(t) \geq 0$. The effective renewable power harvested in $[0,H]$ is denoted by $R(t) \geq 0$. Moreover, $D(t) \geq 0$ denotes the power effectively (after losses) drawn from the storage device at time t.

2.2.2 Electricity Pricing Scheme

Let $P(t)$ denote the energy prices offered by the utility in $[0,H]$, and $W(t)$ be the rates[3] at which renewable energy is sold back to the utility. Then, assuming a linear pricing scheme, the energy cost incurred by the facility in $[0,H]$ is:

$$\chi = \int_0^H P(t)\,[L(t) - X(t)] - W(t)Y(t)dt, \tag{2.1}$$

where $X(t)$ is the power discharged from the local storage to feed the load, and thus satisfies $X(t) \leq L(t)\ \forall\, t$. And $Y(t)$ is the renewable power injected into the grid to obtain credits in return. The total power drawn from the storage is thus $D(t) = X(t) + Y(t)$.

[3] In practice $W(t) \leq P(t)\ \forall\, t$.

2.2.3 Energy Storage Device

State Equation

Let $\tilde{D}(t)$ denote the power drawn from the storage device to effectively deliver $D(t) = X(t) + Y(t)$ at its output. Then, the energy $J(t)$ stored at time $t \geq 0$, can be determined from:

$$J(t) = J(0) + \int_0^t [\varsigma R(x) - \tilde{D}(x)]dx, \tag{2.2}$$

where $0 \leq \varsigma \leq 1$ is the charging efficiency rate. Since the storage device has a limited capacity $\Psi > 0$, the following inequality should hold for all t: $0 \leq J(t) \leq \Psi$.

As seen in Eq. 2.2, the storage device is only charged with renewable energy. This assumption is made following the net metering scenario considered in this chapter. Current regulation only allows for energy from a renewable source to be injected into the grid. Hence, for simplicity[4] we have assumed that the storage device can only be charged with renewable energy harvested locally.

Discharging Model

The relationship between $\tilde{D}(t)$ and $D(t)$ is modelled by using an arbitrary function $\mathscr{F} : [0,\infty) \to [0,\infty)$, i.e.

$$\tilde{D}(t) = \mathscr{F}[D(t)], \tag{2.3}$$

which can be tuned to reflect empirical properties of any practical storage system. The function $\mathscr{F}(\cdot)$ is assumed to be continuous, convex, and strictly increasing.

If we want to use Peukert's model, we should define $\mathscr{F}[D(t)]$ as:

$$\mathscr{F}[D(t)] = \max\left\{Q_{\text{No}}\left[\frac{D(t)}{Q_{\text{No}}}\right]^{\kappa}, D(t)\right\}, \tag{2.4}$$

[4]If battery charging from the grid and net metering are allowed concurrently, then the utility will need to monitor the production of renewable energy at each of their eligible customers and impose the corresponding limits to comply with the regulation.

which follows from (1.5). Moreover, the following definition can be used to make the problem more tractable and obtain results in closed form:

$$\mathscr{F}\left[D(t)\right] = Q_{\text{No}}\left[\frac{D(t)}{Q_{\text{No}}}\right]^{\kappa}. \tag{2.5}$$

Eq. (2.5) can substitute (2.4) without errors only when $D(t) \geq Q_{\text{No}}$. A "systematic" error is introduced by using (2.5) instead of (2.4) when $D(t) < Q_{\text{No}}$. However, this error approaches 0 as $\kappa \to 1^{+}$.

To preserve the health of the batteries in the storage system, the discharging power is bounded according to the largest current that the batteries can deliver at any time t. Therefore, the maximum discharging power allowed at any time t is $\tilde{D}_{\max}$, i.e. $\tilde{D}(t) \leq \tilde{D}_{\max}\ \forall\, t$.

2.3 Problem Formulation

We formulate the following optimization problem to minimize the energy bill incurred by the facility in $[0,H]$:

$$\text{P2.0:} \quad \min_{X(t),Y(t)} \quad \int_0^H P(t)\left[L(t)-X(t)\right]dt - \int_0^H \left[W(t)Y(t)\right]dt$$

subject to the following constraints:

$$0 \leq J(t) \leq \Psi, \tag{2.6a}$$

$$J(H) = J(0), \tag{2.6b}$$

$$\tilde{D}(t) \leq \tilde{D}_{\max}, \tag{2.6c}$$

$$X(t) \leq L(t), \tag{2.6d}$$

$$X(t) \geq 0,\ Y(t) \geq 0,\ \forall\, t\ \in\ [0,H]. \tag{2.6e}$$

In P2.0, $D(t) = X(t) + Y(t)$ and $\tilde{D}(t)$ are related by (2.3), whereas $\tilde{D}(t)$ and $J(t)$ are related by (2.2). The constraint (2.6b) ensures the continuity of the energy level over

different optimization periods [152]. This constraint is a rudimentary way of accounting for future planning periods in the optimization problem. If (2.6b) is removed, then the optimal policy may[5] yield $J(H) = 0$, which will surely affect future planning periods. Constraint (2.6b) implies:

$$\int_0^H \tilde{D}(t)dt = \varsigma \int_0^H R(t)dt, \tag{2.7}$$

i.e. the total energy discharged in $[0,H]$ is equal to the total energy harvested in $[0,H]$. The constraint (2.6c) ensures that the amount of power drawn from the storage system at any time t is bounded according to the maximum current that the batteries can deliver.

The term $P(t)L(t)$ does not depend on the decision variables $X(t)$ or $Y(t)$, and hence can be removed from the objective function in P2.0. Moreover, we can write P2.0 as a maximization problem by multiplying its objective by (-1):

$$\text{P2.1:} \quad \max_{X(t),Y(t)} \quad \int_0^H [P(t)X(t) + W(t)Y(t)]\,dt$$

subject to constraints (2.6a)–(2.6e). In P2.1, $D(t)$ and $\tilde{D}(t)$ are related by (2.3), whereas $\tilde{D}(t)$ and $J(t)$ are related by (2.2).

2.4 Proposed Strategies

In the following we propose three strategies to solve P2.1 assuming exact knowledge of $R(t)$, $P(t)$, $L(t)$, and $W(t)$ in $[0,H]$. P2.1 is infeasible if $\tilde{D}_{\max}$ is not large enough to permit the discharging of the total energy harvested in $[0,H]$, as required by the constraint (2.6b). Therefore, in this section we will assume that P2.1 is feasible, i.e. $\tilde{D}_{\max}$ is large enough to satisfy the constraint (2.6b).

Moreover, if $\mathscr{F}(\cdot)$ is a linear function, then the optimization problem P2.1 reduces to a linear program. Similarly, if $\mathscr{F}(\cdot)$ is modelled after Peukert's Law, and $\tilde{D}_{\max} < Q_{\mathsf{No}}$,

[5] This requires a sufficiently large $\tilde{D}_{\max}$ to ensure full renewable energy utilization in $[0,H]$.

then following (1.5), Peukert's effect will not manifest in the discharging operation, and again, P2.1 reduces to a linear program. In this thesis, we assume that $\mathscr{F}(\cdot)$ is in general non-linear, and if it is modelled after Peukert's Law, then we assume that $\tilde{D}_{\max} > Q_{\mathsf{No}}$, thus allowing the storage device to operate in either regime (linear or non-linear).

2.4.1 Solution by Discretisation in Time

In this section, we propose a solution to P2.1 through discretisation in time, which illustrates the computational complexity involved and therefore motivates a solution in the continuous-time domain. We divide the time interval $[0,H]$ into N slots, each one of duration Δt, i.e., $\Delta t = H/N$. Let $\mathbf{d} \in \mathbb{R}_+^N$ and $\mathbf{p} \in \mathbb{R}_+^N$ represent respectively the power drawn from the storage and the energy prices over N time slots. These vectors are obtained by uniformly sampling their corresponding continuous-time functions at a rate of $1/\Delta t$ samples per unit of time, e.g.,

$$d(k) = D(k\Delta t). \tag{2.8}$$

Let $\tilde{\mathbf{d}} \in \mathbb{R}_+^N$ and $\mathbf{d} \in \mathbb{R}_+^N$ denote, respectively, the vectors containing the samples of $\tilde{D}(t)$ and $D(t)$, i.e.

$$\tilde{d}(k) = \tilde{D}(k\Delta t), \quad d(k) = D(k\Delta t). \tag{2.9}$$

Then we can approximate (2.3) by using a piece-wise linear function as follows:

$$d(k) \approx G[\tilde{d}(k)] \triangleq \begin{cases} \alpha_1 \tilde{d}(k) - \beta_1 & \tilde{d}(k) \leq \Phi_1 \\ \alpha_2 \tilde{d}(k) - \beta_2 & \Phi_1 < \tilde{d}(k) \leq \Phi_2 \\ & \vdots \\ \alpha_M \tilde{d}(k) - \beta_M & \Phi_{M-1} < \tilde{d}(k) \end{cases}, \tag{2.10}$$

where M represents the number of linear segments used to approximate (2.3), and α_i, β_i and Φ_i are parameters chosen to minimize the approximation error. Specifically, $\Phi_2, \ldots, \Phi_{M-1}$ can be chosen as a uniform partition of $[0, \tilde{D}_{\max}]$, and the α_i's and β_i's can then be obtained by solving the following optimization problem:

$$\text{P2. A:} \quad \min_{\alpha_1,\ldots,\alpha_M;\beta_1,\ldots,\beta_M} \quad \int_0^{\tilde{D}_{\max}} \left[\mathscr{F}^{-1}(x) - G(x)\right]^2 dx,$$

where $\mathscr{F}^{-1}(\cdot)$ is the inverse function of $\mathscr{F}(\cdot)$, i.e. $\mathscr{F}^{-1}(\mathscr{F}(x)) = \mathscr{F}(\mathscr{F}^{-1}(x)) = x$. P2.A can be solved numerically. In Appendix A.1 we show an analytical method to find an approximate solution to P2.A.

To simplify P2.1, (2.10) can be replaced with the following set of linear inequality constraints:

$$d(k) \leq \alpha_i \tilde{d}(k) - \beta_i, \; i \in \{1, \ldots, M\}. \tag{2.11}$$

Maximizing the objective in P2.1 requires (2.11) to be satisfied with equality, i.e.,

$$d(k) = \min_i \left\{ \alpha_i \tilde{d}(k) - \beta_i \right\}, \; i \in \{1, \ldots, M\}. \tag{2.12}$$

The right hand side in (2.12) can be shown to be another way to define $G(\cdot)$, which is equivalent to (2.10). To see this, notice that $G(\cdot)$ is a concave[6] piece-wise linear function, which can be written as the point-wise minimum of a set of affine functions.

An approximate solution to P2.1 can then be obtained by solving:

$$\text{DP2. 1:} \quad \max_{\mathbf{x},\mathbf{y}} \quad \Delta t \sum_{k=1}^{N} \left[p(k)x(k) + w(k)y(k)\right]$$

s.t. (2.6b), (2.11) and:

$$0 \leq J(k\Delta t) \leq \Psi, \tag{2.13a}$$

[6] $G(\cdot)$ is assumed to be a valid approximation of $\mathscr{F}^{-1}(\cdot)$, which is concave because $\mathscr{F}(\cdot)$ is assumed to be continuous, strictly increasing and convex [177].

$$x(k) \leq \ell(k), \tag{2.13b}$$

$$\tilde{d}(k) \leq \tilde{D}_{\max} \; \forall \; k. \tag{2.13c}$$

In DP2.1, $d(k) = x(k) + y(k)$, and $J(k\Delta t)$ and $\tilde{d}(k)$ are connected by equation (2.2) after introducing discretisation, i.e.

$$J(k\Delta t) = J(0) + \Delta t \sum_{j=1}^{k} \left[\varsigma r(j) - \tilde{d}(j) \right],$$

where $r(k) = R(k\Delta t)$. Moreover, (2.13a) implies:

$$J(0) + \Delta t \sum_{j=1}^{k} \left[\varsigma r(j) - \tilde{d}(j) \right] \geq 0, \; \forall \; k$$

and

$$J(0) + \Delta t \sum_{j=1}^{k} \left[\varsigma r(j) - \tilde{d}(j) \right] \leq \Psi, \; \forall \; k,$$

which hints to a recursive relationship that can be captured by a triangular matrix. In fact, if we let $\mathbf{A} \in \mathbb{R}^{N \times N}$ be a lower triangular matrix such that $A(i,j) = 1 \; \forall \; i \geq j$. Then, DP2.1 can be cast in matrix form as follows:

$$\text{LP2.1:} \quad \max_{\mathbf{x},\mathbf{y},\mathbf{d},\tilde{\mathbf{d}}} \quad \Delta t \left(\mathbf{p}^T \mathbf{x} + \mathbf{w}^T \mathbf{y} \right)$$

s.t. $d(k) = x(k) + y(k)$, $0 \leq x(k) \leq \ell(k) \; \forall \; k$, and:

$$\begin{pmatrix} -\Delta t \mathbf{A} & \mathbf{0} \\ \Delta t \mathbf{A} & \mathbf{0} \\ -\alpha_1 \mathbf{I} & \mathbf{I} \\ -\alpha_2 \mathbf{I} & \mathbf{I} \\ \vdots & \vdots \\ -\alpha_M \mathbf{I} & \mathbf{I} \\ \Delta t \mathbf{1}^T & 0, 0, \ldots, 0 \end{pmatrix} \begin{pmatrix} \tilde{\mathbf{d}} \\ \mathbf{d} \end{pmatrix} \preceq \begin{pmatrix} \Psi - J(0) - \varsigma \Delta t \mathbf{A} \mathbf{r} \\ J(0) + \varsigma \Delta t \mathbf{A} \mathbf{r} \\ -\beta_1 \mathbf{1} \\ -\beta_2 \mathbf{1} \\ \vdots \\ -\beta_M \mathbf{1} \\ \varsigma \Delta t \mathbf{1}^T \mathbf{r} \end{pmatrix} \tag{2.14}$$

The last inequality

$$\Delta t \mathbf{1}^T \tilde{\mathbf{d}} \leq \varsigma \Delta t \mathbf{1}^T \mathbf{r}$$

implies $J(0) = J(H)$. To see this, notice that $\Delta t \mathbf{1}^T \tilde{\mathbf{d}}$ is the total energy drained from the storage system in $[0, H]$, if $\Delta t \mathbf{1}^T \tilde{\mathbf{d}}$ is upper bounded by the total renewable energy

harvested in $[0,H]$, then maximizing the objective in LP2.1 requires $\Delta t\mathbf{1}^T\tilde{\mathbf{d}} = \varsigma\Delta t\mathbf{1}^T\mathbf{r}$. The last equality implies that the entire energy harvested in $[0,H]$ is drained from the storage system, which yields $J(H) = J(0)$.

As expected, the complexity of LP2.1 increases as N grows. In particular, the number of variables involved in the problem is directly proportional to the number of samples considered in $[0,H]$, and a new constraint is introduced for each linear segment that is added to $G(\cdot)$ to approximate (2.3).

2.4.2 Solution by Evolutionary Strategies

We propose a strategy based on evolutionary algorithms to design the discharging operation across the entire optimization interval. The advantage of this strategy over linearisation and discretisation in time is that the non-linear relationship (2.3) can be handled directly. However, the result obtained with this strategy may not be the optimal. Evolutionary strategies are, in general, used to obtain high-performing suboptimal solutions, especially to problems that are analytically intractable.

The proposed strategy, shown in Algorithm 1, consists of an iterative routine that explores the feasible set of the discharging vectors $\tilde{\mathbf{d}}$'s using evolutionary operators such as mutation and recombination. The fitness of each candidate is evaluated by computing the resulting expenditure, i.e. the lower the resulting cost, the higher the fitness score. To compute the resulting cost from a candidate $\tilde{\mathbf{d}}$, the first step is to determine $\mathbf{d}$ from (2.3), and then the vectors $\mathbf{x}$ and $\mathbf{y}$ can be obtained by using the following policy:

$$x(k) = \min\{d(k), \ell(k)\}, \tag{2.15}$$

and $y(k) = d(k) - x(k)$. This policy follows because the assumed compensation for renewable power injected into the grid is at most equal to the retail electricity prices $P(t)$, i.e. $W(t) \leq P(t)$.

Algorithm 1 Evolutionary Strategy for Energy Management

```
Define initial population
Generations=1
while Generations < Maximum do
    Apply mutation operator
    Recombine the mutated candidates
    Evaluate fitness of the offspring
    Select the survivors
    Generations=Generations+1
end while
```

In the following we describe the main characteristics of the algorithm:

- Initial population: For simplicity, we consider a unitary population, which is seeded by a flat discharging profile, e.g. $\tilde{d}(k) = \frac{J(0)}{N\Delta t} \; \forall \; k, J(0) > 0$.

- Fitness evaluation: Let $\tilde{\mathbf{d}}_c$ represent a candidate solution, then its fitness score is the additive inverse of the energy cost incurred when the discharging operation is $\tilde{\mathbf{d}}_c$. If a given vector $\tilde{\mathbf{d}}$ results in an infeasible[7] operation, then its fitness score is $-\infty$.

- Mutation operator: We implement isotropic Gaussian mutations with varying mutation strength (variance) as follows: let $\tilde{\mathbf{d}}_m$ represent the candidate solution after mutating the individual $\tilde{\mathbf{d}}$, then:

$$\tilde{d}_m(j) = \min\{\tilde{d}(j)\exp(\mathsf{Y}), \tilde{D}_{\max}\}, \tag{2.16}$$

  where $\mathsf{Y} \sim \mathscr{N}\left(0, \sigma^2\right)$. The variance of Y can be chosen as a non-increasing function of the generation number. In this way, as the evolutionary algorithm progresses, the search space is narrowed down, which allows us to fine tune the discharging profile. We may however get stuck in a local optimum.

- Parent selection and recombination: The mutated candidate solutions are recombined using the addition operation, re-scaling is implemented to ensure that the offspring satisfies the causality constraint. Let $\tilde{\mathbf{d}}_1$ and $\tilde{\mathbf{d}}_2$ represent two candidate solutions,

[7] Infeasible candidate solutions violate at least one of the constraints considered in the problem.

their offspring $\tilde{\mathbf{d}}_{12}$ is thus:

$$\tilde{\mathbf{d}}_{12} = \mathsf{SF}\left(\tilde{\mathbf{d}}_1 + \tilde{\mathbf{d}}_2\right),$$

where $\mathsf{SF} > 0$ is a scaling factor chosen to ensure that $\tilde{\mathbf{d}}_{12}$ satisfies the causality constraint. All individuals in the population participate in recombination, hence the algorithm does not require parent selection criteria.

- Selection of survivors: As the population size remains constant, we specify a selection criterion to choose the individual that survives in each generation. Our selection criterion is deterministic and fitness-based, i.e., the fittest individual remains in the population.

2.4.3 Solution by Calculus of Variations

In this section, we propose a different technique to solve the optimization problem. This approach is simpler than the strategies presented in Secs. 2.4.1 and 2.4.2 because it does not rely on iterative algorithms to solve the optimization problem. Instead, the solution is obtained by determining the roots of a function. Moreover, in some particular cases these roots can be obtained analytically, and hence the solution to the optimization problem can be determined directly by plugging the input data into the resulting formula.

Required Simplifications

We introduce some simplifications which will allow us to tackle the problem in continuous time by using calculus of variations. Specifically,

- Proper storage initialization: For tractability, we will assume that

$$J(0) = \varsigma \int_0^H R(t)dt. \tag{2.17}$$

Proposition 2.4.1. *If* $J(0) = \varsigma \int_0^H R(t)dt$*, and* $\tilde{D}(t)$ *satisfies (2.7), then* $J(t) \geq 0 \; \forall \, t$.

Proof. See Appendix B.1. ■

- Large storage capacity: We will assume that Ψ is large enough so as to avert wastage of renewable energy due to overflow. Specifically,

  Proposition 2.4.2. *Let*

  $$\Psi \geq 2\varsigma \int_0^H R(x)dx$$

  then $J(t) \leq \Psi \; \forall \, t$.

  Proof. See Appendix B.2. ■

- Relaxation of constraint (2.6c): We substitute (2.6c) with:

  $$\int_0^H \tilde{D}(t)dt \leq H\tilde{D}_{\max}. \tag{2.18}$$

  Moreover:

  Proposition 2.4.3. *P2.1 is infeasible if*

  $$\varsigma \int_0^H R(x)dx > H\tilde{D}_{\max}.$$

  Proof. The proof is immediate from inspecting (2.7) and (2.18). ■

- $W(t) = P(t) \; \forall \; t$: By introducing this assumption, we can disregard the constraint (2.6d), and as a result we only need to determine the optimal $D(t) = X(t) + Y(t)$. Specifically, we design $D(t)$ to maximize $\int_0^H P(t)D(t)dt$, and then obtain $X(t)$ and $Y(t)$ by using the following policy:

  $$X(t) = \min\{L(t), D(t)\}, \tag{2.19}$$

and

$$Y(t) = D(t) - X(t). \tag{2.20}$$

Any other power allocation policy between $X(t)$ and $Y(t)$ is optimal, as long as it satisfies (2.20). Therefore, when designing $D(t) = X(t) + Y(t)$ we can ignore the constraint (2.6d), because we can always choose $X(t)$ from (2.19).

Simplified Formulation

Following the Propositions 2.4.1 and 2.4.2, we can disregard the constraint (2.6a). Moreover, assuming that the problem is feasible, i.e.

$$\varsigma \int_0^H R(x)dx < H\tilde{D}_{\max},$$

we can disregard the constraint (2.18) and the optimization problem becomes:

$$\text{P2.2:} \quad \max_{D(t)} \quad \int_0^H P(t)D(t)dt$$

subject to:

$$\int_0^H \mathscr{F}\left[D(t)\right] dt = J(0). \tag{2.21}$$

P2.2 can be tackled by using calculus of variations. And depending on the properties of $\mathscr{F}(\cdot)$, we may be able to obtain a solution in closed form. The following theorem provides a necessary condition to solve P2.2, and the closed-form solution obtained when $\mathscr{F}(\cdot)$ is given by (2.5).

Theorem 2.4.1. *Subject to (2.21), a necessary condition to maximize the functional* $\int_0^H P(t)D(t)dt$ *is:*

$$-P(t) + \lambda \mathscr{F}'\left[D(t)\right] = 0, \tag{2.22}$$

where $\mathscr{F}'[x] = \frac{d}{dx}\mathscr{F}[x]$, *and* $\lambda \in \mathbb{R}_+$. *Moreover, if* $\mathscr{F}[x] = Q_{\mathsf{No}}\left[\frac{x}{Q_{\mathsf{No}}}\right]^{\kappa}$, *with* $Q_{\mathsf{No}} > 0$

and $\kappa > 1$*, then, subject to (2.21), (2.22) yields:*

$$D(t) = D^*(t) \triangleq Q_{\text{No}} \left[\frac{P(t)}{\lambda \kappa} \right]^{\frac{1}{\kappa-1}}, \tag{2.23}$$

where

$$\lambda = \frac{1}{\kappa \left[\dfrac{J(0)}{Q_{\text{No}} \displaystyle\int_0^H P(t)^{\frac{\kappa}{\kappa-1}} dt} \right]^{\frac{\kappa-1}{\kappa}}}. \tag{2.24}$$

Proof. See Appendix B.3. ■

Analysis of the Special Case (Simplified Peukert's Model)

If $\mathscr{F}(\cdot)$ is given by (2.5), which we refer to as simplified Peukert's model, then to maximize the functional $\int_0^H P(t)D(t)dt$, $D(t)$ should be directly proportional to $P(t)^{\frac{1}{\kappa-1}}$. Thus, we can say that in such a scenario the discharging operation should track the signal obtained after raising the instantaneous energy price to a power determined by the efficiency of the storage device. Therefore, the higher the unit energy price, the larger the optimal amount of power to be drawn from the storage. Moreover, $\frac{1}{\kappa-1}$ is a modulating exponent, analogous to the Q-factor of a passband filter, with $\kappa \to 1^+$ yielding a more selective response.

The analytical results obtained with this approach may provide valuable insights to design online strategies. The result in Theorem 2.4.1 only requires an estimate of the total renewable energy harvested over the planning horizon to determine the optimal discharging operation without any further knowledge of specific renewable energy arrivals in the future.

By letting $\mathscr{F}[D(t)]$ be defined as in (2.5), we are assuming that the discharging operation follows Peukert's Law and that the discharging power is above the nominal, i.e. $D(t) \geq Q_{\text{No}} \; \forall \, t$. Since Peukert's Law underestimates the remaining charge when

the battery is subject to time-varying discharging rates or temperatures [23], the use of this simplification should be understood as a means to illustrate the procedure to solve P2.2. It is also important to state that by using this simplification we are able to obtain elegant results, which may provide insights that can be used in the design of real-time optimization strategies.

Alternative Formulation

We can alternatively solve the problem P2.1 in terms of $\tilde{D}(t)$ and then obtain the *effective* $D(t)$ by using $\mathscr{F}^{-1}(\cdot)$. To solve P2.1 in terms of $\tilde{D}(t)$, we formulate the following problem:

$$\text{P2.3:} \quad \max_{\tilde{D}(t)} \quad \int_0^H P(t)\mathscr{F}^{-1}\left[\tilde{D}(t)\right] dt$$

s.t.

$$\int_0^H \tilde{D}(t)dt = J(0). \tag{2.25}$$

P2.3 can also be tackled using the results in Theorem 2.4.1. Specifically, if $\mathscr{F}[D(t)]$ is given by (2.5), then we obtain the following expression for optimal $\tilde{D}(t)$ denoted by $\tilde{D}^*(t)$:

$$\tilde{D}^*(t) \triangleq Q_{\text{No}} \left[\frac{P(t)}{\lambda \kappa}\right]^{\frac{\kappa}{\kappa-1}}, \tag{2.26}$$

where λ is given by (2.24).

The advantage of this formulation is that we reduce the chances of overestimating $J(t)$ because we directly optimize $\tilde{D}(t)$. In contrast, when we solve P2.1, we optimize $D(t)$, which may require real-time adjustments in practical implementations as the storage device may[8] be unable to deliver the required $\tilde{D}(t)$ over a given period of time.

[8]This may happen when the estimate of $\mathscr{F}(\cdot)$ carries measurement errors.

2.5 Numerical Results

In this section we evaluate the performance of the proposed strategies assuming arbitrary price trajectories. The function $D(t)$ and the vector $\mathbf{d}$ are referred to as the discharging profiles in continuous and discrete time respectively. As such, they represent the amount of power drawn from the storage system over $[0,H]$. Throughout this section we will assume that the function $\mathscr{F}(\cdot)$ models Peukert's Law, i.e. is given by (2.4) and we will investigate the effects of using the simplified expression (2.5).

Table 2.1: Simulation parameters (offline optimization strategies).

H	1
Δt	0.02
$R(t)$	$50\sin(5t-1)+50$
ς	1
κ	1.2
Q_{No}	$\Delta t\sum_{i=1}^{N} R(i)$
M	10
$P(t)$	$\sin(10t)+1$
$W(t)$	$P(t)$
$J(0)$	$\Delta t\sum_{i=1}^{N} R(i)$
Ψ	$2J(0)$
$\tilde{D}_{\max}$	$6Q_{\mathsf{No}}$

2.5.1 Effect of the Simplifications Introduced

We start by evaluating the effect of introducing the simplification (2.5). Hence, we consider the parameters shown in Table 2.1 and the following linear inequalities used to approximate (2.4) in $[Q_{\mathsf{No}},\tilde{D}_{\max}]$:

$$D(t) \leq \mathscr{L}_1(\tilde{D}(t)) \triangleq 0.79\tilde{D}(t)+13.71$$

$$D(t) \leq \mathscr{L}_2(\tilde{D}(t)) \triangleq 0.75\tilde{D}(t)+16.90$$

$$D(t) \leq \mathscr{L}_3(\tilde{D}(t)) \triangleq 0.73\tilde{D}(t)+19.97$$

$$D(t) \leq \mathscr{L}_4(\tilde{D}(t)) \triangleq 0.71\tilde{D}(t)+22.96$$

$$D(t) \leq \mathscr{L}_5(\tilde{D}(t)) \triangleq 0.69\tilde{D}(t) + 25.87$$

$$D(t) \leq \mathscr{L}_6(\tilde{D}(t)) \triangleq 0.68\tilde{D}(t) + 28.71$$

$$D(t) \leq \mathscr{L}_7(\tilde{D}(t)) \triangleq 0.67\tilde{D}(t) + 31.50$$

$$D(t) \leq \mathscr{L}_8(\tilde{D}(t)) \triangleq 0.66\tilde{D}(t) + 34.24$$

$$D(t) \leq \mathscr{L}_9(\tilde{D}(t)) \triangleq 0.65\tilde{D}(t) + 36.94$$

We can therefore express $D(t)$ as:

$$D(t) \approx \min_i \left\{ \mathscr{L}_i(\tilde{D}(t)) \right\}, \; i \in \{1, \ldots, 9\}. \tag{2.27}$$

These inequalities approximate (2.4) in the range $Q_{\mathsf{No}} \leq \tilde{D}(t) \leq \tilde{D}_{\max}$. The range $0 \leq \tilde{D}(t) \leq Q_{\mathsf{No}}$ does not require approximation according to (2.4). We start by evaluating the accuracy of this approximation by directly comparing (2.4) and (2.27). The comparison is shown in Fig. 2.2. As seen, the number of linear segments is sufficiently large to provide an acceptable approximation.

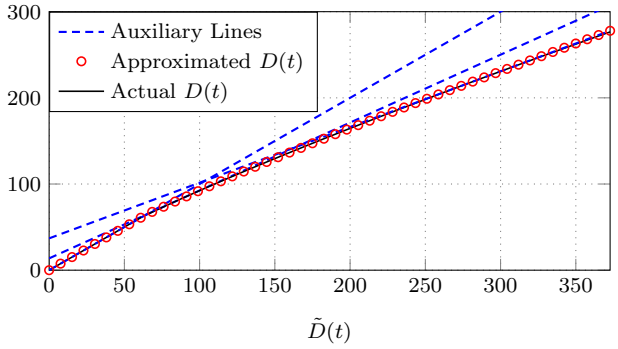

Figure 2.2: Eq. (2.4) and the approximation (2.27).

2.5.2 Comparison between the Proposed Strategies

Considering the parameters listed in Table 2.1, we determine the optimal discharging operation –$D(t)$– by solving P2.1 through linearisation and discretisation in time and the results are shown in Fig. 2.3. As observed, the strategy seeks to discharge larger

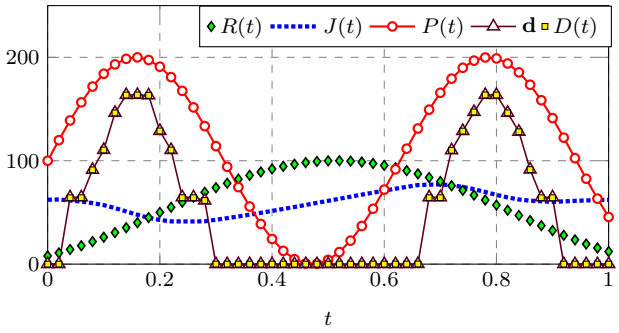

Figure 2.3: Renewable energy arrival profile, energy stored over time, and pricing function. The discharging profile obtained directly through linearisation and discretisation in time is $\mathbf{d}$. The discharging profile obtained from $\tilde{\mathbf{d}}$ through (2.4) is denoted by $D(t)$.

amounts of power when the prices are high. Moreover, an acceptable match between the $D(t)$ obtained by solving the linear program and denoted by $\mathbf{d}$, and the $D(t)$ obtained from $\tilde{D}(t)$ through (2.4) is seen. The energy stored over time is also shown, as well as the prices, and the renewable energy profile, which resembles the output of a solar panel.

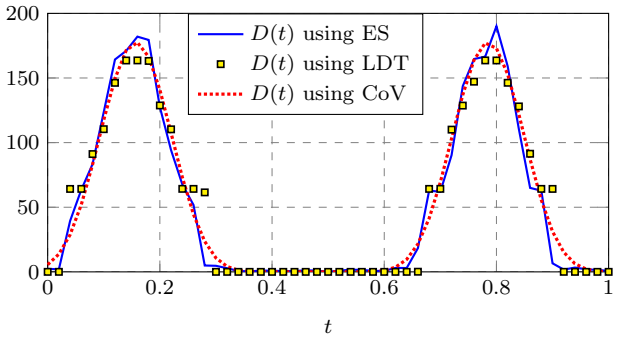

Figure 2.4: Optimal discharging profile obtained through linearisation and discretisation in time (LDT), evolutionary strategies (ES), and calculus of variations (CoV).

In Fig. 2.4 we show the optimal discharging profiles obtained by using the three proposed strategies for the price and renewable power trajectories shown in the Fig. 2.3. The simulation parameters are again the ones listed in Table 2.1. The discharging profile obtained by using the evolutionary strategy took one thousand generations, and

the variance of Υ was kept constant at 0.01 throughout all the iterations. The similarities between the discharging profiles obtained by using different methods are remarkable. Differences are also observed when $D(t) < Q_{\mathsf{No}}$, which follows from the relaxation (2.5), introduced to simplify Peukert's Law. This simplification introduces an error when $D(t) < Q_{\mathsf{No}}$.

In Fig. 2.5 we have plotted the value of $\int_0^H P(t)D(t)dt$, optimized by using calculus of variations, and linearisation following discretisation in time, for different values of $J(0) = \varsigma \int_0^H R(t)dt$, while maintaining $\Psi = 2J(0)$. To avoid loss of generality, we have considered random energy prices drawn from a standard uniform distribution, i.e. $p(k) \sim \mathscr{U}(0,1)$, and computed the mean performance by averaging over the results obtained in ten thousand realisations. To that end, we have considered $Q_{\mathsf{No}} = 20$ and $\kappa = 1.3$, while other parameters are left unchanged from Table 2.1. The linear inequalities used to approximate (2.4) in $[Q_{\mathsf{No}}, \tilde{D}_{\max}]$ have been obtained by using the method described in Appendix A.1, with the partition's midpoints $\{x_2, x_3, \ldots, x_{10}\}$ defined as follows:

$$x_i = (0.4i + 0.6)\, Q_{\mathsf{No}},\ i \in \{2, \ldots, 10\}.$$

As seen in Figs. 2.5 and 2.6, both strategies agree up to some gap which depends on whether the simplifications introduced to obtain the solution in (2.23) are justified. At this point, it is worth emphasizing that the result obtained with the strategy based on linearisation and discretisation approaches the optimal performance as we increase the sampling frequency, and add more linear segments to accurately represent $\mathscr{F}(\cdot)$. In contrast, whenever the simplifications introduced are justified, the strategy based on calculus of variations is able to provide a solution whose accuracy can be improved without the need to solve the optimization problem with an increased number of variables and

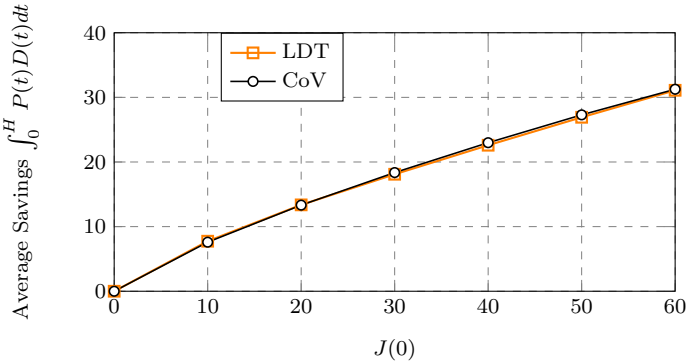

Figure 2.5: Performance of the strategies based on linearisation and discretisation in time (LDT), and calculus of variations (CoV) with $\tilde{D}_{\max} = 300$.

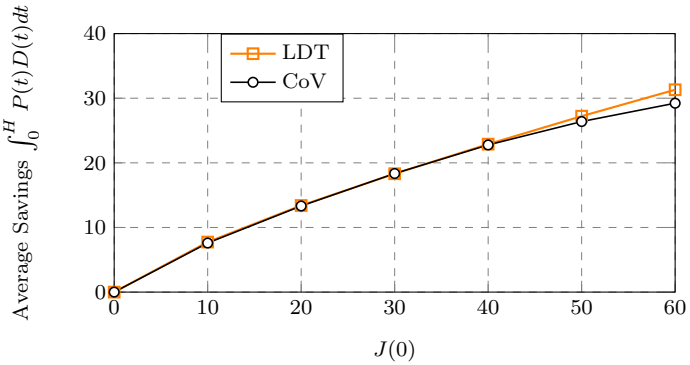

Figure 2.6: Performance of the strategies based on linearisation and discretisation in time (LDT), and calculus of variations (CoV) with $\tilde{D}_{\max} = 200$.

constraints.

2.5.3 Performance of the Evolutionary Strategy

In the following we provide further simulation results to evaluate the performance of the evolutionary strategy (ES). The discharging profile shown in Fig. 2.4 was obtained in a single execution. But since the mutation operations are random, a slightly different result is obtained in each run. We therefore compute mean values and standard deviations to determine the variability of the results. In Fig. 2.7 we have plotted the average discharging profile obtained after fifty iterations, and also the profiles obtained by adding

and subtracting two standard deviations from the mean. The average discharging profile and the standard deviations were estimated by using the results obtained in ten thousand realisations.

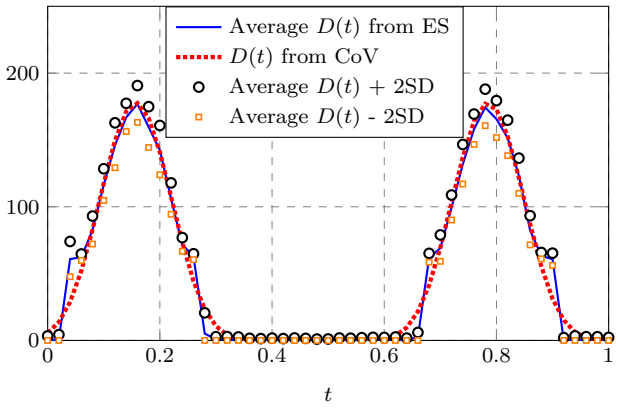

Figure 2.7: Average discharging profile obtained after fifty iterations using the evolutionary algorithm. The discharging profile obtained by using calculus of variations (CoV) is also shown. SD stands for standard deviation.

As observed in Fig. 2.7, the standard deviations of the N designed variables are all relatively small. In fact, deviations of two times their magnitude are still close to the average discharging profile. This follows despite the small number of iterations considered in each realisation, which shows that even as few as 50 generations may be enough to obtain acceptable results.

2.5.4 Comparison with Existing Strategies

We consider the following simulation parameters $\kappa = \{1.01, 1.05, 1.2\}$, $Q_{\mathsf{No}} = 200$, $M = 10$, $\tilde{D}_{\max} = +\infty$, $P(t) \sim \mathscr{U}(0,1)$, $W(t) = P(t)$, $\Delta t = 0.02$, $J(0) \in [10, 200]$, and $R(t) = 0 \; \forall \, t$. The linear inequalities used to approximate (2.4) in $[Q_{\mathsf{No}}, \tilde{D}_{\max}]$ are computed for each value of κ according to the method described in Appendix A.1. We then compare the performance of the strategy based on calculus of variations with the one of existing proposals. The existing energy management strategies are based on dynamic

programming [62] or linear programming techniques [67], and ignore the non-linear relationship between $D(t)$ and $\tilde{D}(t)$. In Fig. 2.8, we have plotted the optimal value of $\int_0^H P(t)D(t)dt$ against $J(0)$, the energy initially available in the storage system. As observed, if the storage device is nearly linear, i.e. $\kappa \to 1^+$, then the performance gap between the proposed strategy and the existing in the literature is negligible. However, if $\kappa > 1$, then the proposed strategy outperforms the ones in the literature. The performance gap grows with κ. In works such as [62] and [67] the performance metric is the final energy cost, and hence the cost function is non-increasing with respect to the storage capacity. In contrast, in Fig. 2.8 we plot the savings obtained with both the proposed and existing strategies, hence the curves are non-decreasing with respect to the storage capacity.

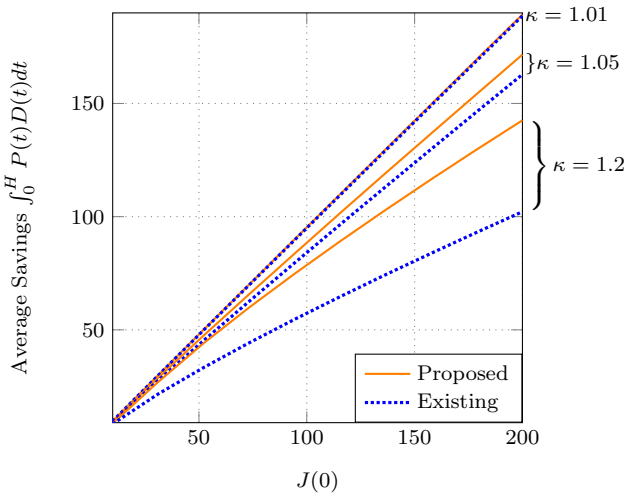

Figure 2.8: Comparison with existing works. Energy savings ($) versus energy initially available in the storage $J(0)$.

2.5.5 Further Insights

In Fig. 2.9 we show the optimal discharging profile obtained by using calculus of variations for the price trajectory $P(t) = \sin(10t) + 1$, and assuming different values of κ.

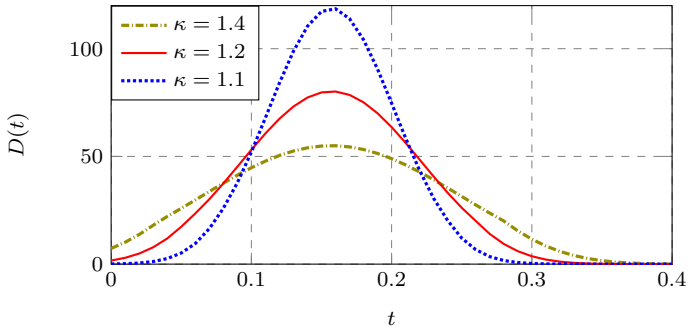

Figure 2.9: Optimal discharging profile obtained by using calculus of variations, while varying Peukert's exponent κ.

Since the function $\sin(10t)+1$ is periodic, only half of the discharging operation is shown, the other half is similar. As observed, the closer is κ to 1, the sharper is the discharging profile. This result follows because the power loss associated with Peukert's effect is negligible when $\kappa \to 1^+$, and the optimization strategy encourages leveraging high pricing periods.

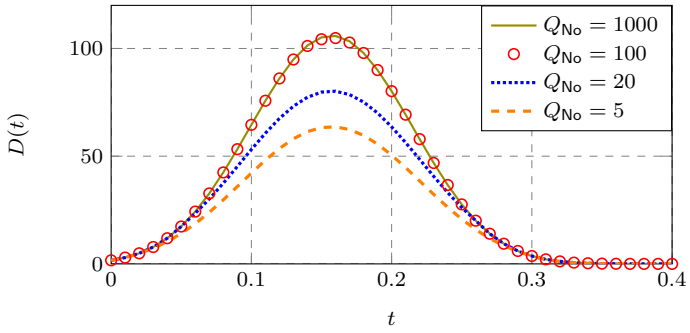

Figure 2.10: Optimal discharging profile obtained by using calculus of variations, while varying Q_{No}, the nominal output power of the storage device.

In Fig. 2.10 we show the optimal discharging profile obtained by using calculus of variations for the price trajectory $P(t) = \sin(10t)+1$, and assuming different values of Q_{No}. As observed, not always increasing Q_{No} results in larger instantaneous power withdrawals, even during peak pricing periods. The expression for optimal $D(t)$ in terms of Q_{No} diverges as $Q_{\mathsf{No}} \to \infty$. However, it does not mean that the optimal $D(t)$

can be increased unlimitedly because it also has to satisfy the constraint (2.21).

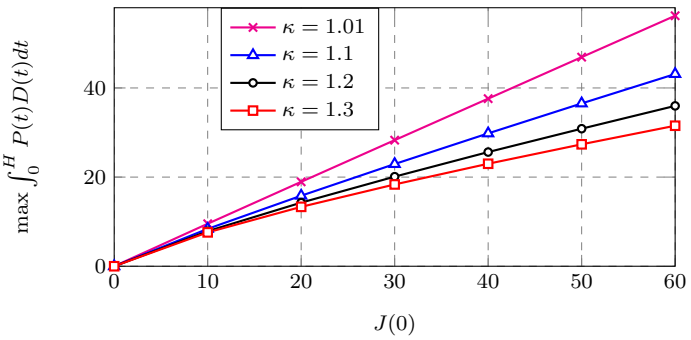

Figure 2.11: Performance of the strategy based on calculus of variations when Peukert's exponent takes on different values.

Considering random energy prices drawn from a standard uniform distribution, in the following we investigate the effect of κ and Q_{No} in the average optimal value of $\int_0^H P(t)D(t)dt$, as we vary $J(0)$. Again, we consider the following simulation parameters: $Q_{\mathsf{No}} = 20$, $\tilde{D}_{\max} = 120$, $\kappa = 1.2$, and we average over ten thousand realisations. In Fig. 2.11 we have plotted the average optimal value of $\int_0^H P(t)D(t)dt$ obtained when the optimal $D(t)$ is determined through calculus of variations, and the value of $J(0)$ increases from 0 to 60. As observed, the relationship between the value of $\int_0^H P(t)D(t)dt$ and $J(0)$ becomes closer to a linear relationship as $\kappa \to 1$, which is expected because the non-linear effects fade as $\kappa \to 1$.

In Fig. 2.12 we have plotted the average optimal value of $\int_0^H P(t)D(t)dt$ obtained when the optimal $D(t)$ is determined through calculus of variations, and the value of $J(0)$ increases from 0 to 80. To obtain the lines in Fig. 2.12 we have considered $\kappa = 1.2$. As observed, increasing Q_{No} increases the optimal $\int_0^H P(t)D(t)dt$ up to a point where it is no longer necessary to have a larger Q_{No} to avoid the losses derived from Peukert's effect.

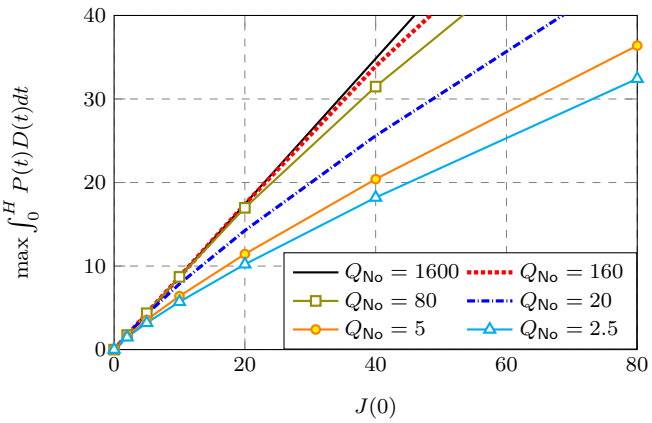

Figure 2.12: Performance of strategy using calculus of variations, for varying Q_{No}, nominal output power of storage device.

2.6 Summary

Assuming dynamic electricity pricing, we have formulated a mathematical problem to minimize the expenditure incurred by a non-deferrable load facility over a finite planning horizon. We have assumed that the facility is equipped with a renewable energy harvester and a storage device. Moreover, our storage model has taken into account the non-linear relationship between the discharging rate and the remaining charge at all times.

We have then solved the constrained optimization problem by using three methods: discretisation and linearisation, evolutionary strategies, and calculus of variations. The performance of the solution obtained through discretisation and linearisation depends on the sampling frequency, and the number of linear inequalities employed. The method based on evolutionary strategies uses an iterative randomized search, and delivers potentially different results in each run. However, it can provide acceptable results with as few as fifty iterations. The method based on calculus of variations provides an analytical solution, which can be expressed in closed form if the discharging model allows it.

The simulation results, which assumed a discharging model based on Peukert's Law,

have shown agreement between the three methods, and provided the following insights:

- The three proposed strategies achieve comparable performance. However, the strategy based on linearisation and discretisation in time requires an adequate sampling rate, and a fair number of linear inequalities. The more linear inequalities are considered, the more accurate is their representation of the non-linear relationship between $D(t)$ and $\tilde{D}(t)$, and the higher its performance. The method based on evolutionary strategies can be tuned to incur different computational costs, either by varying the sampling rate, or the number of generations. However, it does not guarantee the optimality of the solution obtained, and its results can vary across runs. The strategy based on calculus of variations is able to obtain an acceptable performance and does not require the execution of an iterative algorithm. Hence, it has a clear advantage over the other two.

- The strategies available in the literature disregard the nonlinearity of the storage device and hence incur a performance loss. The proposed strategies outperform the state of the art, especially when the storage device exhibits high non-linearity, e.g. when Peukert's exponent is strictly larger than 1.

- Increasing the efficiency of the storage system enhances the performance of the proposed strategies. The theoretical upper bound is determined by the results obtained when the storage device is lossless and linear.

- In general, increasing the nominal output power of the storage device leads to a performance enhancement, because it widens the linear region of operation, and thus reduces the losses derived from non-linear effects such as Peukert's. However, this performance gain is curbed at some point, a result that follows because the total energy discharged over the optimization horizon is limited. This result can provide

an indication for proper storage sizing and design, especially because it shows the existence of a critical storage capacity, above which no further improvement can be achieved.

It is worth emphasizing the following:

- When Peukert's model was applied, the relaxation introduced to obtain closed-form analytical solutions did not lead to a considerable performance loss, at least for the values of κ, the Peukert's exponent, that fall within its practical limits.
- The proper storage initialization led to a significant simplification of the problem because it allowed us to disregard the causality constraint. This in turn led us to find analytical results by using optimization techniques in continuous time.
- It is encouraging to see that a randomized search, which starts from a flat discharging profile, is, within an acceptable number of iterations, able to achieve a result which is very similar to the one obtained analytically.

In the optimization problem formulated in this chapter we have enforced continuity of the energy stored over subsequent optimization periods. In the next chapters we will consider a more general setting, in which the energy left unused at the end of the optimization horizon is given a value, and will formulate the optimization problem in terms of such a value.

Chapter 3

Online Energy Management Strategies

In this chapter we propose online strategies to minimize the energy bill incurred by a non-deferrable load facility over a finite planning horizon. We assume that the facility is equipped with a renewable energy harvester and a storage device. Unlike the solutions in Chapter 2, the strategies proposed in this chapter do not require exact knowledge of the future renewable energy arrivals or the future power requirements of the facility.

Initially, we propose an online algorithm that uses estimates of future renewable energy arrivals and power requirements, which are obtained through forecasting techniques such as a first-order linear predictor, or an auto-regressive integrated moving average (ARIMA) time series model. We also propose a time-inhomogeneous Markov chain model to predict renewable energy arrivals, which we later incorporate in our proposed forecasting-based algorithm.

In this chapter, we also propose an online strategy which does not rely on estimates of future renewable energy arrivals. The proposed strategy is based on continuous-time optimal control theory, does not require extensive computations, and, unlike existing works, takes into account the non-linearity of the discharging operation.

3.1 Contributions

The two major contributions of this chapter are:

- We propose an online strategy to minimize the expenditure incurred by a non-

deferrable load facility over a finite planning horizon. The facility is equipped with a renewable energy harvester and a storage device. The proposed strategy is designed by assuming a general model for the storage device, which is able to account for the non-linear relationship between the discharging rate and the remaining charge. The proposed strategy uses estimates of future renewable energy arrivals and future load requirements, which are obtained through forecasting techniques such as a first-order linear predictor or an ARIMA time series model. We also introduce a time-inhomogeneous Markov chain model to forecast renewable energy arrivals. The proposed model has some advantages over existing prediction strategies, since it is simpler, uses bounded random variables[1], and can be continuously improved with new observations.

- We propose an online strategy that does not require estimates of future renewable energy arrivals, and is based on analytical results, thus making it simpler than the strategies based on statistical forecasting. To devise this strategy, we solve a constrained optimization problem in continuous time. We specifically minimize a non-linear functional, which depends on the control signal, and the total renewable energy stored over time. By using a continuous-time optimization approach we can obtain analytical solutions, which we use to devise an online strategy that does not require extensive computations. The proposed strategy is model-independent,[2] and has significantly less reliance on renewable energy forecasts, which can be used to further reduce the complexity of existing solutions.

[1] Signals with additive Gaussian noise have unbounded support.

[2] The proposed strategy is not affected by the statistical distribution of the renewable energy generation process.

3.2 System Model

For completeness, we state the fundamental assumptions in this section. The system model is the same as the one described in Sec. 2.2.

3.2.1 General Setup

We consider a facility which is permanently connected to the grid as represented in Fig. 2.1 by a base station. The facility is equipped with a storage device, and a renewable energy harvester represented in Fig. 2.1 by a solar panel. The renewable energy management unit (REMU) is in charge of implementing the designed power flows between the different entities in the system.

The power consumed by the facility is assumed to be non-deferrable, and denoted by $L(t)$. The renewable power harvested is $R(t)$, and the effective (after losses) power drawn from the storage device is $D(t)$. The planning horizon is $[0,H]$, where H can be made arbitrarily large, as long as the physical properties of the components in the system remain constant in $[0,H]$.

3.2.2 Electricity Pricing Scheme

We consider time-varying energy prices denoted by $P(t)$. Moreover, the REMU is allowed to sell renewable energy to the utility following a net metering policy. As in Chapter 2, the renewable energy is sold back to the utility at rates denoted by $W(t)$.

The net energy bill χ incurred over the period $[0,H]$, under this linear pricing scheme is thus:

$$\chi = \int_0^H P(t)\left[L(t) - X(t)\right] - W(t)Y(t)dt, \tag{3.1}$$

where $X(t)$ is the power drawn from the storage to feed the local load, and $Y(t)$ is the renewable power injected into grid. Again, the total power drawn from the storage

device is $D(t) = X(t) + Y(t)$.

3.2.3 Energy Storage Device

Let $J(t)$ denote the energy stored at time t, and $\tilde{D}(t)$ denote the power drained from the storage device when $D(t) = X(t) + Y(t)$ is effectively drawn from its terminals. Then $J(t)$ can be determined as follows:

$$J(t) = \int_0^t \left[\varsigma R(x) - \tilde{D}(x)\right] dx + J(0), \tag{3.2}$$

where $0 \leq \varsigma \leq 1$ is the charging efficiency, and $J(0)$ is the energy initially stored in the system. The storage device is only charged with renewable energy, for the reason explained in Sec. 2.2.3.

Let Ψ denote the available storage capacity, then $0 \leq J(t) \leq \Psi$ holds at all times. The first inequality $0 \leq J(t)$ implies:

$$\int_0^t \tilde{D}(x)dx \leq \varsigma \int_0^t R(x)dx + J(0), \ \forall\, t, \tag{3.3}$$

a condition often referred to as the causality constraint. Moreover, $J(t) \leq \Psi$ imposes the following constraint on $\tilde{D}(t)$:

$$\int_0^t \tilde{D}(x)dx \geq \varsigma \int_0^t R(x)dx + J(0) - \Psi, \ \forall\, t. \tag{3.4}$$

As in Chapter 2, the relationship between $\tilde{D}(t)$ and $D(t)$ is assumed arbitrary:

$$\tilde{D}(t) = \mathscr{F}\left[D(t)\right], \tag{3.5}$$

where $\mathscr{F}(\cdot)$ is a continuous, convex, and strictly increasing function defined in $[0, \infty)$.

Again, if we want to use Peukert's model, we define $\mathscr{F}\left[D(t)\right]$ as in Eq. (2.4). And if we need to use simplified Peukert's model, we set $\mathscr{F}\left[D(t)\right]$ as in Eq. (2.5).

To preserve the health of the battery system, and define its region of operation, the

maximum discharging power allowed at any time t is $\tilde{D}_{\max}$, i.e. $\tilde{D}(t) \leq \tilde{D}_{\max}\ \forall\, t$.

3.3 Problem Formulation and Genie-Aided Solution

We consider a more general version of the problem formulated in Sec. 2.3. In the following formulation we account for the value of the residual energy in the storage device at the end of the planning horizon. This generalizes the formulation in Sec. 2.3, which simply forces the residual energy to be equal to the energy initially stored in the system $J(0)$.

3.3.1 Continuous-Time Formulation

We let K denote the unit price of the energy remaining in the storage device at the end of the optimization horizon, i.e. we assume that the energy left unused at $t = H$ has a bequest value of $KJ(H)$. Then, we cast the energy bill minimization problem as follows:

$$\text{P3.0:} \quad \min_{X(t),Y(t)} \qquad \chi - KJ(H)$$

s.t. $X(t) \leq L(t)$, $\tilde{D}(t) \leq \tilde{D}_{\max}\ \forall\, t$, and (3.3)–(3.4). In P3.0, $D(t) = X(t) + Y(t)$ and $\tilde{D}(t)$ are related according to Eq. (3.5), and $\tilde{D}(t)$ and $J(t)$ are related according to Eq. (3.2).

3.3.2 Discrete-Time Formulation

We can obtain an approximate solution to P3.0 by introducing discretisation, i.e. by sampling the functions $P(t)$, $L(t)$, $R(t)$, $D(t)$, and $\tilde{D}(t)$ at a uniform rate of $1/\Delta t$ samples per unit of time. We specifically consider N samples, i.e. $\Delta t = \frac{H}{N}$, and denote the uniformly sampled vectors by lower case bold letters as follows: $\mathbf{p}$, $\boldsymbol{\ell}$, $\mathbf{r}$, $\mathbf{d}$, $\tilde{\mathbf{d}} \in \mathbb{R}_+^N$. That is, for $k \in \{1,2,\ldots,N\}$, we have:

$$\begin{aligned} p(k) = P(k\Delta t),\ \ell(k) = L(k\Delta t),\ d(k) = D(k\Delta t), \\ j(k) = J(k\Delta t),\ \tilde{d}(k) = \tilde{D}(k\Delta t),\ r(k) = R(k\Delta t). \end{aligned} \tag{3.6}$$

Therefore, in the discrete domain, P3.0 can be cast as follows:

$$\text{P3.1:} \quad \min_{\mathbf{x},\mathbf{y}} \qquad \Delta t \left[\sum_{k=1}^{N} p(k) \left[\ell(k) - x(k) \right] - w(k) y(k) \right] - KJ(H),$$

s.t. $d(k) = x(k) + y(k)$, $x(k) \leq \ell(k)$, $\forall\, k$, and:

$$0 \leq j(k) \leq \Psi \tag{3.7a}$$

$$\tilde{d}(k) \leq \tilde{D}_{\max} \tag{3.7b}$$

$$d(k) = \mathscr{F}^{-1}\left[\tilde{d}(k)\right],\ k \in \{1,\ldots,N\}. \tag{3.7c}$$

As explained in Chapter 2, $\mathscr{F}^{-1}(\cdot)$ can be approximated with a piece-wise linear function, and hence Eq. (3.7c) can be replaced with a set of linear inequalities.

3.3.3 Genie-Aided Solution

In the following we derive the matrix formulation of P3.1, which is required to handle the problem to a solver, and thus obtain a genie-aided solution. Let $\mathbf{A}$ denote a lower triangular matrix with $A(i,j) = 1\ \forall\, i \geq j$, and $\eta = J(H)$, then we can cast P3.1 in matrix form as follows:

$$\text{LP3.1:} \quad \max_{\mathbf{x},\mathbf{y},\mathbf{d},\tilde{\mathbf{d}},\eta} \quad \Delta t \left(\mathbf{p}^T\mathbf{x} + \mathbf{w}^T\mathbf{y}\right) + K\eta$$

s.t. $d(k) = x(k) + y(k)$, $x(k) \leq \ell(k)$, $\tilde{d}(k) \leq \tilde{D}_{\max}$, $\forall\, k$, and:

$$\begin{pmatrix} -\Delta t\mathbf{A} & \mathbf{0} & \mathbf{0} \\ \Delta t\mathbf{A} & \mathbf{0} & \mathbf{0} \\ -\alpha_1\mathbf{I} & \mathbf{I} & \mathbf{0} \\ -\alpha_2\mathbf{I} & \mathbf{I} & \mathbf{0} \\ \vdots & \vdots & \vdots \\ -\alpha_M\mathbf{I} & \mathbf{I} & \mathbf{0} \\ \Delta t\mathbf{1}^T & 0,\ldots,0 & 0,\ldots,1 \end{pmatrix} \begin{pmatrix} \tilde{\mathbf{d}} \\ \mathbf{d} \\ \eta \end{pmatrix} \preceq \begin{pmatrix} \Psi - J(0) - \varsigma\Delta t\mathbf{A}\mathbf{r} \\ J(0) + \varsigma\Delta t\mathbf{A}\mathbf{r} \\ -\beta_1\mathbf{1} \\ -\beta_2\mathbf{1} \\ \vdots \\ -\beta_M\mathbf{1} \\ \varsigma\Delta t\mathbf{1}^T\mathbf{r} + J(0) \end{pmatrix} \tag{3.8}$$

3.4 Forecasting Techniques

In this section we briefly describe some forecasting techniques that can be part of the proposed online strategy. For ease of exposition, we explain how these techniques can be used to predict future renewable energy arrivals. Similar methods can be used to estimate the energy consumption of the facility within the entire planning horizon. Advanced forecasting techniques can also be incorporated in the proposed algorithm.

3.4.1 First-Order Linear Predictor

Let $\mathbf{r} \in \mathbb{R}_+^N$ denote renewable power arrivals over N time slots. Then, to use a first-order linear predictor we assume that $\mathbf{r}$ evolves according to the following model:

$$r(k+1) = \mathsf{coeff}_k r(k) + \mathsf{noise}, \tag{3.9}$$

where $\mathsf{coeff}_k \in \mathbb{R}_+$, and noise is a random variable whose distribution can be chosen to reflect practical properties of $r(k+1)$ such as bounds. The coefficient coeff_k can be obtained from historical records. In particular, if $\mathbb{E}[\mathsf{noise}] = 0$, taking expectation on both sides of (3.9) yields:

$$\mathsf{coeff}_k = \frac{\mathbb{E}[r(k+1)]}{\mathbb{E}[r(k)]}. \tag{3.10}$$

Hence, if we assume that the model parameters are known, i.e. $\mathsf{coeff}_1, \ldots, \mathsf{coeff}_{N-1}$, then we can estimate $r(k+1)$ as the argument of:

$$\text{P3.2:} \quad \min_{\hat{r}(k+1)} \quad \mathbb{E}\left[\left(r(k+1) - \hat{r}(k+1) \right)^2 \mid r(k) \right].$$

The solution to P3.2 can be obtained by recognizing that the objective function is convex in $\hat{r}(k+1)$. Thus expanding it, and applying linearity yields:

$$\mathbb{E}\left[\left(r(k+1) - \hat{r}(k+1) \right)^2 \mid r(k) \right] = \mathbb{E}\left[r(k+1)^2 \mid r(k) \right] - 2\hat{r}(k+1)\mathbb{E}\left[r(k+1) \mid r(k) \right] + \hat{r}(k+1)^2.$$

The first-order optimality condition $\frac{\partial}{\partial \hat{r}(k+1)} \mathbb{E}\left[(r(k+1) - \hat{r}(k+1))^2 \mid r(k) \right] = 0$ implies:

$$\hat{r}(k+1) = \mathbb{E}[r(k+1) \mid r(k)] = \mathsf{coeff}_k r(k) + \mathbb{E}[\mathsf{noise}]. \tag{3.11}$$

To estimate $r(k+2)$ when $t = k$, we use our estimate of $r(k+1)$, i.e.

$$\hat{r}(k+2) = \mathsf{coeff}_{k+1} \hat{r}(k+1) + \mathbb{E}[\mathsf{noise}].$$

We name this approach *first-order linear predictor* because the model assumes that the mean values of adjacent sample points are linearly related, i.e. the mean of the output depends linearly on the mean of the previous sample. Unlike the first-order standard autoregressive process, the parameters in our model change over time, i.e. in general we have $\mathsf{coeff}_1 \neq \mathsf{coeff}_2 \neq \ldots \neq \mathsf{coeff}_{N-1}$.

3.4.2 Auto-Regressive Integrated Moving Average Time Series

We explained the basics of the Auto-Regressive Integrated Moving Average (ARIMA) model in Sec. 1.2.5. In the following we briefly describe the forecasting approach undertaken when the underlying model is assumed to be an ARIMA(m,n,q) process. In this thesis we will assume that the model has been identified from existing data, and hence we do not discuss model identification techniques. To implement our proposed strategies we resort to identification algorithms built-in to numerical software such as R [178].

As explained in Sec. 3.4.1, to minimize the mean-squared error, the estimates must be determined by computing the expected value of the output conditioned on the information available at the current time. To write the forecasting equation, we first define

the following auxiliary variables:

$$r_{\mathsf{diff}}(k) = \begin{cases} r(k), & n = 0 \\ r(k) - r(k-1), & n = 1 \\ r(k) - r(k-1) - [r(k-1) - r(k-2)] = r(k) - 2r(k-1) + r(k-2), & n = 2 \\ \vdots & \end{cases}$$

where $n \in \mathbb{N}$ is the second parameter in the ARIMA(m,n,q) model. Then, assuming that we have exact knowledge of the model parameters, we can write the forecasting equation as follows:

$$\begin{aligned} \hat{r}_{\mathsf{diff}}(k) &= \mathbb{E}[r_{\mathsf{diff}}(k) \mid r_{\mathsf{diff}}(k-1), \ldots, r_{\mathsf{diff}}(0)] \\ &= \eta_0 + \eta_1 r_{\mathsf{diff}}(k-1) + \ldots + \eta_m r_{\mathsf{diff}}(k-m) \\ &\quad + \theta_1 \omega(k-1) + \theta_2 \omega(k-2) + \ldots + \theta_q \omega(k-q), \end{aligned} \tag{3.12}$$

where $\boldsymbol{\omega}$ is an i.i.d. Gaussian process, i.e. $\omega(i) \sim \mathcal{N}(0, \sigma^2)$.

3.4.3 Time-Inhomogeneous Markov Chain

We propose a time-inhomogeneous Markov chain model to forecast renewable energy arrivals.

Definition

Let $\mathcal{S} = \{E_1, E_2, \ldots\}$ denote the finite state space, and $E_x,\ x \in \{1, \ldots, |\mathcal{S}|\}$ be defined by dividing the output of the energy harvester into $|\mathcal{S}|$ segments. Let Λ denote the maximum power that the energy harvester can deliver, and $s(k)$ denote the state in the kth time slot. Then $s(k) = E_x$, with $x \in \{1, \ldots, |\mathcal{S}| - 1\}$, if and only if $r(k) \in \left[(x-1)\frac{\Lambda}{|\mathcal{S}|}, x\frac{\Lambda}{|\mathcal{S}|}\right)$, and $s(k) = E_{|\mathcal{S}|}$ if and only if $r(k) \in \left[(|\mathcal{S}| - 1)\frac{\Lambda}{|\mathcal{S}|}, \Lambda\right]$. The transition probabilities in the Markov chain described above are assumed to be time-varying to reflect inter-hour dependencies in the renewable energy generation.

Use in Forecasting

Let $\hat{r}(k)$ denote the estimated power arrival at time slot k, then we choose $\hat{r}(k)$ as the argument of the following optimization problem:

$$\text{P3.3:} \quad \min_{\hat{r}(k)} \quad \mathbb{E}\left[\left(r(k)-\hat{r}(k)\right)^2 \mid s(k-1)=E_x\right].$$

To find E_x we simply determine in which interval the recorded $r(k-1)$ falls. If $r(k-1)$ is not yet available, we use $\hat{r}(k-1)$ instead:

$$E_x = \begin{cases} E_1, & \text{if } 0 \le \hat{r}(k-1) < \frac{\Lambda}{|\mathcal{S}|} \\ E_2, & \text{if } \frac{\Lambda}{|\mathcal{S}|} \le \hat{r}(k-1) < 2\frac{\Lambda}{|\mathcal{S}|} \\ \vdots & \\ E_{|\mathcal{S}|}, & \text{if } (|\mathcal{S}|-1)\frac{\Lambda}{|\mathcal{S}|} \le \hat{r}(k-1) \le \Lambda \end{cases} \tag{3.13}$$

To compute $\mathbb{E}\left[\left(r(k)-\hat{r}(k)\right)^2 \mid s(k-1)=E_x\right]$ we assume that $r(k-1) \mid s(k-1)=E_x$ is uniformly[3] distributed in the interval $\left[(x-1)\frac{\Lambda}{|\mathcal{S}|}, x\frac{\Lambda}{|\mathcal{S}|}\right)$. Therefore, the conditional distribution of $r(k) \mid s(k-1)=E_x$ can be obtained by using the law of total probability. Specifically, to simplify notation let $r_k := r(k)$, hence $r_k \mid \{s(k)=E_x\} \sim \mathscr{U}\left([x-1]\frac{\Lambda}{|\mathcal{S}|}, x\frac{\Lambda}{|\mathcal{S}|}\right)$, and by the law of total probability, we have:

$$f_{r_k}(r_k) = \begin{cases} \frac{|\mathcal{S}|}{\Lambda} P\left(s(k)=E_1\right), & 0 \le r_k < \frac{\Lambda}{|\mathcal{S}|} \\ \frac{|\mathcal{S}|}{\Lambda} P\left(s(k)=E_2\right), & \frac{\Lambda}{|\mathcal{S}|} \le r_k < \frac{2\Lambda}{|\mathcal{S}|} \\ \vdots & \\ \frac{|\mathcal{S}|}{\Lambda} P\left(s(k)=E_{|\mathcal{S}|}\right), & \frac{\Lambda(|\mathcal{S}|-1)}{|\mathcal{S}|} \le r_k \le \Lambda \end{cases} \tag{3.14}$$

Proposition 3.4.1. *Let r_k be distributed according to (3.14), then*

[3]The uniform distribution reflects total uncertainty about $r(k)$ given that we know its lower and upper bounds.

$\mathbb{E}\left[(r_k - \hat{r}_k)^2 \mid s(k-1) = E_x\right]$ *attains its minimum at:*

$$\hat{r}_k = \frac{\Lambda}{2|\mathcal{S}|} \sum_{i=1}^{|\mathcal{S}|} [2i-1]\, P\left(s(k) = E_i \mid s(k-1) = E_x\right). \tag{3.15}$$

Proof. See Appendix B.5. ■

3.5 Online Optimization with Forecasts

In this section we propose an online strategy to solve P3.1. The proposed strategy uses forecasting techniques to estimate future renewable energy arrivals and future energy consumption.

3.5.1 Forecasts Update Rate

Our strategy uses predictions at an intra-day level. We estimate $\mathbf{r}$ and $\boldsymbol{\ell}$ at the beginning of the optimization horizon, and update the predictions only when the observations (measurements) deviate from the forecasts by a given threshold. We measure these deviations by computing the relative forecast errors, defined as follows: Let $r(k)$ denote the energy arrival at time slot k, and $\ell(k)$ the energy consumed by the facility in the same time slot. If $\hat{r}(k)$ and $\hat{\ell}(k)$ denote respectively our estimates of $r(k)$ and $\ell(k)$, then, the relative forecast errors are:

$$\mathsf{rfe}_r = \frac{|r(k) - \hat{r}(k)|}{r(k)}, \tag{3.16}$$

and

$$\mathsf{rfe}_\ell = \frac{|\ell(k) - \hat{\ell}(k)|}{\ell(k)}. \tag{3.17}$$

Notice that rfe_r and rfe_ℓ are updated in each time slot. The acceptable values of rfe_r and rfe_ℓ are respectively denoted by ε_r and ε_ℓ.

3.5.2 Constraints Handling

In the following we introduce a policy to handle the causality constraint, and the constraint derived from the limited storage capacity. Let $\mathbf{d}^*$ denote the optimal $\mathbf{d}$, obtained by solving LP3.1 using estimates of $\mathbf{r}$ and $\boldsymbol{\ell}$, then $d^*(k)\Delta t$ is the optimal renewable energy to be drawn from the battery within the kth time slot. We avert wastage of renewable energy by implementing the following policy: If $\mathsf{overflow} = \Psi - [j(k-1) + r(k)\Delta t - d^*(k)\Delta t] > 0$, then the energy drawn from the storage device is increased[4] to $d^*(k)\Delta t + \mathsf{overflow}$. Similarly, if $\mathsf{overflow} < 0$, then the energy discharged is decreased to $d^*(k)\Delta t + \mathsf{overflow}$.

Next, we discuss the approaches to handle the occurrence of negative outputs in the stochastic models for the renewable energy arrivals, and the power consumption. Clearly, power and energy quantities must be positive. However, the time series models explained in Sec. 3.4 may lead to negative outputs when the stochastic component of the model is assumed of unbounded support. This is the case of the ARIMA(m,n,q) model, where $\boldsymbol{\omega}$ is a Gaussian i.i.d. random process. There are two ways to handle this issue:

1. By using a mathematical transformation: A mathematical transformation can lead to a simplified time series model, or constrain the forecast to stay positive [178]. The following is the procedure used in statistics to ensure that time series models do not return negative values:

   A. Apply the Box-Cox transformation. The Box-Cox transform with parameter λ

[4] If $d^*(k)\Delta t + \mathsf{overflow} > \ell(k)\Delta t$ then, the excess renewable energy is injected into the grid.

is defined as follows:

$$r_{\mathsf{trans}}(k) = \begin{cases} \log[r(k)] & \text{if } \lambda = 0 \\ \frac{[r(k)]^{\lambda}-1}{\lambda} & \text{otherwise} \end{cases}. \tag{3.18}$$

As seen, if $\lambda = 0$ then a logarithmic[5] transformation is used, whereas if $\lambda \neq 0$, then a power transformation is used [178]. In this thesis we use a logarithmic transformation, i.e. a Box-Cox transformation with $\lambda = 0$.

B. Adjust the ARIMA model to the Box-Cox transformed data. The model identification is performed on the transformed data. The best model is chosen according to criteria such as the Akaike information criterion (AIC). This step can be completed in R by using built-in functions such as `auto.arima()`.

C. Forecast using the obtained model in Step B. The estimates can be obtained by using the forecasting equation (3.12).

D. Back-transform the data to the original scale. This step is required to have the estimated quantities in the original units of measurement.

2. By imposing bounds on the outputs: When generating the corresponding random samples we can impose a lower and an upper bound on the output. In this way, we ensure that the generated samples are within the practical limits. The disadvantage of this approach is that further estimation errors are introduced when the forecasting equations are not updated to account for bounded innovations (errors).

3.5.3 Proposed Algorithm

With the considerations discussed in Secs. 3.5.1 and 3.5.2, we propose the strategy shown in **Algorithm** 2. The following is a description of the key steps in the algorithm:

[5]The default base for the logarithmic operation is Euler's number e.

- *Training of the statistical model:* In this step we use historical records to identify the statistical models. We specifically use maximum likelihood estimators implemented in functions such as `auto.arima()` and `markovchainFit()`. More details on these model identification algorithms can be found in [179] and [180].

- *Initialize the estimates* $\hat{\mathbf{r}}$ *and* $\hat{\boldsymbol{\ell}}$*:* We determine our first estimates of $\mathbf{r}$ and $\boldsymbol{\ell}$ by using mean values or observations from the previous day.

- *Solve the optimization problem using the estimates* $\hat{\mathbf{r}}$ *and* $\hat{\boldsymbol{\ell}}$*:* We solve the optimization problem by using the initial estimates in order to determine the first course of action before the planning horizon starts.

- *Updating of estimates and decision variables:* As observations (measurements) are recorded, we update the estimates and the decision variables. The decision variables are updated by solving the optimization problem with the newly available information and the refined estimates. If the measurements do not deviate from the predictions significantly we continue using the same estimates and do not update the decision variables. In this way, the number of mathematical operations required by the algorithm can be reduced.

- *Battery state estimation and adjustment of discharging quantity:* The decision variables are updated in each of the time slots if they lead to any constraint violation.

- *Termination:* The algorithm finalizes when the number of time slots has covered the entire planning horizon.

Algorithm 2 Forecasting-based online optimization algorithm

Train the statistical models for $\mathbf{r}$ and $\boldsymbol{\ell}$
Initialize the estimates $\hat{\mathbf{r}}$ and $\hat{\boldsymbol{\ell}}$
Solve optimization problem using $\hat{\mathbf{r}}$ and $\hat{\boldsymbol{\ell}}$
Estimate $j(0)$
for $k = 1$ **to** N **do**
  Measure $r(k)$ and $\ell(k)$
  if $\mathsf{rfe}_r > \varepsilon_r$ OR $\mathsf{rfe}_\ell > \varepsilon_\ell$ **then**
    if $\mathsf{rfe}_r > \varepsilon_r$ **then**
      Update $\hat{\mathbf{r}}$
    end if
    if $\mathsf{rfe}_\ell > \varepsilon_\ell$ **then**
      Update $\hat{\boldsymbol{\ell}}$
    end if
    Solve optimization problem using updated estimates
  end if
  Update $\mathbf{j}$: $j(k) = j(k-1) + \Delta t \left[\varsigma r(k) - \tilde{d}(k)\right]$
  Adjust $d(k)$ if $j(k) > \Psi$ or $j(k) < 0$
end for

3.6 Online Optimization without Forecasts

We propose an online strategy to solve P3.1, which does not require predictions of future renewable energy arrivals or the execution of iterative routines. In some cases, the decision variables can be optimized by plugging the available information into a formula. In the more general case, the optimal operation is determined by computing the roots of a function defined by the optimality condition.

The proposed strategy is based on Pontryagin's Maximum Principle [25]. Pontryagin's Maximum Principle is a set of necessary conditions for a constrained control trajectory, i.e. $D(t)$, to maximize a functional such as (3.1), which also depends on $J(t)$, a dynamic system that evolves according to (3.2). Thus, to use Pontryagin's Maximum Principle, we write (3.2) in differential form. Differentiating both sides of (3.2) yields:

$$\frac{dJ}{dt} = \varsigma R(t) - \tilde{D}(t). \tag{3.19}$$

The solution to (3.19) uniquely determines $J(t)$ for any given initial condition $J(0)$.

3.6.1 Constraints Relaxations

The following are propositions that describe some simplifications introduced and their implications. These simplifications are required to make the optimization problem P3.1 tractable. As a result, the proposed strategy can only be applied in scenarios in which these simplifications are justified.

Proposition 3.6.1. *Let $J(0) > 0$, $J(t)$ satisfy (3.19) with $R(t) \geq 0 \ \forall \ t$, and $\tilde{D}(t) = \theta(t)J(t)$, for any non-negative function $\theta(t)$. Then $J(t) > 0, \ \forall \ t$.*

Proof. The solution to (3.19) in terms of $\theta(t) = \frac{\tilde{D}(t)}{J(t)}$ can be obtained by multiplying both sides of (3.19) by the integrating factor:

$$F(t) = \exp\left(\int \theta(t)dt\right), \tag{3.20}$$

which leads to:

$$F(t)\left[\frac{d}{dt}J(t) + \theta(t)J(t)\right] = \varsigma R(t)F(t). \tag{3.21}$$

By noting that $\frac{d}{dt}F(t) = \theta(t)F(t)$, the equation (3.21) reduces to:

$$\frac{d}{dt}\left[J(t)F(t)\right] = \varsigma R(t)F(t). \tag{3.22}$$

Clearly, the solution to (3.22) is:

$$J(t) = \frac{\varsigma \int_0^t R(x)\exp\left[\int \theta(x)dx\right]dx}{\exp\left[\int \theta(t)dt\right]} + J(0). \tag{3.23}$$

Therefore, if $R(t) \geq 0 \ \forall \ t$, and $J(0) > 0$ then $J(t) > 0 \ \forall \ t$ regardless of the choice of $\theta(t)$. ■

Proposition 3.6.2. *Let $\Psi \geq J(0) + \varsigma \int_0^H R(x)dx$ and $J(t)$ satisfy (3.19), then $J(t) \leq \Psi \ \forall \ t$.*

Proof. The proof is similar to the proof of Proposition 2.4.2, which can be found in Appendix B.2. We thus briefly summarize the argument: Since $\tilde{D}(t) \geq 0 \; \forall \, t$, we have:

$$\int_0^t \left[\varsigma R(x) - \tilde{D}(x)\right] dx + J(0) \leq J(0) + \varsigma \int_0^H R(x)dx, \; \forall \, t, \tag{3.24}$$

and by adding this inequality to $J(0) + \varsigma \int_0^H R(x)dx \leq \Psi$, we obtain $J(t) \leq \Psi \; \forall \, t$. ■

Finally, for tractability we will assume that $\tilde{D}_{\max}$ is large enough to disregard the constraint (3.7b), and will solve the problem by assuming $W(t) = P(t) \; \forall \, t$.

3.6.2 Simplified Problem and Solution

For ease of notation let $\mathscr{G}(x) = \mathscr{F}^{-1}(x) \; \forall \, x$. Then, using the results in Propositions 3.6.2 and 3.6.1, we cast $P0$ as a savings maximization problem in terms of $\theta(t)$ as follows:

$$\text{P3.4:} \quad \max_{\theta(t)} \quad \int_0^H P(t)\mathscr{G}\left[\theta(t)J(t)\right] dt + KJ(H),$$

st. (3.19). In P3.4 we have ignored the constraints (3.2) and (3.4) following the Propositions 3.6.1 and 3.6.2. The solution to P3.4 can be obtained by using Pontryagin's Maximum Principle as explained in the next theorem:

Theorem 3.6.1. *Let $\Psi \geq \varsigma \int_0^H R(t)dt + J(0)$, $J(0) > 0$, $dJ(t) = \varsigma R(t) - \theta(t)J(t)dt$, $K > 0$, and $J(t) > 0 \; \forall \, t$, then a necessary condition for $\theta(t)$ to maximize $\int_0^H P(t)\mathscr{G}(\theta J)\, dt + KJ(H)$ is:*

$$P(t)\frac{\partial}{\partial \theta}\mathscr{G}(\theta J) = K. \tag{3.25}$$

Moreover, if $\mathscr{G}[x] = Q_{\mathsf{No}}\left[\frac{x}{Q_{\mathsf{No}}}\right]^{\frac{1}{\kappa}}$, with $Q_{\mathsf{No}} > 0$ and $\kappa > 1$, then (3.25) yields:

$$\theta(t) = \theta^*(t) \triangleq \frac{Q_{\mathsf{No}}}{J(t)}\left[\frac{P(t)}{\kappa K}\right]^{\frac{\kappa}{\kappa-1}}. \tag{3.26}$$

Proof. See Appendix B.4. ■

Observations based on the result (3.26):

- The result in Eq. (3.26) indicates that P3.4 can be solved without any knowledge of future renewable energy arrivals when $J(t) > 0 \ \forall \ t$. This is a consequence of the assumed infinite energy storage capacity and the unlimited discharging rate. The result in (3.26) is meant to minimize the losses incurred in the discharging operation, at the time the consumption of renewable energy is spread across $[0,H]$ by using the ratio $\frac{P(t)}{K}$ as a reference. The scheduling criterion only depends on $\frac{P(t)}{K}$ and the storage parameters Q_{No} and κ.

- For the result in Eq. (3.26) to be valid, $J(0)$ and $R(t)$ must be such that $J(t) > 0 \, \forall \, t \ \in [0,H]$. Hence, an interpretation of Eq. (3.26) is that it is meant to continuously allocate the consumption of $J(t)$ in $[t,H)$ for each $t \in [0,H)$. This allocation policy not only spreads the energy consumption to minimize the losses from the discharging operation, but also takes into account the energy prices in $[0,H]$ and the bequest value of $J(H)$ in order to maximize the objective in P3.4. Moreover, since the storage capacity and the discharging rate are unlimited, this optimal discharging policy is not affected by the future state of the storage device or the future renewable energy arrivals.

- The result in Eq. (3.26) is model-independent as it does not depend on the statistical distribution of $R(t)$. Hence, this strategy can be applied independently of the renewable energy source, i.e. it is not restricted to solar energy management systems.

- $\theta^*(t)$ is directly proportional to Q_{No}. In fact, the larger nominal output power the storage device has, the smaller the loss incurred as the linear region of the discharging operation spans from 0 to Q_{No}.

- $\theta^*(t)$ is inversely proportional to $K^{\frac{\kappa}{\kappa-1}}$. The larger K, the less energy is used in $[0,H]$, thus increasing $J(H)$, which is assumed valued at $KJ(H)$.

- A constant pricing function implies a constant consumption rate $\theta(t)J(t)$. The optimal strategy should also minimize the loss derived from the discharging operation.

- The next proposition discusses the impact of the values of K in the optimal discharging profile $\theta^*(t)$:

  Proposition 3.6.3. *If $K > P(t)\ \forall\ t$, $\mathscr{G}[x] = Q_{\mathsf{No}}\left[\frac{x}{Q_{\mathsf{No}}}\right]^{\frac{1}{\kappa}}$, with $Q_{\mathsf{No}} > 0$ and $\kappa \to 1^+$, then $J(H) \to J(0) + \varsigma \int_0^H R(x)dx$, and the optimal $\theta(t)$ satisfies:*

$$\lim_{\kappa \to 1^+} \theta^*(t) = 0\ \forall\ t. \tag{3.27}$$

  Proof. The result in (3.27) follows from:

$$\lim_{\kappa \to 1^+} \frac{Q_{\mathsf{No}}}{J(t)} \left[\frac{P(t)}{\kappa K}\right]^{\frac{\kappa}{\kappa-1}} = 0, \tag{3.28}$$

  which can be shown by noting that $\lim_{\kappa \to 1^+} \left[\frac{P(t)}{\kappa K}\right]^{\frac{\kappa}{\kappa-1}} = 0$. If $\theta^*(t) = 0\ \forall\ t$, then by the energy conservation principle, we have $J(H) = J(0) + \varsigma \int_0^H R(x)dx$. ■

  Proposition 3.6.3 implies that very little power is used during the planning horizon and most of the energy is left for future consumption.

3.7 Numerical Results and Discussion

We present numerical results to draw further insights regarding the performance of the proposed strategies. For concreteness, in this section we will assume that $\mathscr{G}[x]$ is defined according to Peukert's model and will evaluate the impact of using its simplified version $\mathscr{G}[x] = Q_{\mathsf{No}}\left[\frac{x}{Q_{\mathsf{No}}}\right]^{\frac{1}{\kappa}}$, instead of $\mathscr{G}[x] = \min\left\{Q_{\mathsf{No}}\left[\frac{x}{Q_{\mathsf{No}}}\right]^{\frac{1}{\kappa}}, x\right\}$.

Table 3.1: Simulation parameters (online optimization strategies).

H	1
Δt	0.01
$R(t)$	$50\sin(5t-1)+50$
ς	1
κ	1.3
Q_{No}	$\int_0^H R(t)dt$
M	10
$P(t)$	$50\sin(10t)+150$
$W(t)$	$50\sin(10t)+150$
K	111.27
$J(0)$	$\int_0^H R(t)dt$
Ψ	$J(0)+\int_0^H R(t)dt$
$\tilde{D}_{\max}$	$6Q_{\mathsf{No}}$

3.7.1 Online Optimization without Forecasts

Comparison with the Genie-Aided Approach

We compare the performance of the algorithm proposed in Sec. 3.6, against the genie-aided solution obtained in Sec. 3.3. We consider the simulation parameters shown in Table 3.1, and the following are the linear inequalities that we use to approximate (2.4) in $[Q_{\mathsf{No}}, \tilde{D}_{\max}]$:

$$D(t) \leq \mathscr{L}_1(\tilde{D}(t)) \triangleq 0.71\tilde{D}(t) + 18.54$$

$$D(t) \leq \mathscr{L}_2(\tilde{D}(t)) \triangleq 0.67\tilde{D}(t) + 22.50$$

$$D(t) \leq \mathscr{L}_3(\tilde{D}(t)) \triangleq 0.64\tilde{D}(t) + 26.26$$

$$D(t) \leq \mathscr{L}_4(\tilde{D}(t)) \triangleq 0.62\tilde{D}(t) + 29.86$$

$$D(t) \leq \mathscr{L}_5(\tilde{D}(t)) \triangleq 0.60\tilde{D}(t) + 33.33$$

$$D(t) \leq \mathscr{L}_6(\tilde{D}(t)) \triangleq 0.58\tilde{D}(t) + 36.70$$

$$D(t) \leq \mathscr{L}_7(\tilde{D}(t)) \triangleq 0.56\tilde{D}(t) + 39.98$$

$$D(t) \leq \mathscr{L}_8(\tilde{D}(t)) \triangleq 0.55\tilde{D}(t) + 43.18$$

$$D(t) \leq \mathscr{L}_9(\tilde{D}(t)) \triangleq 0.54\tilde{D}(t) + 46.31$$

In Fig. 3.1, we have plotted the discharging operations obtained with the proposed algorithm and the genie-aided strategy. The discharging operation obtained with the genie-aided strategy takes the form of a piece-wise linear function because of the discretisation and the linearisation introduced. The battery state obtained with the genie-aided strategy is denoted by $\mathbf{j}^* \in \mathbb{R}_+^N$, and the battery state obtained with the proposed strategy based on Pontryagin's Maximum Principle is denoted by $J^*(t)$. The similarities between the two are remarkable, especially considering that $\theta^*(t)$ was designed without any knowledge of future renewable energy arrivals. A separation between the two lines can be seen when the discharging power is below $Q_{\mathsf{No}} \approx 62$. This follows in this particular scenario because we have used the results derived by assuming (2.5) instead of (2.4), which introduces errors when $\tilde{D}(t) < Q_{\mathsf{No}}$. Although this mismatch is reduced as $\kappa \to 1^+$.

If we assume that the relationship between $D(t)$ and $\tilde{D}(t)$ is $D(t) = \mathscr{G}\left[\tilde{D}(t)\right] \triangleq Q_{\mathsf{No}}\left[\frac{\tilde{D}(t)}{Q_{\mathsf{No}}}\right]^{\frac{1}{\kappa}}$, even when $D(t) \leq Q_{\mathsf{No}}$, then, as shown in Fig. 3.2, the mismatch between the discharging profile obtained through linearisation and the one obtained by applying Pontryagin's Maximum Principle is considerably reduced. To obtain the results in Fig. 3.2 we have considered the parameters in Table 3.1, except for $M = 26$. The linear segments used to approximate $\mathscr{G}(\cdot)$ in the interval $[0, \tilde{D}_{\max}]$ have been obtained by using the method in Appendix A.1, with the partition's midpoints $\{x_1, x_2, \ldots, x_{26}\}$ defined as follows:

$$\begin{aligned} x_i &= 0.1 \times Q_{\mathsf{No}} \times i,\ i \in \{1,\ldots,9\}, \\ x_i &= (0.2i - 0.8)\, Q_{\mathsf{No}}\ i \in \{10,\ldots,26\}. \end{aligned} \tag{3.29}$$

Finally, we compare the performance of the online strategy based on Pontryagin's

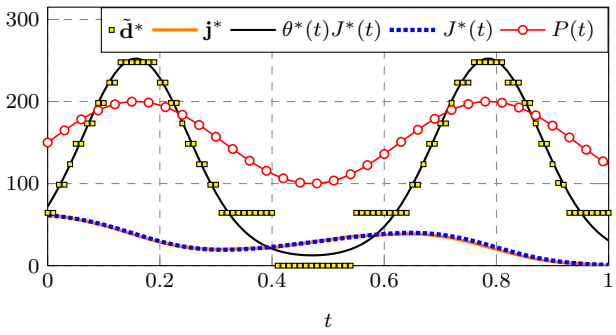

Figure 3.1: Discharging profile obtained by using the online strategy proposed in Sec. 3.6, and the genie-aided strategy.

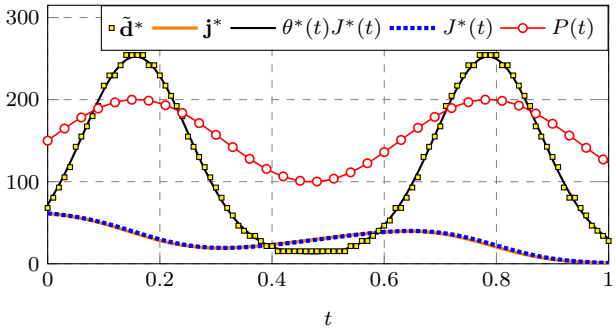

Figure 3.2: Discharging profile obtained by using the online strategy proposed in Sec. 3.6, and the genie-aided strategy. Simplified Peukert's model applies in both approaches.

Maximum Principle, and the genie-aided strategy obtained by solving P3.1 through discretisation and linearisation. To simplify notation, we define:

$$\Upsilon[\theta(t)] \triangleq \int_0^H P(t) Q_{\mathsf{No}} \left(\frac{\theta(t) J(t)}{Q_{\mathsf{No}}} \right)^{\frac{1}{\kappa}} dt + KJ(H).$$

We then consider the following simulation parameters: $\Delta t = 0.01$, $p(k) \sim \mathscr{U}(1,2)$, $K = 0.7 \frac{1}{N} \sum_{k=1}^{N} p(k)$, $r(k) \sim \mathscr{U}(0,100)$, $\kappa = 1.3$, $Q_{\mathsf{No}} = 20$, and $\tilde{D}_{\max} = \{200, 80\}$, and plot the results in Figs. 3.3 and 3.4. As observed in Fig. 3.4, the online strategy incurs a performance degradation when the simplifications introduced to obtain the result in (3.26) are not justified. However, when the simplifications can be justified, the proposed online strategy, which does not require any knowledge of future renewable energy arrivals, achieves the same performance as the genie-aided strategy.

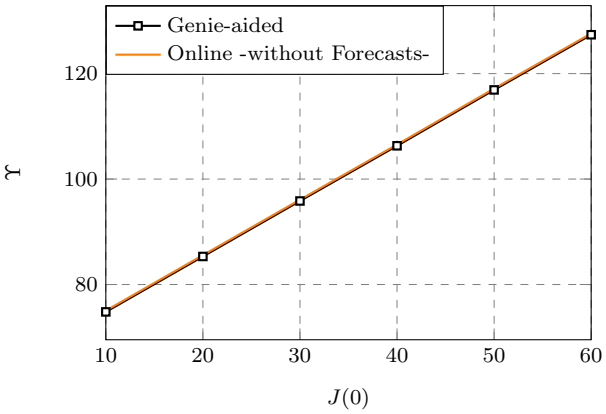

Figure 3.3: Performance of the online strategy proposed in Sec. 3.6, with $\tilde{D}_{\max} = 200$.

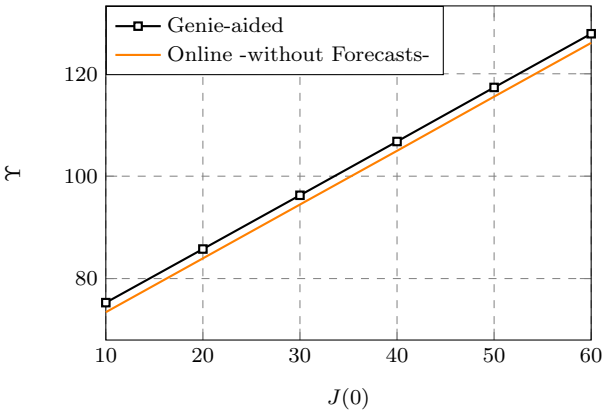

Figure 3.4: Performance of the online strategy proposed in Sec. 3.6, with $\tilde{D}_{\max} = 80$.

3.7.2 Online Optimization with Forecasts

We now evaluate the performance of the proposed forecasting-based strategies. Since in this section we have assumed $W(t) = P(t)\ \forall\, t$, the forecasting strategies are used to estimate future renewable energy arrivals, as no information about the load is required[6] when $W(t) = P(t)\ \forall\, t$. From [181], we obtain data containing the typical output power of a photovoltaic panel (PVP) located in Southern California. The characteristics and exact location of the PVP are shown in Table 3.2. The weather data source chosen to

[6]Load forecasting is required to design $X(t)$, however, when $W(t) = P(t)\ \forall\, t$ we can design $D(t)$ and then determine $X(t)$ from (2.19), as discussed in Sec. 2.4.3.

Table 3.2: Characteristics of the photovoltaic system (Southern California).

Location	System size	Tilt, Azimuth	Inverter efficiency	DC to AC size ratio	Losses
32.7° N, 117.2° W	4 kW (DC)	20°, 180°	96%	1.1	14%

Table 3.3: Characteristics of the time series (data from PVWatts calculator).

Hours	Training period	Optimization period	Samples per day
6:00 - 17:00	June 1 - June 30	6:00 - 17:00	$N = 12$

obtain the time series was the typical meteorological year database 3 (TMY3). TMY data suit the purpose of our simulations because they represent typical, as opposed to extreme conditions.[7]

Other characteristics of the data that we use to train our statistical models are listed in Table 3.3. The time series generated by the PVWatts calculator [181], and R's built-in functions such as `auto.arima()` and `markovchainFit()`, are used to identify the ARIMA and Markov chain models. For more details on the model identification algorithms please refer to [179], [180].

First-Order Linear Predictor

We assume energy prices measured in United States Dollars (USD), and drawn from a standard uniform distribution over the 12-hour period shown in Table 3.3. We also consider $\Delta t = 1$, $\varsigma = 1$, $\varepsilon = 0$, $\tilde{D}_{\max} = \frac{\Psi}{\Delta t}$, $Q_{\mathsf{No}} = \frac{\Psi}{\Delta t}$, and varying storage capacities measured in kilo-watt-hour (kWh). Since $\tilde{D}_{\max} = \frac{\Psi}{\Delta t}$ and $Q_{\mathsf{No}} = \frac{\Psi}{\Delta t}$, the storage device operates in its linear regime at all times, and the value of κ is irrelevant. The following are the model parameters, which were obtained by averaging over 1 month of data retrieved from [181], as indicated in Table 3.3: $\mathsf{coeff}_1 = 2.51$, $\mathsf{coeff}_2 = 1.91$, $\mathsf{coeff}_3 = 1.36$, $\mathsf{coeff}_4 = 1.29$ $\mathsf{coeff}_5 = 1.09$, $\mathsf{coeff}_6 = 1.05$, $\mathsf{coeff}_7 = 0.89$, $\mathsf{coeff}_8 = 0.81$, $\mathsf{coeff}_9 =$

[7] TMY data cannot be used to design or determine if systems meet worst-case conditions [182]. However, that is not the purpose of our simulations.

0.79, $\text{coeff}_{10} = 0.61$, $\text{coeff}_{11} = 0.50$. For the stochastic model in (3.9), we consider normally distributed errors with zero mean and variance $\sigma^2 = 0.14$. We also constrain the outputs to be in the interval $[0, 3.35]$ kW.

We implement Algorithm 2, and compare its performance with the genie-aided solution. We plot the results obtained after averaging over ten thousand[8] realisations in Fig. 3.5. As observed, there is a small performance gap between the two strategies, and this gap decreases as the storage capacity grows. This result suggests that the forecasting errors become less influential as Ψ grows, which is sensible because a large storage capacity allows the algorithm to schedule the discharging operation with more freedom, e.g. without forcing energy consumption to reserve storage space.

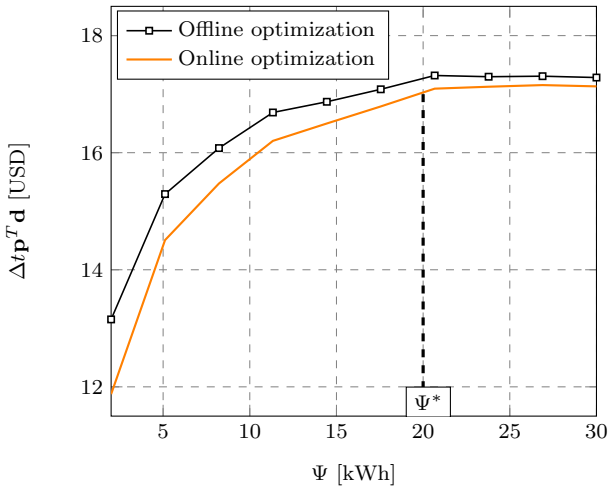

Figure 3.5: Average performance of the proposed online strategy considering random energy rates drawn from a standard uniform distribution (USD), and using the first-order linear predictor for forecasting.

Auto-Regressive Integrated Moving Average Time Series

Assuming energy prices measured in USD, and drawn from a standard uniform distribution, in the following we evaluate the performance of Algorithm 2 when the renewable

[8] In Appendix A.2 we provide a discussion on how this number (ten thousand) was decided.

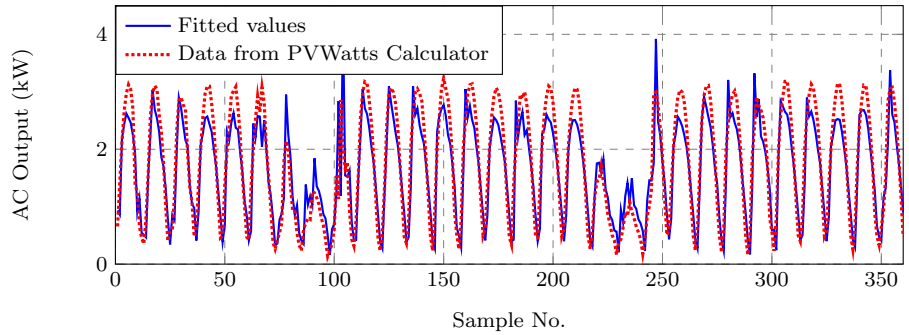

Figure 3.6: Training data and values obtained with the fitted model.

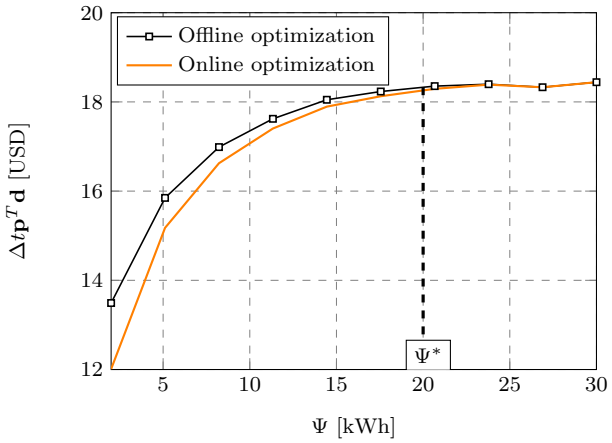

Figure 3.7: Average performance of the proposed online strategy considering random energy rates drawn from a standard uniform distribution (USD), and using the ARIMA time series model for forecasting.

energy arrivals follow an ARIMA time series model. We consider a planning horizon of duration 12 hours, i.e. $N = 12$, with simulation parameters $\Delta t = 1$, $\varsigma = 1$, $\varepsilon = 0$, and $\tilde{D}_{\max} = Q_{\mathsf{No}} = \frac{\Psi}{\Delta t}$. The storage capacities are allowed to vary, and are measured in kWh. Since $\tilde{D}_{\max} = \frac{\Psi}{\Delta t}$ and $Q_{\mathsf{No}} = \frac{\Psi}{\Delta t}$, the storage device operates in its linear regime at all times, and the value of κ is irrelevant.

We then use the function `auto.Arima()` to obtain the following ARIMA(2,0,2) model as the best fit for our training data:

$$r(k) = 1.71 + 1.49r(k-1) - 0.72r(k-2) - 0.28\omega(k-1) - 0.16\omega(k-2) + \omega(k),$$

with σ^2 estimated as 0.14. Both the training data and the fitted values obtained with the ARIMA(2,0,2) model are shown in Fig. 3.6. In this particular scenario, the initial ARIMA model is an ARMA$(2,2)$ model. But since this model is updated daily, the parameters m, n and q may change as data are added to the training sequence, thus justifying the use of a general model.

We consider ten thousand realisations, and in all of them the output of the model is upper bounded by 3.35kW according to the data obtained from the PVWatts calculator [181]. We also use the Box-Cox transformation with $\lambda = 0$ to ensure that the outputs of the model are always positive.

In Fig. 3.7, we have plotted the daily cost saving against the storage size obtained by using the proposed online algorithm and the genie-aided strategy. As seen, the gap between the two strategies approaches 0 as Ψ reaches 30. Moreover, increasing the storage capacity beyond Ψ^* does not affect the cost savings. The rationale behind this result may be the following: Ψ^* is the smallest storage capacity required to shift the largest possible consumption of renewable energy to the peak pricing periods, for $\Psi > \Psi^*$, the causality constraint impedes scheduling a larger amount of energy, hence the improvement is negligible.

Time-Inhomogeneous Markov Chain

We use the data obtained from [181], and the function `markovchainFit` to train our Markov chain model. We specifically consider five states defined respectively by the intervals: $[0, 0.67)$, $[0.67, 1.34)$, $[1.34, 2.01)$, $[2.01, 2.68)$, and $[2.68, 3.35]$. The obtained transition probability matrices are shown in Table A.1 of Appendix A.3, where we only show sourcing states with non-zero probability of occurrence.

We consider the following scenario: $N = 12$, $\Delta t = 1$, $\varepsilon = 0$, $\varsigma = 1$, $\tilde{D}_{\max} = Q_{\mathsf{No}} = \frac{\Psi}{\Delta t}$,

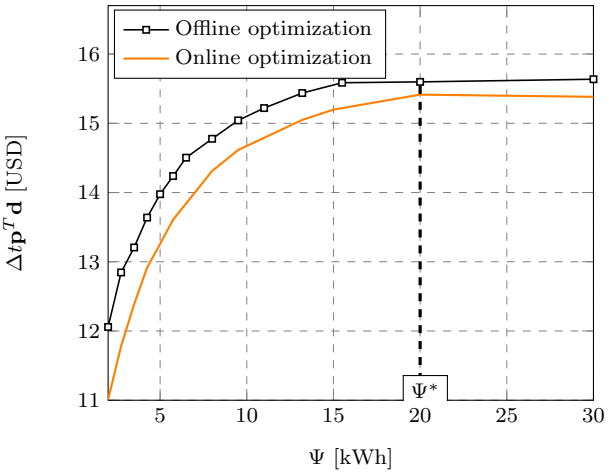

Figure 3.8: Average performance of the proposed online strategy considering random energy rates in USD, and drawn from a standard uniform distribution, and Markovian renewable energy arrivals.

and $p(k) \sim \mathscr{U}(0,1)$, and varying storage capacities measured in kWh. Since $\tilde{D}_{\max} = \frac{\Psi}{\Delta t}$ and $Q_{\mathsf{No}} = \frac{\Psi}{\Delta t}$, the storage device operates in its linear regime at all times, and the value of κ is irrelevant. We then benchmark the average performance of Algorithm 2 against the genie-aided solution. We specifically consider ten thousand realisations, and plot the results in Fig. 3.8. As observed, the performance gap between the genie-aided strategy and the proposed algorithm decreases as Ψ grows. Again, it is seen that there is a critical storage capacity Ψ^* above which no further savings can be achieved.

In the last part of this section we determine the confidence intervals of the results presented in Figs. 3.5, 3.7, and 3.8. Hence, in Figs. 3.9 and 3.10 we show the average percentage gap between the genie-aided result (GAR) and the online result (OR) for the three forecasting techniques employed. Moreover, we also show the one - standard deviation (1-SD) confidence interval. As shown, for the three techniques, the worst deviation occurred when the storage capacity was the smallest considered, i.e. $\Psi =$ 2kWh. Similarly, in all the three techniques, the worst average gap occurred when the storage capacity was the smallest considered. Finally, storage capacities of at least

20kWh led to remarkably small performance gaps, which on average did not reach a 5% deviation from the GAR.

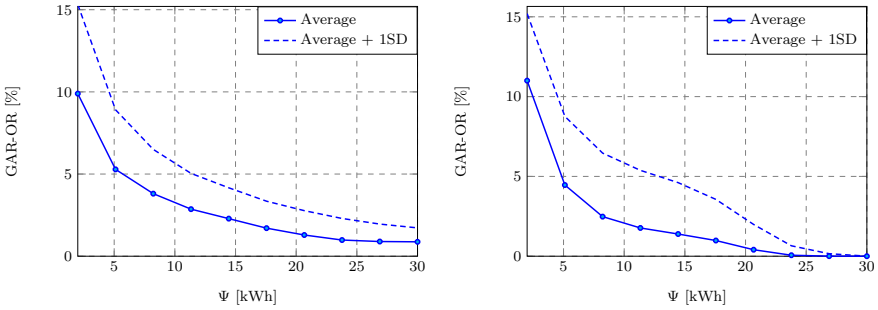

Figure 3.9: Confidence interval for the performance gap defined as genie-aided result (GAR) - online result (OR) in relative terms (%). Forecasting-based online algorithms using linear predictors (left) and ARIMA (right).

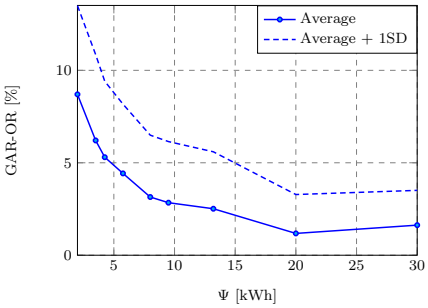

Figure 3.10: Confidence interval for the performance gap defined as genie-aided result (GAR) - online result (OR) in relative terms (%). Forecasting-based online algorithm using Markov chains.

3.8 Summary

We have proposed several online strategies to minimize the energy bill incurred by a non-deferrable load facility over a finite planning horizon. We have assumed that the facility is equipped with a renewable energy harvester and a storage device. We have then proposed strategies based on forecasting techniques such as a first-order linear predictor, an ARIMA time series model, or a time-inhomogeneous Markov chain. Unlike the proposals in the literature, these new strategies take into consideration the non-linear characteristics of the energy storage device, and also pricing policies such as

net metering.

We have also proposed an online strategy, which is based on Pontryagin's Maximum Principle, and does not require estimates of future renewable energy arrivals. The proposed strategy is model-independent, and uses analytical results, which are obtained by solving the optimization problem in continuous time. As a result, it is simpler than strategies based on repetitive computations.

We have obtained the following insights from our analysis and numerical results:

- Proper storage sizing has allowed us to eliminate the overflow-related constraint, which has considerably simplified the optimization problem, and has ultimately led to an analytical result.

- To eliminate the causality constraint in the optimization problem, we have forced the discharging power to be proportional to the energy available in the storage device at all times. That is, instead of designing $\tilde{D}(t)$ we have opted to optimize the ratio $\frac{\tilde{D}(t)}{J(t)}$, which has enabled a powerful simplification, and allowed us to derive results in analytic form. In practice, this substitution represents the continuous feedback that we require to design the control signal $\tilde{D}(t)$, so as to satisfy the causality constraint at all times.

- If the bequest value of the energy left unused at the end of the planning horizon can be properly assessed, then reliance on forecasts can be eliminated by using Pontryagin's Maximum Principle. This is perhaps the most interesting finding in this chapter. We have shown both analytically and through simulations, that estimates of future renewable energy arrivals are not required if the bequest value of $J(H)$ is given, and the discharging rate and storage capacity are unlimited.

- There is a storage capacity Ψ^*, above which no further cost reduction can be achieved,

and as a result, the optimal energy management strategy only requires $\Psi \geq \Psi^*$. The critical storage capacity Ψ^* depends on the local generation capacity, and the efficiency of the charging/discharging operations.

Chapter 4

Cooperative Renewable Energy Management

In this chapter, we propose strategies to minimize the energy bill incurred by a group of cooperating facilities over a finite planning horizon. The facilities are equipped with renewable energy harvesters and storage devices, and their loads are assumed to be non-deferrable. Unlike previous solutions, the strategies proposed in this chapter assume that the participating facilities, e.g. households, base stations, or buildings, are enabled to share renewable energy, either through the smart grid or dedicated power lines. The proposed strategies can be used to optimize the use of renewable energy in cellular networks, whose base stations are subject to different pricing signals, power consumption profiles, and renewable energy harvesting conditions.

We first consider a system architecture in which each facility is equipped with its own renewable energy harvester and storage device. With this consideration, we propose using the smart grid as a medium for the participating facilities to share renewable energy in order to minimize their collective energy bill. We specifically design the optimal energy sharing strategy by solving a constrained optimization problem.

Thereafter, we consider a second architecture, in which all the participating facilities have shared access to an energy farm where renewable power is harvested and stored. With this consideration we design the optimal access policy, and also determine the optimal rate at which the renewable energy should be utilised. We then compare the performance of the two proposed strategies and draw the appropriate conclusions.

In this chapter we also investigate cooperative energy management strategies which do not require exact knowledge of future renewable energy arrivals. We particularly focus on the second architecture, and devise a strategy to minimize the average[1] energy cost incurred by all the participants over a finite planning horizon.

4.1 Contributions

The following are the main contributions of this chapter:

- We propose two genie-aided strategies to minimize the energy bill incurred by a group of facilities, e.g base stations, or households, over a finite planning horizon. The power consumed by the facilities is assumed to be non-deferrable, and the group is assumed to have renewable energy harvesting and storage capabilities. The first strategy assumes that each facility is equipped with its own renewable energy harvester and storage device. To design this strategy we formulate and solve a constrained optimization problem, in which the decision variables determine the optimal energy sharing strategy among the facilities. The second proposed strategy assumes that all the facilities have shared access to an energy farm where renewable power is harvested and stored. In this scenario we seek to optimize the participants' access policy, and determine the optimal rate at which the renewable energy should be utilised. The results presented in this chapter can be used to determine performance bounds of cooperative energy management strategies in practical deployments. Moreover, these results can provide insights that can help engineers to determine the most cost-effective designs.

- Assuming centralized renewable energy generation and storage, we devise a strategy to minimize the average energy cost incurred by all the facilities over a finite planning

[1]The average energy cost is computed across realisations of the stochastic process that models the amount of renewable energy available over time.

horizon. The proposed strategy determines the optimal rate at which the renewable energy should be utilised, and also takes into account its uncertainty over time. Unlike existing works, we use a continuous-time approach, which makes the problem more tractable, and allows us to obtain explicit analytical solutions. We specifically show how the stochastic optimization problem boils down to solving Bellman's equation, which, in continuous time, is a deterministic differential equation. A simplification that cannot be obtained if we formulate the problem using discrete-time signals [183].

4.2 Energy Management with Distributed Generation and Storage

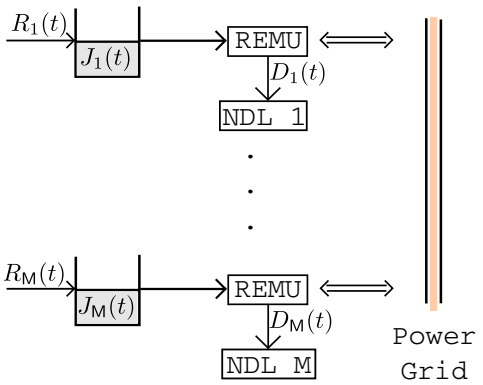

Figure 4.1: Distributed generation and storage. Set of M non-deferrable loads (NDLs). REMU stands for Renewable Energy Management Unit.

4.2.1 System Model

We consider a set of M facilities, each one of them permanently connected to the power grid as shown in Fig. 4.1. Each facility is equipped with its own renewable energy harvester and storage device. Moreover, we assume that the facilities can share renewable energy through the grid.

The renewable power transferred from the facility j to the facility $i \neq j$, over the planning horizon $[0,H]$, is denoted by $T_{j,i}(t)$, where $t \in [0,H]$ is the time index. As in previous chapters, the planning horizon can be as large as desired, but the physical

properties of the components in the system (such as the storage device) are assumed to remain constant in $[0, H]$.

The total power received by the facility i from other facilities is $V_i(t)$, i.e.:

$$V_i(t) = \sum_{j=1,\ j\neq i}^{\mathsf{M}} T_{j,i}(t),\ \forall\, t. \tag{4.1}$$

Notice that (4.1) does not include transmission losses, which follows because the energy transfers between facilities do not need to happen physically. The facilities inject energy into the grid, and the utility registers the operation to deliver the same amount of energy at the destination. In that respect, the utility is assumed to have sufficient[2] delivery capacity within the network of facilities. The transmission losses are then borne by the utility, which charges a fee for the service.

Let $L_i(t)$ and $D_i(t)$ denote respectively the power consumed and drawn from the storage device by the ith facility. Then, we impose the following constraint on $D_i(t) + V_i(t)$:

$$D_i(t) + V_i(t) \leq L_i(t)\ \forall\, t. \tag{4.2}$$

By introducing this constraint we ensure that no renewable energy is sold to the utility or grid operator,[3] i.e. all the harvested renewable energy must be consumed by the participants, or left stored for future use. These assumptions are introduced to avoid unjustified financial gains, given that different prices take place across different locations.

Energy Storage Device

To simplify notation, we assume energy storage devices with the same characteristics (e.g. capacity) across all the participating facilities. The non-linear relationship between the discharging rate and the remaining charge is modelled by using an arbitrary function

[2]This is a sensible assumption because the energy generated by a single harvester is smaller than the energy delivered by the distribution system to a set of loads in a given geographical area.

[3]The renewable energy is injected into the grid only if it is to be transferred to another facility.

$\mathscr{F} : [0,\infty) \to [0,\infty)$, which is continuous, convex, and strictly increasing. Hence, the following relationship holds between the total power drained from the storage device $\tilde{D}_i(t)$, and the power effectively delivered $D_i(t) + \sum_{j=1, j\neq i}^{\mathsf{M}} T_{i,j}(t)$:

$$\tilde{D}_i(t) = \mathscr{F}\left(D_i(t) + \sum_{j=1, j\neq i}^{\mathsf{M}} T_{i,j}(t) \right). \tag{4.3}$$

For simplicity we will assume that the same function $\mathscr{F}(\cdot)$ applies to all the storage devices. Let $R_i(t)$ and $J_i(t)$ denote respectively the renewable power harvested, and the energy available in the storage device at facility i, then:

$$J_i(t) = J_i(0) + \int_0^t \left[\varsigma R_i(\tau) - \tilde{D}_i(\tau) \right] d\tau, \tag{4.4}$$

where $0 \leq \varsigma \leq 1$ is the charging efficiency rate, assumed the same for all the storage devices across participating facilities.

Total Energy Cost

The participating facilities are deployed across a given geographical area and each facility is, in general, subject to different time-varying energy prices and power consumption profiles. Let $P_i(t) > 0, \forall\, t$ denote the energy prices offered by the utility to the ith facility. Then, assuming a linear pricing scheme the energy cost incurred by all the facilities in $[0,H]$ is:

$$\chi = \sum_{i=1}^{\mathsf{M}} \int_0^H P_i(t) \left[L_i(t) - D_i(t) - \mathsf{df} V_i(t) \right] dt, \tag{4.5}$$

where $0 \leq \mathsf{df} \leq 1$ is a discount factor, which models the transfer fees, e.g. $\mathsf{df} = 1$ represents free power transfers.

In this section we assume that the utility does not purchase renewable power from its customers because the purpose of the energy management strategies is to encourage participants to cooperate and maximize their consumption of renewable energy. This

objective can be accomplished through energy sharing and by leveraging the power grid infrastructure.

4.2.2 Problem Formulation

To simplify notation we introduce the following definition:

$$\mathbf{T}(t) = \begin{pmatrix} T_{1,1}(t) & T_{1,2}(t) & \dots & T_{1,\mathsf{M}}(t) \\ T_{2,1}(t) & T_{2,2}(t) & \dots & T_{2,\mathsf{M}}(t) \\ \vdots & \vdots & \ddots & \vdots \\ T_{\mathsf{M},1}(t) & T_{\mathsf{M},2}(t) & \dots & T_{\mathsf{M},\mathsf{M}}(t) \end{pmatrix}. \tag{4.6}$$

Note that $T_{i,i}(t)$ can be seen as the renewable power that the ith facility transfers to itself, or said otherwise, uses locally. Therefore we define $T_{i,i}(t) \triangleq D_i(t)\ \forall\, t$, and the energy bill minimization problem can be formulated as follows:

$$\text{P4.A:} \quad \min_{\mathbf{T}(t)} \sum_{i=1}^{\mathsf{M}} \left(\int_0^H P_i(t) \left[L_i(t) - T_{i,i}(t) - \mathsf{df} \sum_{j=1,\ j\neq i}^{\mathsf{M}} T_{j,i}(t) \right] dt \right)$$

s.t.

$$0 \leq J_i(t) \leq \Psi, \tag{4.7a}$$

$$\sum_{j=1}^{\mathsf{M}} T_{j,i}(t) \leq L_i(t), \tag{4.7b}$$

$$\sum_{j=1}^{\mathsf{M}} T_{i,j}(t) \leq D_{\max},\ \forall\, t,\ \forall\, i. \tag{4.7c}$$

In P4.A, $D_i(t)$ is related to $\tilde{D}_i(t)$ through (4.3), and $J_i(t)$ is related to $\tilde{D}_i(t)$ through (4.4). The objective function in P4.A is the total energy cost incurred by all the facilities in $[0,H]$. Moreover, the constraint (4.7a) is introduced to restrict the energy stored over time, i.e. $J_i(t)$, to the interval $[0,\Psi]$, where Ψ is the storage capacity, which is the same for all the facilities. The constraint (4.7b) is introduced to restrict the total renewable power consumed by the ith facility to the interval $[0,L_i(t)]$. The constraint (4.7c) is

introduced to upper bound the total power discharged from each of the storage devices.

4.2.3 Proposed Strategy

We propose a strategy to solve P4.A based on linearisation and discretisation in time. As explained in Sec. 2.4.1, we can use linearisation to replace (4.3) with a set of linear inequalities. Let $N = \frac{H}{\Delta t}$ denote the number of slots of length Δt in the planning horizon $[0, H]$. Then the discrete-time version of P4.A can be cast as follows:

$$\text{P4.AD:} \quad \min_{\mathbf{T}(k\Delta t),\, k\in\{1,\dots,N\}} \sum_{i=1}^{\mathsf{M}} \left(\Delta t \sum_{k=1}^{N} P_i(k\Delta t) \left[L_i(k\Delta t) - T_{i,i}(k\Delta t) - \mathsf{df} \sum_{j=1,\ j\neq i}^{\mathsf{M}} T_{j,i}(k\Delta t) \right] \right)$$

s.t.

$$0 \leq J_i(k\Delta t) \leq \Psi, \tag{4.8a}$$

$$\sum_{j=1}^{\mathsf{M}} T_{j,i}(k\Delta t) \leq L_i(k\Delta t), \tag{4.8b}$$

$$\sum_{j=1}^{\mathsf{M}} T_{i,j}(k\Delta t) \leq D_{\max}, \tag{4.8c}$$

$$\sum_{j=1}^{\mathsf{M}} T_{i,j}(k\Delta t) = G[\tilde{D}_i(k\Delta t)],\ \forall\, k\ \forall\, i, \tag{4.8d}$$

where $G[\cdot]$ was defined in Eq. (2.10). In P4.AD, we no longer consider (4.3) because we have introduced (4.8d). The relationship between $J_i(k\Delta t)$ and $\tilde{D}_i(k\Delta t)$ is (4.4). To avoid introducing new notation, we have used the definition of $\mathbf{T}(t)$ to formulate P4.AD. However, P4.AD has been formulated to optimize $\mathbf{T}(t)$ only at specific points $t = k\Delta t$ with $k \in \{0,\dots,N\}$. Therefore, P4.AD can be cast as a linear program and solved numerically.

4.3 Energy Management with Centralized Generation and Storage

4.3.1 System Model

We consider a set of M facilities, each one of them permanently connected to the power grid as shown in Fig. 4.2. All the facilities share access to a single renewable energy

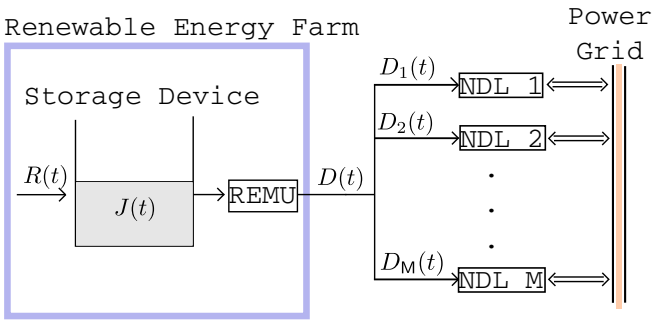

Figure 4.2: Centralized generation and storage. Set of M non-deferrable loads (NDLs). REMU stands for Renewable Energy Management Unit.

harvester and storage device. Since all the participants have shared access to the same renewable energy reserve, no power transferred is allowed among the facilities.

We consider the planning horizon $[0,H]$, where H is such that the physical properties of the components in the system remain constant in $[0,H]$. We let $L_i(t)$ and $D_i(t)$ denote respectively the power consumed, and drawn from the central storage by the ith facility. Since potentially different pricing signals apply across facilities, the following constraint is imposed on $D_i(t)$ in order to avoid unjustified financial gains:

$$D_i(t) \leq L_i(t) \; \forall \, t. \tag{4.9}$$

As a result, no locally harvested renewable energy is injected into the grid.

Energy Storage Device

The storage capacity of the energy farm is $\mathsf{M}\Psi$. That is, the total storage capacity is the same as in the distributed model described in Sec. 4.2.

Again, we assume a non-linear relationship between $D(t) = D_1(t) + \ldots + D_{\mathsf{M}}(t)$, the total power effectively drawn from the central storage, and $\tilde{D}(t)$, the power drained before losses:

$$\tilde{D}(t) = \mathscr{F}\left[D(t)\right], \tag{4.10}$$

where $\mathscr{F} : [0,\infty) \rightarrow [0,\infty)$ is assumed to be continuous, convex, and strictly increasing.

Let $R(t)$ and $J(t)$ denote respectively the renewable power harvested, and the energy available at the central storage at time t, then:

$$J(t) = J(0) + \int_0^t \left[\varsigma R(\tau) - \tilde{D}(\tau)\right] d\tau. \tag{4.11}$$

Total Energy Cost

The energy price offered by the utility to the ith participant is denoted by $P_i(t) > 0, \forall\, t$. Hence, assuming a linear pricing scheme the energy cost incurred by all the facilities is:

$$\chi = \sum_{i=1}^{\mathsf{M}} \int_0^H P_i(t) \left[L_i(t) - D_i(t)\right] dt. \tag{4.12}$$

4.3.2 Problem Formulation

The optimization problem can be formulated as follows:

$$\text{P4.B:} \quad \min_{D_1(t),\ldots,D_{\mathsf{M}}(t)} \sum_{i=1}^{\mathsf{M}} \left(\int_0^H P_i(t) \left[L_i(t) - D_i(t)\right] dt \right)$$

s.t.

$$0 \leq J(t) \leq \mathsf{M}\Psi, \ \forall\, t \tag{4.13a}$$

$$D_i(t) \leq L_i(t), \ \forall\, t, \ \forall\, i \tag{4.13b}$$

$$D_1(t) + \ldots + D_{\mathsf{M}}(t) \leq D_{\max}, \ \forall\, t. \tag{4.13c}$$

In P4.B, $D(t) = D_1(t) + D_2(t) + \ldots + D_{\mathsf{M}}(t)$ and $\tilde{D}(t)$ are related through (4.10), whereas $\tilde{D}(t)$ and $J(t)$ are related through (4.11).

4.3.3 Proposed Strategy

We can obtain an approximate solution to P4.B by introducing discretisation and by replacing the non-linear relationship (4.10) with a set of linear inequalities as proposed in

previous solutions. The discrete-time representation of P4.B can be written as follows:

$$\text{P4.BD:} \quad \min_{D_1,\ldots,D_{\mathsf{M}}} \sum_{i=1}^{\mathsf{M}} \Delta t \left(\sum_{k=1}^{N} P_i(k\Delta t)\,[L_i(k\Delta t) - D_i(k\Delta t)] \right)$$

s.t.

$$0 \leq J(k\Delta t) \leq \mathsf{M}\Psi, \tag{4.14a}$$

$$D_i(k\Delta t) \leq L_i(k\Delta t), \tag{4.14b}$$

$$D_1(k\Delta t) + \ldots + D_{\mathsf{M}}(k\Delta t) \leq D_{\max}, \tag{4.14c}$$

$$D_1(k\Delta t) + \ldots + D_{\mathsf{M}}(k\Delta t) = G[\tilde{D}(k\Delta t)],\ \forall\, k,\ \forall\, i. \tag{4.14d}$$

To solve P4.BD we no longer need to consider the non-linear relationship (4.10) because $D_1(k\Delta t) + \ldots + D_{\mathsf{M}}(k\Delta t)$ and $\tilde{D}(k\Delta t)$ are now related through (4.14d). The relationship between $J(\cdot)$ and $\tilde{D}(\cdot)$ is (4.11). To avoid introducing new notation, the same symbols $D_1(t), \ldots, D_{\mathsf{M}}(t)$ have been used to formulate P4.BD. However, P4.BD is formulated to optimize the trajectories $D_1(t), \ldots, D_{\mathsf{M}}(t)$ only at specific points $t = k\Delta t,\ k \in \{0, \ldots, N\}$. Therefore, P4.BD can be cast as a linear program and solved numerically.

4.4 Further Results on Energy Management with Centralized Generation

In this section we further investigate the model with centralized renewable energy generation and obtain additional results after introducing some simplifying approximations. We specifically consider the following simplifications:

1. We assume that the storage capacity is large enough to avert energy waste from battery overflow i.e., we disregard the constraint $J(t) \leq \mathsf{M}\Psi\ \forall\, t$, and hence (4.13a) simplifies to:

$$\int_0^t \tilde{D}(\tau)d\tau \leq J(0) + \int_0^t \varsigma R(\tau)d\tau,\ \forall\, t \in\ [0, H]. \tag{4.15}$$

2. We assume that $D_{\max}$ is large enough so as to ignore the constraint (4.13c).

3. We remove the constraint (4.13b), which in practice assumes that the loads are much larger than the production of renewable energy at all times.

4. We assume that $J(H)$ has a bequest value of $P(H)J(H)$, where $P(H) = \max\{P_1(H), P_2(H), \ldots, P_{\mathsf{M}}(H)\}$. This assumes that the energy left unused at the end of the optimization period can be sold at the highest price in the market at time $t = H$, which is $P(H)J(H)$.

After introducing the simplifications described above, P4.B can be written as follows:

$$\text{P4.B1:} \quad \max_{D_1,\ldots,D_{\mathsf{M}}} \sum_{i=1}^{\mathsf{M}} \left(\int_0^H P_i(t) D_i(t) dt \right) + P(H)J(H)$$

s.t. (4.10), (4.11), (4.15) and $D(t) = D_1(t) + D_2(t) + \ldots + D_{\mathsf{M}}(t)$.

In P4.B1 we have removed the term $\sum_{i=1}^{\mathsf{M}} \int_0^H P_i(t)L_i(t)dt$ from the objective function because it does not depend on the optimization variables $D_i(t)$. Moreover, P4.B1 has been formulated as a maximization problem to remove the negative sign from the objective function.

4.4.1 Offline Optimization

In this section, we obtain an approximate solution to P4.B1 by introducing some simplifications. Although this is a genie-aided solution, it provides insights that we will use in Sec. 4.4.2 to propose an online strategy.

Partitioning of $[0,H]$ and auxiliary variables γ_j

To tackle P4.B1, we propose a partitioning scheme for the interval $[0,H]$. Specifically, if $P_1(t), P_2(t), \ldots, P_{\mathsf{M}}(t)$ are of bounded variation,[4] then we can find a partition $\mathcal{P} =$

[4]Let $f : \mathbb{R} \to \mathbb{R}$ be a finite function. If for any $x,\ y \in [a,b]$, there exists a constant C, such that $|f(x) - f(y)| \leq C|x - y|$ then $f(\cdot)$ is of bounded variation in $[a,b]$ [184]. Intuitively, a finite function is of bounded variation if it does not change *too fast*. Therefore it is reasonable to assume that practical pricing functions must be of bounded variation.

$\{t_0, t_1, \ldots, t_N\}$ of $[0, H]$ such that for all intervals $[t_{j-1}, t_j]$, $j \in \{1, \ldots, N\}$, there exists $k_j \in \{1, 2, \ldots, \mathsf{M}\}$ such that $P_{k_j}(t) \geq P_i(t)\ \forall\ i$ and $\forall\ t \in [t_{j-1}, t_j]$. This partitioning scheme is illustrated in Fig. 4.3. As seen, we can determine $\mathcal{P}$ by computing the values of t at which $P_1(t), P_2(t), \ldots, P_{\mathsf{M}}(t)$ intersect. This excludes intervals $[a, b]$, in which all prices $P_i(t)$ are equal, i.e. $P_i(t) = P_1(t),\ \forall\ i,\ \forall\ t \in [a, b]$. In such intervals, *any* $P_i(t)$ satisfies $P_i(t) \geq P_j(t),\ \forall\ j \neq i$.

The cardinality of the sequence $\mathcal{P} = \{t_0, t_1, \ldots, t_N\}$ is $N + 1$, and determines the number of subintervals in which $\mathcal{P}$ divides $[0, H]$, e.g if $t_0 = 0$ and $t_N = H$, then the number of subintervals is N. For simplicity, in the rest of this thesis we refer to this number as the cardinality of the partition. We will be particularly interested in partitions with the smallest cardinality, among other criteria.

To solve P4.B1 using this partitioning scheme, we introduce the following definition: Let γ_j be the renewable energy drawn from the central storage by all the facilities in $[t_{j-1}, t_j]$ i.e.,

$$\gamma_j = \int_{t_{j-1}}^{t_j} \tilde{D}(t)dt,\ j \in \{1, 2 \ldots, N\}. \tag{4.16}$$

Using (4.10), γ_j can be written in terms of $D(t) = D_1(t) + D_2(t) + \ldots + D_{\mathsf{M}}(t)$:

$$\gamma_j = \int_{t_{j-1}}^{t_j} \mathscr{F}\left[D(t)\right] dt. \tag{4.17}$$

Next, we solve P4.B1 in two steps. In the first step, we formulate a constrained optimization problem to obtain the optimal $D_1(t),\ D_2(t), \ldots, D_{\mathsf{M}}(t)$ in terms of the auxiliary variables $\gamma_j,\ j \in \{1,\ 2, \ldots, N\}$. In the second step, we plug the obtained optimal trajectories in the objective function and optimize with respect to $\gamma_1, \ldots, \gamma_N$.

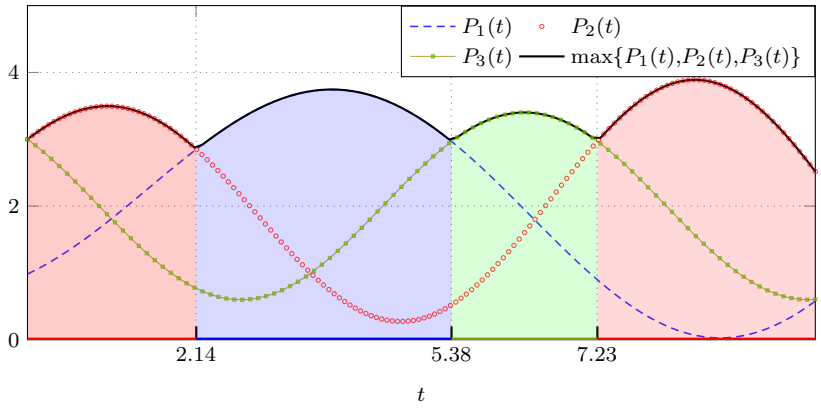

Figure 4.3: Illustration of the proposed partitioning scheme for $[0,H]$. In this case, we consider three pricing profiles.

Optimal trajectories $D_1(t),\ D_2(t),\ldots,D_{\mathsf{M}}(t)$

Using the auxiliary variables $\gamma_j,\ j \in \{1,\ldots,N\}$ and the partitioning scheme defined in Sec. 4.4.1, we formulate the following optimization problem to obtain the optimal $D_1(t),D_2(t),\ldots,D_{\mathsf{M}}(t)$ in terms of $\gamma_j,\ j \in \{1,2,\ldots,N\}$.

$$\text{P4.B2:} \quad \max_{D_1,\ldots,D_{\mathsf{M}}} \sum_{j=1}^{N} \left(\int_{t_{j-1}}^{t_j} \left[\sum_{i=1}^{\mathsf{M}} P_i(t) D_i(t) \right] dt \right) + P(H)J(H)$$

s.t. (4.15) and (4.17) with $D(t) = D_1(t) + D_2(t) + \ldots + D_{\mathsf{M}}(t)$.

To simplify notation, we define:

$$\zeta = \sum_{j=1}^{N} \gamma_j,$$

and use the following result to solve P4.B2:

Lemma 4.4.1. *Let $J(0) \geq \zeta$, and $D(t)$ satisfy (4.17), then:*

$$\int_0^t \mathscr{F}\left[D(\tau)\right] d\tau \leq J(0) + \int_0^t R(\tau) d\tau,\ 0 \leq t \leq H. \tag{4.18}$$

Proof. From (4.17) we have:

$$\int_0^t \mathscr{F}\left[D(\tau)\right] d\tau \leq \sum_{j=1}^{N} \gamma_j,\ 0 \leq t \leq H. \tag{4.19}$$

Moreover, $0 \leq \int_0^t \varsigma R(\tau)d\tau,\ \forall\, t$. Hence, from (4.19) we have:

$$\int_0^t \mathscr{F}\left[D(\tau)\right]d\tau \leq \zeta + \int_0^t \varsigma R(\tau)d\tau,\ 0 \leq t \leq H. \tag{4.20}$$

Finally, (4.18) can be obtained by adding (4.20) to the inequality $\zeta \leq J(0)$. ■

Following Lemma 4.4.1, if $J(0) \geq \zeta$, then, we can disregard the constraint (4.15) because $J(0) \geq \zeta$ implies (4.18), which is (4.15) with $\tilde{D}(t) = \mathscr{F}\left[D(t)\right]$. Moreover, we can remove $P(H)J(H)$ from the objective function in P4.B2 because, given $\gamma_1, \ldots, \gamma_N$, $J(H)$ does not depend on the optimization variables $D_1(t), \ldots, D_{\mathsf{M}}(t)$. In fact, by the principle of conservation of energy, we have:

$$J(H) = J(0) - \sum_{j=1}^{N} \gamma_j + \int_0^H \varsigma R(t)dt. \tag{4.21}$$

To simplify notation, let ρ denote the objective function in P4.B2, i.e.,

$$\rho = \sum_{j=1}^{N} \int_{t_{j-1}}^{t_j} \left[\sum_{i=1}^{\mathsf{M}} P_i(t)D_i(t)\right] dt + P(H)J(H),$$

then using the result in Lemma 4.4.1 and (4.21), we enunciate the following theorem:

Theorem 4.4.1. *Let $J(0) \geq \zeta$, $P_i(t),\ i \in \{1, \ldots, \mathsf{M}\}$ be of bounded variation, and $\mathcal{P} = \{t_0, t_1, \ldots, t_N\}$ denote the smallest[5] partition of $[0, H]$ such that for all intervals $[t_{j-1}, t_j],\ j \in \{1, 2, \ldots, N\}$, there exists $k_j \in \{1, 2, \ldots, \mathsf{M}\}$ such that $P_{k_j}(t) \geq P_i(t) > 0\ \forall\, i$ and $\forall\, t \in [t_{j-1}, t_j]$. Then, a necessary condition to maximize ρ subject to (4.17) is:*

$$-P_{k_j}(t) + \lambda \mathscr{F}'\left[D_{k_j}(t)\right] = 0,\ \ D_i(t) = 0,\ \forall\, i \neq k_j, \tag{4.22}$$

where $\mathscr{F}'(x) = \frac{d}{dx}\mathscr{F}(x)$, and $\lambda \in \mathbb{R}_+$. Moreover, if $\mathscr{F}(x) = Q_{\mathsf{No}}\left[\frac{x}{Q_{\mathsf{No}}}\right]^{\kappa}$, with $Q_{\mathsf{No}} > 0$

[5]The smallest partition is the one with the smallest cardinality.

and $\kappa > 1$*, then, (4.22) yields:*

$$D_{k_j}(t) = D^*_{k_j}(t) \triangleq \left(\frac{\gamma_j {Q_{\mathsf{No}}}^{\kappa-1}}{\int_{t_{j-1}}^{t_j} P_{k_j}(\tau)^{\frac{\kappa}{\kappa-1}} d\tau} \right)^{\frac{1}{\kappa}} \left[P_{k_j}(t)\right]^{\frac{1}{\kappa-1}}, \tag{4.23}$$

and $D_i(t) = 0$, $\forall\, i \neq k_j$, $\forall\, t \in [t_{j-1}, t_j]$, $\forall\, j$.

Proof. See Appendix B.6. ■

Optimal $\gamma_1, \gamma_2, \ldots, \gamma_N$

We have obtained the optimal $D_1(t), \ldots, D_{\mathsf{M}}(t)$ in terms of γ_j, $j \in \{1, \ldots, N\}$. Now we optimize $\gamma_1, \ldots, \gamma_N$ by solving the auxiliary optimization problem that we formulate next. First, we plug the optimal $D_1(t), \ldots, D_{\mathsf{M}}(t)$ in the objective function of P4.B2, and simplify using:

$$\sum_{i=1}^{\mathsf{M}} P_i(t) D_i(t) = P_{k_j}(t) D^*_{k_j}(t) \;\forall\, t \in [0, H], \tag{4.24}$$

which follows from Theorem 4.4.1. By using (4.21) and (4.24) the objective function can be written as a functional of the optimal trajectory $D^*_{k_j}(t)$, which in turn is a function of the γ_j's:

$$\rho\left[D^*_{k_j}(t)\right] = \sum_{j=1}^{N} \left(\int_{t_{j-1}}^{t_j} P_{k_j}(t) D^*_{k_j}(t) dt \right) + P(H) \left(Z - \sum_{j=1}^{N} \gamma_j \right), \tag{4.25}$$

where $Z = J(0) + \int_0^H \varsigma R(t) dt$, and $D^*_{k_j}(t)$ is the optimal $D_{k_j}(t)$ which can be obtained from (4.22), or from (4.23) if $\mathscr{F}(\cdot)$ follows the definition in (2.5).

To optimize ρ with respect to the γ_j's, we can use Lagrange multipliers. Moreover, if $\mathscr{F}(x) = Q_{\mathsf{No}} \left[\frac{x}{Q_{\mathsf{No}}}\right]^{\kappa}$ then we are able to obtain explicit results as shown in the following lemmas:

Lemma 4.4.2. *Let* $\mathscr{F}(x) = Q_{\mathsf{No}} \left[\frac{x}{Q_{\mathsf{No}}}\right]^{\kappa}$, $Q_{\mathsf{No}} > 0$, $\kappa > 1$, $P(H) > 0$, *and* $D_{k_j}(t) =$

$D^*_{k_j}(t)$, where $D^*_{k_j}(t)$ was defined in (4.23), then ρ attains its maximum at:

$$\gamma_j = Q_{\mathsf{No}} \int_{t_{j-1}}^{t_j} \left[\frac{P_{k_j}(\tau)}{\kappa P(H)} \right]^{\frac{\kappa}{\kappa-1}} d\tau,\ j \in \{1,\ldots,N\}. \tag{4.26}$$

Proof. See Appendix B.7. ■

As seen in (4.26), $P(H) = 0$ leads to an indeterminate form. However, if $R(t) = 0\ \forall\ t$, then, there exists an expression for optimal γ_j, which is valid for $P(H) = 0$. We present this result in the following lemma:

Lemma 4.4.3. *Let $\mathscr{F}(x) = Q_{\mathsf{No}} \left[\frac{x}{Q_{\mathsf{No}}} \right]^{\kappa}$, $Q_{\mathsf{No}} > 0$, $\kappa > 1$, $P(H) = 0$, $R(t) = 0\ \forall\ t$, and $D_{k_j}(t) = D^*_{k_j}(t)$, where $D^*_{k_j}(t)$ was defined in (4.23), then ρ attains its maximum at:*

$$\gamma_j = J(0) \frac{\Omega_j}{\sum_{n=1}^{N} \Omega_n}, \tag{4.27}$$

where:

$$\Omega_j = \int_{t_{j-1}}^{t_j} P_{k_j}(\tau)^{\frac{\kappa}{\kappa-1}} d\tau,\ j \in \{1,2,\ldots,N\}.$$

Proof. See Appendix B.7. ■

The results in Lemma 4.4.3 are also valid when the following constraint is enforced:

$$J(H) = J(0),$$

and $J(0)$ is initialized as follows:

$$J(0) = \varsigma \int_0^H R(t)dt.$$

In this case, $R(t)$ can take on any non-negative values in $[0,H]$.

4.4.2 Stochastic Optimization

In this section, we formulate a stochastic optimization problem to minimize the expected energy bill incurred by all the participants in $[0,H]$. The expected energy bill is

obtained by averaging over the ensemble of $J(t)$.

Unlike the offline strategy proposed in Sec. 4.4.1, the strategy that we propose in this section does not require any assumptions regarding the initialization of the storage device. Moreover, it only uses practically available, causal information of $J(t)$.

Stochastic model for $J(t)$

We use the following stochastic differential equation to model the random process $J(t)$:

$$dJ(t) = [\mu(t) - \theta(t)]J(t)dt + \mathsf{noise}, \tag{4.28}$$

where $\mathbb{E}[\mathsf{noise}] = 0$, $\mu(t)$ is a deterministic function of t, which represents the relative growth/contraction rate of $J(t)$, and $\theta(t)J(t)$ is the power intentionally drawn from the energy farm. A similar stochastic differential equation has been used in [185] to model renewable energy reserves under uncertainty.

In practice, $\mu(t)$ can be estimated for a fixed $J(0)$, by setting $\theta(t) = 0 \ \forall \ t$, and computing:

$$\mu(t) \approx \frac{\overline{J(t+\Delta t)} - \overline{J(t)}}{\overline{J(t)}}, \tag{4.29}$$

where $\overline{X(t)}$ represents the estimated mean value of $X(t)$, and Δt is the chosen discretization step. This model is flexible because $\mu(t)$ can be chosen arbitrarily to match statistical properties of the process such as its time-varying mean value. Moreover, $\mu(t)$ can take on negative values to represent phenomena such as leakage or self-discharge [6], [95].

According to (4.28), the consumption rate of renewable energy is $\theta(t)J(t)$, i.e. $\tilde{D}(t) = \theta(t)J(t)$. This assumption does not incur any loss of generality because $\theta(t)$ can be designed arbitrarily. Moreover, by using this substitution we automatically ensure that $\tilde{D}(t) = 0$ if $J(t) = 0$.

If the noise term in (4.28) takes on large negative values, then $J(t)$ may drop below 0. This is unrealistic because $J(t)$ models energy. To prevent $J(t)$ from taking negative values, we define the noise term as follows:

$$\mathsf{noise} = \sigma J(t) d\mathscr{W}, \tag{4.30}$$

where $d\mathscr{W} \sim \mathscr{N}(0, dt)$, and σ is a parameter which allows us to control the noise power. With this noise model, the energy reserve can, within a time interval of duration dt, go up or down in proportion to $J(t)$. As a result, if $J(0) > 0$, then $J(t) > 0 \; \forall \, t$, as we will show in Theorem 4.4.2. Moreover, this model makes physical sense because $J(t)$ can have a wider range of excursion when $J(t)$ is large. In contrast, if $J(t)$ is small, then so is its range of movement, since it cannot go below 0.

After replacing (4.30) in (4.28), we obtain the following stochastic differential equation:

$$dJ(t) = [\mu(t) - \theta(t)] J(t) dt + \sigma J(t) d\mathscr{W}. \tag{4.31}$$

Theorem 4.4.2. *Let $d\mathscr{W} = \mathscr{W}(t + dt) - \mathscr{W}(t)$, where $\mathscr{W}(t)$ is the standard Wiener process, then the solution to (4.31) is:*

$$J(t) = \mathsf{K}(t) \exp\left(\sigma \mathscr{W}(t)\right), \tag{4.32}$$

where:

$$\mathsf{K}(t) = J(0) \exp\left[\int_0^t \left(\mu(\tau) - \theta(\tau) - \frac{1}{2}\sigma^2\right) d\tau\right]. \tag{4.33}$$

Proof. See Appendix B.8. ■

Note that $d\mathscr{W} = \mathscr{W}(t + dt) - \mathscr{W}(t)$ implies $d\mathscr{W} \sim \mathscr{N}(0, dt)$, as previously stated.

Corollary 1 of Theorem 4.4.2: *If $J(0) > 0$, then $J(t) > 0$ for all $t > 0$, and for all realisations of $\mathscr{W}(t)$.*

Proof. By (4.33), $J(0) > 0$ implies $\mathsf{K}(t) > 0 \,\forall\, t$. Hence, by (4.32), we have $J(t) > 0 \,\forall\, t$, and for all realisations of $\mathscr{W}(t)$. ■

Following Corollary 1 of Theorem 4.4.2, all consumption rates of the form $\tilde{D}(t) = \theta(t)J(t)$ are feasible because (4.15) holds for any $\tilde{D}(t) = \theta(t)J(t)$, i.e. $J(t) > 0 \,\forall\, t$ and for any $\theta(t)$.

Corollary 2 of Theorem 4.4.2: *Given that $\mathscr{W}(t)$ is the Wiener process, $J(t)$ has continuous sample paths for all realisations of $\mathscr{W}(t)$.*

Proof. Given the definition of $d\mathscr{W}$, $J(t)$ is an Ito diffusion process because it satisfies (4.31). Therefore, all sample paths of $J(t)$ are continuous [186]. ■

Following Corollary 2 of Theorem 4.4.2, $J(t)$ does not have jump discontinuities. Sudden changes in $J(t)$ are the result of using or harvesting an infinite amount of power, hence, all sample paths of $J(t)$ must be continuous from physical considerations as well.

Corollary 3 of Theorem 4.4.2: *The expected value of $J(t)$ is given by:*

$$\mathbb{E}\left[J(t)\right] = \mathsf{K}(t)\exp\left(\frac{1}{2}\sigma t\right). \tag{4.34}$$

Proof. The result (4.34) follows immediately after taking expectation on both sides of (4.32), and noting that $\mathbb{E}\left[\exp\left(\sigma\mathscr{W}(t)\right)\right] = \exp\left(\frac{1}{2}\sigma t\right)$ [33]. ■

Following Corollary 3 of Theorem 4.4.2, the process $J(t)$ is non-stationary because its mean is time-dependent. This makes physical sense because solar irradiance and wind speed have seasonality.

Formulation of the stochastic optimization problem

To formulate the stochastic optimization problem we first simplify the objective function in P4.B1. Specifically, following Theorem 4.4.1, only one facility will access the

energy farm at any time t. Therefore, we can design $D(t) = D_1(t) + D_2(t) + \ldots + D_{\mathsf{M}}(t)$, and then determine $D_i(t),\ i \in \{1,2,\ldots,\mathsf{M}\}$ by using an indicator variable $\mathcal{I}_i$ as follows:

$$D_i(t) = \mathcal{I}_i D(t), \tag{4.35}$$

where $\mathcal{I}_i = 1$ if the ith facility has access to the energy farm, and $\mathcal{I}_i = 0$ otherwise.

Further, the ith facility has access to the energy farm in $[t_{j-1}, t_j]$ if $P_i(t) \geq P_k(t)\ \forall\, k \in \{1,2,\ldots,\mathsf{M}\}$ and $\forall\ t \in [t_{j-1}, t_j]$. As a result, we can design $D(t)$ by assuming that the price offered by the utility is $P(t) = \max_i\{P_i(t)\}\ \forall\ t$, which yields the following simplification:

$$\sum_{i=1}^{\mathsf{M}} \int_0^H P_i(t) D_i(t) dt = \int_0^H P(t) D(t) dt. \tag{4.36}$$

Moreover, by using $D(t) = \mathscr{G}\left[\tilde{D}(t)\right]$ and $\tilde{D}(t) = \theta(t) J(t)$, we can write $\int_0^H P(t) D(t) dt$ in terms of $\theta(t)$:

$$\int_0^H P(t) D(t) dt = \int_0^H P(t) \mathscr{G}\left[\theta(t) J(t)\right] dt. \tag{4.37}$$

By using (4.36) and (4.37), we can then cast the optimization problem in terms of $\theta(t)$ as follows:

$$\text{P4.B3:} \qquad \max_{\theta(t)}\ \ \mathbb{E}\left[\int_0^H P(t) \mathscr{G}\left[\theta(t) J(t)\right] dt + P(H) J(H)\right],$$

where the expected value in P4.B3 is taken over the ensemble of $J(t)$, which evolves according to (4.31). Since $\tilde{D}(t) = \theta(t) J(t)$, the constraint (4.15) can be disregarded because following Theorem 4.4.2 all the realisations of $J(t)$ are ensured to satisfy $J(t) > 0\ \forall\, t$, regardless of the choice of $\theta(t)$.

Solution by Continuous-Time Dynamic Programming

To solve P4.B3, we assume knowledge of $P(t)$, and the initial state of the storage device $J(0)$. At any time t, the value of $J(\tau)$ is only known for $\tau \leq t$. We then use the following

steps to obtain a solution by continuous-time dynamic programming:

1. We define the value function and apply Bellman's principle. The value function associated with our problem is:

$$V(t,J) = \max_{\theta} \quad \mathbb{E}_{t,J}\left[\int_t^H P(x)\mathscr{G}\left[\theta(x)J(x)\right]dx + P(H)J(H)\right], \tag{4.38}$$

where $\mathbb{E}_{t,J}[\cdot]$ denotes expectation over the ensemble of $J(\cdot)$ assuming knowledge of the process up to time t. By applying Bellman's principle [187], we obtain:

$$V(t,J) = \max_{\theta} \quad \mathbb{E}_{t,J}\left[\int_t^{t+\Delta t} P(x)\mathscr{G}\left[\theta(x)J(x)\right]dx + V(t+\Delta t, J+\Delta J)\right]. \tag{4.39}$$

From its definition, the value function satisfies the following boundary condition:

$$V(H,J) = P(H)J(H). \tag{4.40}$$

2. We derive the Hamilton-Jacobi-Bellman equation. Let $0 < \nu < 1$, then by the rectangular approximation of definite integrals, for small Δt we have:

$$\int_t^{t+\Delta t} P(x)\mathscr{G}\left[\theta(x)J(x)\right]dx \approx P(t+\nu\Delta t)\mathscr{G}\left[\theta(t+\nu\Delta t)J(t+\nu\Delta t)\right]\Delta t. \tag{4.41}$$

After replacing (4.41) in (4.39) we obtain:

$$V(t,J) = \max_{\theta} \quad \mathbb{E}_{t,J}\left[\Delta t P(\bar{t})\mathscr{G}\left[\theta(\bar{t})J(\bar{t})\right] + V(t+\Delta t, J+\Delta J)\right], \tag{4.42}$$

where $\bar{t} = t + \nu\Delta t$. Moreover, by the Taylor approximation we have:

$$V(t+\Delta t, J+\Delta J) = V(t,J) + \frac{\partial V}{\partial t}\Delta t + \frac{\partial V}{\partial J}\Delta J + \frac{1}{2}\frac{\partial^2 V}{\partial J^2}(\Delta J)^2 + o(\Delta t). \tag{4.43}$$

Substituting (4.43) into (4.42) and, dividing by Δt, we obtain:

$$0 = \max_{\theta} \mathbb{E}_{t,J}\left[P(\bar{t})\mathscr{G}\left[\theta(\bar{t})J(\bar{t})\right] + \frac{\partial V}{\partial t} + \frac{\partial V}{\partial J}\frac{\Delta J}{\Delta t} + \frac{1}{2}\frac{\partial^2 V}{\partial J^2}\frac{(\Delta J)^2}{\Delta t}\right]. \tag{4.44}$$

Therefore, by letting $\Delta t \to 0$, we obtain the following equation, known as the

Hamilton-Jacobi-Bellman equation [183], [187]:

$$0 = \max_{\theta} \mathbb{E}_{t,J}\left[P(t)\mathscr{G}\left[\theta(t)J(t)\right] + \frac{\partial V}{\partial t} + \frac{\partial V}{\partial J}\frac{dJ}{dt} + \frac{1}{2}\frac{\partial^2 V}{\partial J^2}\frac{(dJ)^2}{dt}\right]. \tag{4.45}$$

From (4.31), we have $\mathbb{E}_{t,J}[dJ] = [\mu(t) - \theta(t)]J(t)dt$. Moreover:

Lemma 4.4.4. $\mathbb{E}_{t,J}[(dJ)^2] = [\sigma J(t)]^2 dt$

Proof. From (4.31), we have (time indices left out for brevity):

$$\mathbb{E}_{t,J}\left[(dJ)^2\right] = \mathbb{E}_{t,J}\left[([\mu-\theta]Jdt)^2 + 2\sigma[\mu-\theta]JdtJd\mathscr{W} + (\sigma Jd\mathscr{W})^2\right] = (\sigma J)^2 dt.$$

The last result follows from $\mathbb{E}_{t,J}[(d\mathscr{W})^2] = dt$, $\mathbb{E}_{t,J}[dtd\mathscr{W}] = 0$, and $dt^2 \approx 0$. ■

After replacing $\mathbb{E}_{t,J}[dJ] = [\mu(t) - \theta(t)]J(t)dt$ and $\mathbb{E}_{t,J}[(dJ)^2] = (\sigma J)^2 dt$ in (4.45) we obtain the following partial differential equation:

$$0 = \max_{\theta}\left\{P(t)\mathscr{G}\left[\theta(t)J(t)\right] + \left[\frac{\partial V}{\partial t} + [\mu(t)-\theta(t)]J\frac{\partial V}{\partial J} + \frac{1}{2}\sigma^2 J^2\frac{\partial^2 V}{\partial J^2}\right]\right\}. \tag{4.46}$$

3. We find a candidate solution by using a first-order optimality condition. Since the function $f(\theta) = P\,\mathscr{G}[\theta J] + \left(\frac{\partial}{\partial t} + [\mu-\theta]J\frac{\partial}{\partial J} + \frac{1}{2}(\sigma J)^2\frac{\partial^2}{\partial J^2}\right)V(t,J)$ is concave[6] in θ, we maximize it by introducing this first-order optimality condition $\frac{df}{d\theta} = 0$, which leads to:

$$P(t)\frac{\partial}{\partial\theta}\mathscr{G}\left[\theta J\right] = J(t)\frac{\partial V}{\partial J}. \tag{4.47}$$

Let $\theta^*(t)$ denote the optimal $\theta(t)$. Then (4.46) can be simplified to:

$$0 = P(t)\mathscr{G}\left[\theta^*(t)J(t)\right] + \left[\frac{\partial V}{\partial t} + [\mu(t)-\theta^*(t)]J\frac{\partial V}{\partial J} + \frac{1}{2}\sigma^2 J^2\frac{\partial^2 V}{\partial J^2}\right]. \tag{4.48}$$

4. We solve the Hamilton-Jacobi-Bellman equation, i.e. we find $V(t,J)$ and $\theta^*(t)$ which satisfy (4.48). This step depends on the function $\mathscr{G}[x]$. And for illustration

[6] Note that $\mathscr{G}(x)$ is concave in x because it is the inverse of a convex, strictly increasing and continuous function [177].

purposes, in the rest of this chapter we will assume that $\mathscr{G}(x) = Q_{\mathsf{No}}\left(\frac{x}{Q_{\mathsf{No}}}\right)^{\frac{1}{\kappa}}$, with $Q_{\mathsf{No}} > 0$ and $\kappa > 1$. Thus, from (4.47) we obtain the following candidate solution:

$$V^*(t,J) = \left[\frac{1}{Q_{\mathsf{No}}}\right]^{\phi-1} P(t)[J^{\phi}]\,[\theta^*(t)]^{\phi-1},\ \theta^*(t) > 0,\ \forall\, t, \tag{4.49}$$

where $\phi = \frac{1}{\kappa}$ has been introduced to simplify notation.

We now plug $V^*(t,J)$ in (4.48) and find the conditions under which $\theta^*(\cdot)$ and $V^*(t,J)$ satisfy (4.48). Hence, we start by computing the partial derivative of $V^*(t,J)$ with respect to t:

$$\frac{\partial}{\partial t}V^*(t,J) = \left[\frac{1}{Q_{\mathsf{No}}}\right]^{\phi-1}\left[P'(t)[\theta^*(t)]^{\phi-1}[J^{\phi}] + (\phi-1)P(t)[J(t)]^{\phi}[\theta^*(t)]^{\phi-2}\frac{d}{dt}\theta^*(t)\right],$$

where $P'(t) = \frac{d}{dt}P(t)$. Moreover, the second-order partial derivative of $V^*(t,J)$ with respect to J is:

$$\frac{\partial^2 V^*(t,J)}{\partial J^2} = \phi\,(\phi-1)\left[\frac{1}{Q_{\mathsf{No}}}\right]^{\phi-1} P(t)\,[\theta^*(t)]^{\phi-1}\,[J]^{\phi-2}.$$

After replacing these derivatives into (4.48), we obtain the following condition for optimal $\theta^*(t)$, so that (4.48) is satisfied:

$$\frac{d\theta^*}{dt} = (\theta^*)^2 + y(t)\theta^*, \tag{4.50}$$

with:

$$y(t) = \frac{1}{1-\phi}\left(\phi\mu(t) + \frac{P'(t)}{P(t)}\right) - \frac{1}{2}\sigma^2\phi.$$

The equation (4.50) is a non-linear differential equation that can be solved by appropriate substitutions. The non-trivial[7] solutions to (4.50) are:

$$\theta^*(t) = \frac{\exp\left(\int_0^t y(z)dz\right)}{\frac{1}{\theta^*(0)} - \int_0^t \exp\left(\int_0^x y(\tau)d\tau\right)dx}, \tag{4.51}$$

[7] If $y(t)$ is constant over time, then the trivial solution to (4.50) is $\theta^*(t) = -y(t)$.

where $\theta^*(0)$ can be found by using the boundary condition (4.40):

$$\left[\frac{1}{Q_{\mathsf{No}}}\right]^{\phi-1} P(H)[J(H)]^{\phi}\left[\theta^*(H)\right]^{\phi-1} = P(H)J(H).$$

By assuming $[J(H)]^{\phi} \approx [J(H)]$, which holds true for $\phi \to 1^{-}$, we obtain:

$$\theta^*(H) = Q_{\mathsf{No}}. \tag{4.52}$$

The result in (4.52) can be used to determine $\theta^*(0)$ in (4.51).

5. For $\mathscr{G}(x) = Q_{\mathsf{No}}\left(\frac{x}{Q_{\mathsf{No}}}\right)^{\phi}$ we discuss some special cases:

a. If $y(t)$ is a constant, then so is $\theta^*(t)$. Specifically, the solution to (4.50) is $\theta^*(t) = -y(t)$, i.e.:

$$\theta^*(t) = \frac{1}{2}\sigma^2\phi - \frac{1}{1-\phi}\left(\phi\mu(t) + \frac{P'(t)}{P(t)}\right). \tag{4.53}$$

b. If $\sigma \ll 1$, then:

$$\theta^*(t) = \frac{h(t)}{\frac{h(0)}{\theta^*(0)} - \int_0^t h(x)dx}, \tag{4.54}$$

where

$$h(t) = \left[\exp\left(\phi\int\mu(t)dt\right)P(t)\right]^{\frac{1}{1-\phi}}.$$

In (4.54) we have used $\frac{P'(t)}{P(t)} = \frac{d}{dt}\log[P(t)]$.

c. If $|\mu(t)| \ll 1\ \forall\, t$, and $\sigma \ll 1$, then:

$$\theta^*(t) = \frac{P(t)^{\frac{1}{1-\phi}}}{\frac{P(0)^{\frac{1}{1-\phi}}}{\theta^*(0)} - \int_0^t P(x)^{\frac{1}{1-\phi}}dx}. \tag{4.55}$$

Observation: If $\phi \to 1^{-}$, then $\theta^*(t)$ does not depend on σ because $y(t) \approx \frac{1}{1-\phi}\left(\phi\mu(t) + \frac{P'(t)}{P(t)}\right)$. Contrarily, if $P'(t) = 0$ and $\mu(t) = 0\ \forall\, t$, then the optimal energy consumption rate is $\frac{1}{2}\phi\sigma J(t)$, i.e. $\theta^*(t)$ increases linearly with σ.

6. We discuss the optimality of $\theta^*(t)$ and implementation feasibility: Assume continuous consumption, i.e. $\theta^*(t) > 0 \ \forall \ t \in [0,H]$, and let $P(t)$ be of class[8] C^1, and $J(t) > 0 \ \forall \ t$, then $V^*(t,J)$ is of class $C^{1,2}$, i.e. continuously differentiable in t, and twice continuously differentiable in J. Moreover, from its definition, $V^*(t,J)$ satisfies a polynomial growth condition, hence by the verification theorem [187], $\theta^*(t)$ is optimal because $V^*(t,J)$ satisfies both the boundary condition (4.40), and the Hamilton-Jacobi-Bellman equation.

By Theorem 4.4.2, the consumption rate of renewable energy can be set to $\theta^*(t)J(t)$ at all times. Hence, consuming $\theta^*(t)J(t)$ is always feasible.

4.5 Numerical Results and Discussion

We present numerical results to validate the analysis presented in this chapter. We divide this section into three parts: In the first part, we study the performance of the energy sharing strategy proposed in Sec. 4.2. In the second part, we compare the performance of the energy sharing strategies proposed in Sections 4.2 and 4.3. Finally, in the third part we discuss the performance of the strategy proposed in Section 4.4. Throughout this section we use (2.4) to model the relationship between $D(t)$ and $\tilde{D}(t)$, and between $D_i(t)$ and $\tilde{D}_i(t)$.

4.5.1 Energy Sharing with Distributed Generation and Storage

In this section we investigate the circumstances under which the cooperating facilities resort to renewable energy sharing to minimize their collective expenditure. For simplicity we consider a set of two facilities, and analyse the following scenarios:

- Scenario A: Price signals, loads, renewable energy generation, and battery parameters are all equal across participants. The only difference between the two is the energy

[8] In general, the point-wise maximum of M differentiable functions is almost everywhere differentiable. However, we can regard $P(t)$ as a differentiable approximation of $\max_i\{P_i(t)\}$, which is smooth in $[0,H]$.

Table 4.1: Simulation scenarios (distributed generation and storage).

	Scenario A	Scenario B	Scenario C	Scenario D
H	1			
Δt	0.01			
$R_1(t)$	$15\cos(2\pi t)+20$			0
$R_2(t)$	$15\cos(2\pi t)+20$			
$L_1(t)$	$20\sin(2\pi t-3)+20$			
$L_2(t)$	$L_1(t)$	$20\cos(2\pi t-3)+20$	$L_1(t)$	
ς	1			
κ	1.3			
Q_{No}	50		20	
$D_{\max}$	50		20	
M	2			
$P_1(t)$	$0.5\sin(2\pi t)+1.5$			
$P_2(t)$	$P_1(t)$		$0.5\cos(2\pi t)+1.5$	$P_1(t)$
df	0.9			
Ψ_1	500			
Ψ_2	500			
$J_1(0)$	10	0		
$J_2(0)$	0			

initially available in the battery. The parameters are summarized in Table 4.1. As observed in Fig. 4.4, power is at some point transferred from the participant with more renewable energy locally stored. In this case, the sharing strategy contributes to reducing the energy that the second participant would otherwise draw from the grid.

- Scenario B: Price signals, renewable energy generation, and battery parameters (including the energy initially stored in each of the devices) are all equal across participants. The only difference between the two sets of parameters is the load demand, as shown in Table 4.1. It is observed in Fig. 4.5 that load differences can trigger the energy sharing mechanism, even if the price signals are identical between the participants, and fees are incurred in the energy transfer. This result follows because the proposed strategy seeks to maximize the consumption of renewable energy within $[0,H]$, hence if a facility is unable to consume its renewable energy within the planning horizon, then the excess must be transferred to another facility with a higher

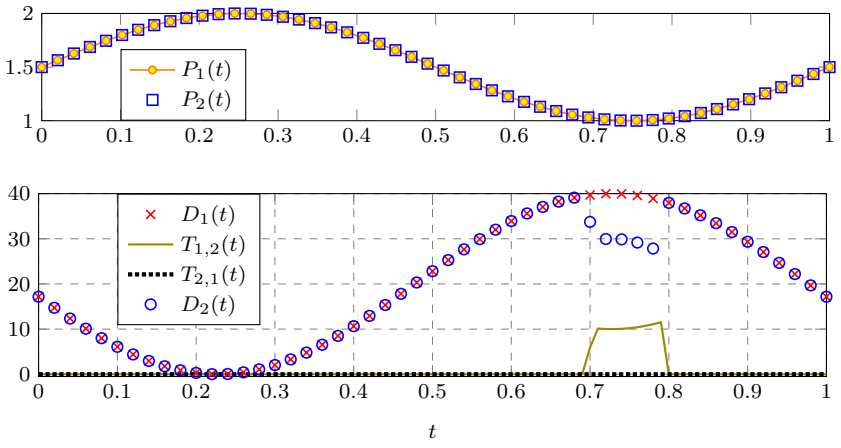

Figure 4.4: Top: Pricing profiles. Bottom: Optimal power flows and renewable energy consumption rate. Simulation parameters as in Scenario A.

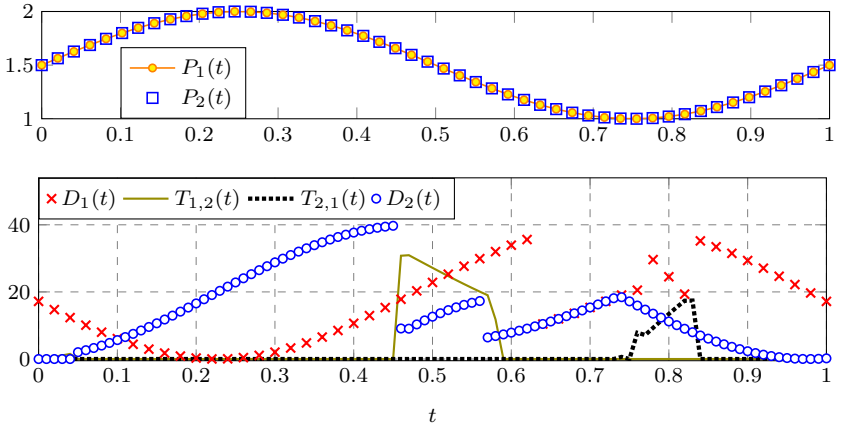

Figure 4.5: Top: Pricing profiles. Bottom: Optimal power flows and renewable energy consumption rate. Simulation parameters as in Scenario B.

load demand.

- Scenario C: Load demands, renewable energy generation, and battery parameters (including the energy initially stored in each of the devices) are all equal across participants. The only difference between the two sets of parameters is in the price signals, as shown in Table 4.1. Again, as observed in Fig. 4.6, price differences trigger the energy sharing mechanism, despite the fees incurred in the energy transfer. This follows

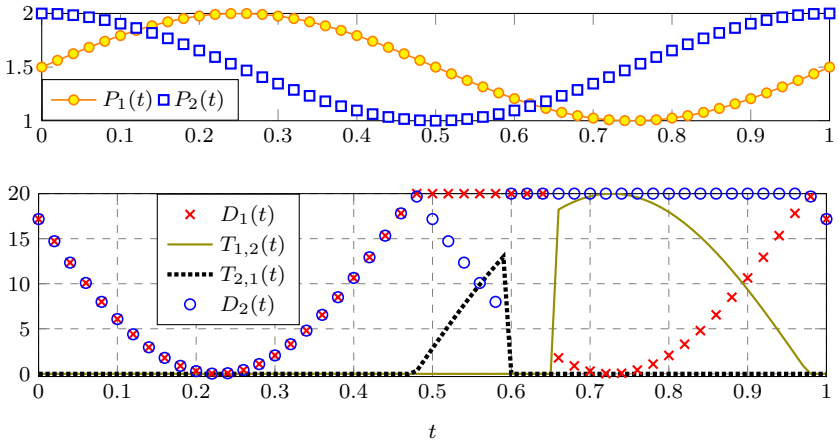

Figure 4.6: Top: Pricing profiles. Bottom: Optimal power flows and renewable energy consumption rate. Simulation parameters as in Scenario C.

because the fee incurred is small, i.e. $\mathsf{df} = 0.9$, and leveraging the price differences can provide a bigger benefit.

- Scenario D: Price signals, loads, and battery parameters –including $J_1(0)$ and $J_2(0)$– are all equal across participants, but the renewable energy generation is different, i.e. $R_1(t) \neq R_2(t)$. As observed in Fig. 4.7, having $R_1(t) \neq R_2(t)$ also triggers the energy sharing strategy, even when $P_1(t) = P_2(t)\ \forall\ t$ and $\mathsf{df} < 1$. Again, this result follows because the proposed strategy seeks to maximize the consumption of renewable energy in $[0,H]$, i.e. if a facility is unable to completely consume its renewable energy, then it must transfer the excess energy to a facility with lower generation capacity.

4.5.2 Distributed vs. Centralized Generation and Storage

In this section we compare the performance of the two architectures studied in this chapter. To that end, we consider the same set of two facilities and the simulation scenarios summarized in Table 4.2.

The parameters not listed in Table 4.2 are common to all the simulation scenarios. Specifically, $P_1(t) = 10\sin(2\pi t) + 10$, $P_2(t) = -10\sin(2\pi t) + 10$, $\mathsf{df} = 1$,

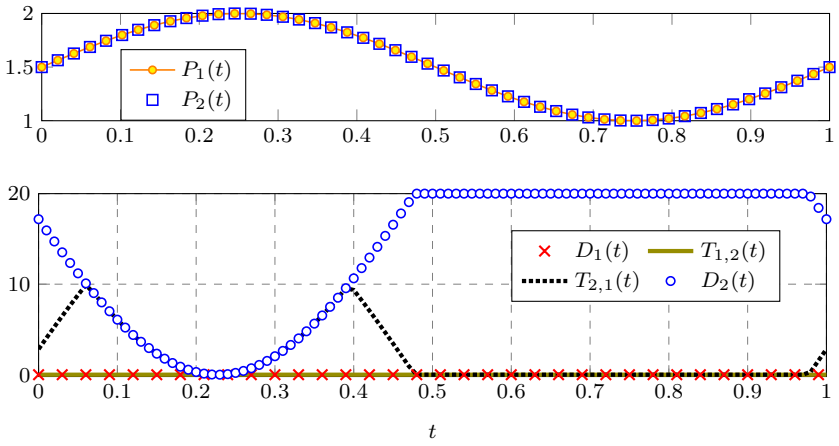

Figure 4.7: Top: Pricing profiles. Bottom: Optimal power flows and renewable energy consumption rate. Simulation parameters as in Scenario D.

Table 4.2: Simulation scenarios (centralized vs. distributed generation and storage).

	Scenario E	Scenario F	Scenario G	Scenario H
H	1			
Δt	0.1			
$R_1(t)$	$\sim \mathscr{U}(0,10)$			
$R_2(t)$	$\sim \mathscr{U}(0,10)$			
$R(t)$	$R_1(t)+R_2(t)$	$\sim \mathscr{U}(0,20)$	$R_1(t)+R_2(t)$	$\sim \mathscr{U}(0,10)+\mathscr{U}(0,10)$
$L_1(t)$	$12\ \forall\, t$			
$L_2(t)$	$12\ \forall\, t$			
ς	1			
κ	1.3			
Q_{No}	12		10	12
$D_{\max}$	12		10	12

$\Psi \in \{0, 0.5, 1, 1.5, 2\}$, $J_1(0) = 0$, $J_2(0) = 0$, $J(0) = 0$. After simulating the scenarios described in Table 4.2 we obtained the following insights:

Scenario E: As shown in Fig. 4.8, in this case both the centralized and distributed architectures lead to a similar performance. The plots shown in Fig. 4.8 were obtained by averaging over the results of ten thousand realisations. The performance similarity follows because the total renewable energy generated in both models is the same, the discount factor df is unitary, i.e. no transfer fees are imposed, and the battery parameters are such that the losses derived from the battery operation are the same in both

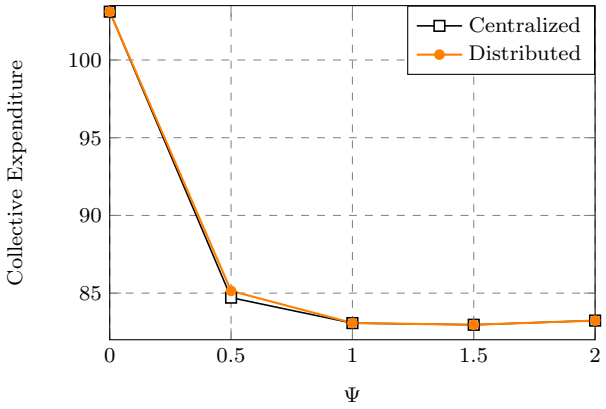

Figure 4.8: Centralized vs. distributed renewable energy generation and storage. Simulation parameters as in Scenario E.

architectures.

Scenario F: In this scenario, we have that $R(t) \neq R_1(t) + R_2(t)$, i.e. the total renewable power generated in the centralized architecture is not necessarily the same as the renewable power harvested in the distributed model. Instead, $R(t)$, $R_1(t)$, and $R_2(t)$ are independent, and $R(t)$ is allowed to take on values drawn from a uniform distribution between 0 and 20. Despite the fact that the average renewable energy harvested is the same in both layouts, the distributed model outperforms the centralized architecture, as shown in Fig. 4.9. This result follows also despite having chosen the other parameters as in Scenario E, which led to strikingly similar results in both models. A possible explanation for this outcome lies in the variance of the renewable power arrivals, which is larger in the model with centralized storage, and the assumed independence of the renewable power generation across different locations.

Scenario G: In this scenario, we decrease $D_{\max}$ and Q_{No} to 10, and introduce two additional constraints, namely $D_1(t) \leq D_{\max}$ and $D_2(t) \leq D_{\max}$, while maintaining other simulation parameters as in Scenario E. As shown in Fig. 4.10, the two architectures lead to different performances in this scenario. There is a performance loss in the centralized model, which results from the additional constraints introduced. This result can

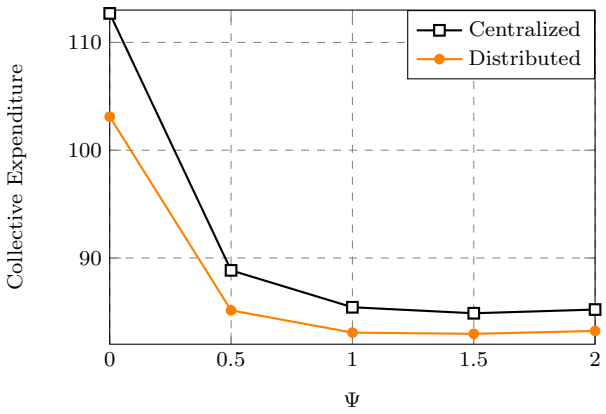

Figure 4.9: Centralized vs. distributed renewable energy generation and storage. Simulation parameters as in Scenario F.

give some insights on how the constraints (4.7c) and (4.13c) affect the performance of the proposed models, and how the battery parameters should be chosen so as to achieve the desired performance.

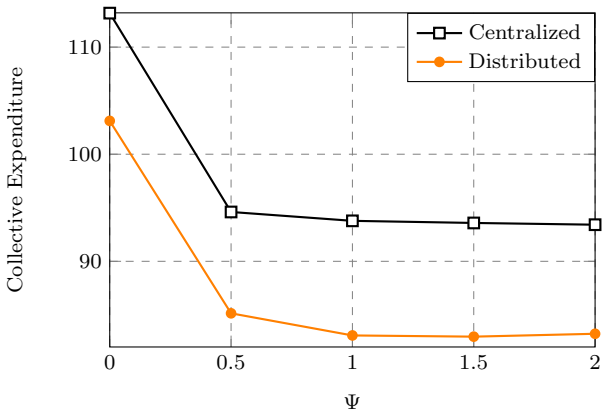

Figure 4.10: Centralized vs. distributed renewable energy generation and storage. Simulation parameters as in Scenario G.

Scenario H: In this scenario, we let $R(t)$ be the sum of two independent random variables drawn from a uniform distribution ranging from 0 to 10. The other parameters are the same as in Scenario E. While the statistical properties of the energy harvested in both models are the same, the realisations of $R_1(t)$, $R_2(t)$ and $R(t)$ are independent. The results obtained show a very similar performance as seen in Fig. 4.11.

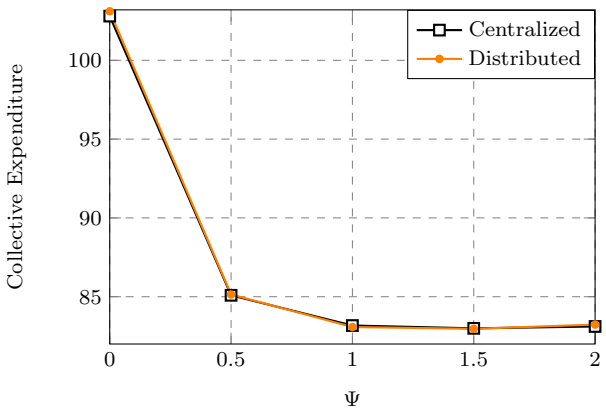

Figure 4.11: Centralized vs. distributed renewable energy generation and storage. Simulation parameters as in Scenario H.

4.5.3 Solution by Continuous-Time Dynamic Programming

We now evaluate our strategy based on continuous-time dynamic programming. Again, we consider the time interval $[0,1]$, and begin by generating sample paths of $J(t)$. In Fig. 4.12, we have plotted two sample paths of $J(t)$, along with the relative growth/contraction rate $\mu(t)$. As expected, the variability of the process increases with σ. Furthermore, $J(t)$ tends to grow when $\mu(t) > 0$, and shrink when $\mu(t) < 0$.

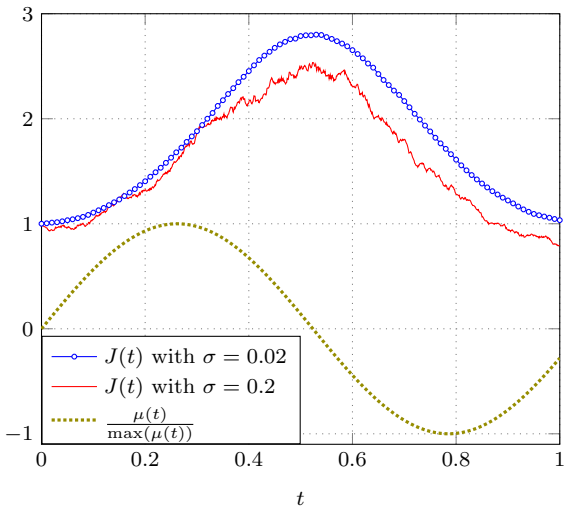

Figure 4.12: Sample paths of $J(t)$ with $J(0) = 1$. The normalized growth (or contraction) rate $\mu(t)$ is also shown.

For simplicity we set $Q_{\mathsf{No}} = 1$, and consider $\mathscr{G}(x) = x^{\phi}$. Hence, to simplify notation, we let ξ denote the objective function in P4.B3, i.e.,

$$\xi = \mathbb{E}\left[\int_0^H P(t)\left[\theta(t)J(t)\right]^{\phi} dt + P(H)J(H)\right],$$

and ξ^* denote the maximum value of ξ, which is attained when $\theta(t) = \theta^*(t)$, $t \in [0,1]$. Other simulation parameters are chosen as follows: $P(t) = 0.5\sin(10t) + 1.5$, and $\mu(t) = \alpha - \frac{P'(t)}{\phi P(t)}$, for some constant α. This setting implies that both $y(t)$ and $\theta^*(t)$ are constant in $[0,H]$. Specifically, $\theta^*(t) = 0.425\sigma - 5.66\alpha$. Moreover, we consider a fixed $\phi = 0.85$, while the initial state of the storage device is $J(0) = 100$.

In Fig. 4.13, we have plotted the obtained ξ for different values of $\theta(t)$, which under the scenario described above must be constant in $[0,H]$. As seen in Fig. 4.13, ξ attains its maximum when $\theta(t) = \theta^*$ for all $t \in [0,H]$. The results shown in Fig. 4.13 were obtained by averaging over ten thousand realisations of $J(t)$ with $\sigma = 0.1$.

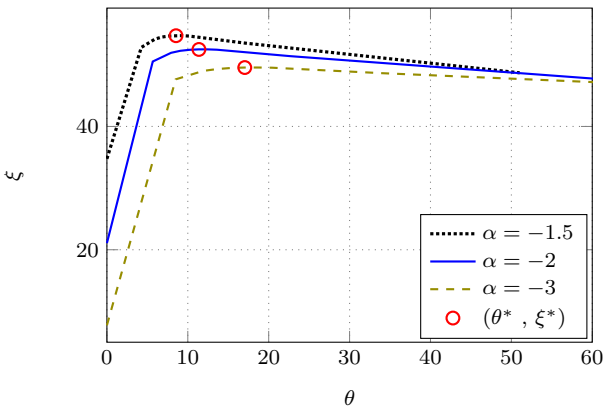

Figure 4.13: Objective function in P4B.3 for different values of θ. Optimal ξ is denoted by ξ^*.

4.6 Summary

In this chapter we have proposed strategies to minimize the energy expenditure incurred by a set of non-deferrable load facilities over a finite planning horizon. We have con-

sidered facilities equipped with renewable energy harvesters and storage devices, and enabled to share renewable energy, either through the smart grid, or dedicated power lines. We have then proposed two genie-aided strategies, and made the corresponding comparisons. To design the first strategy, we have assumed that all the participating facilities are equipped with their own renewable energy harvester and storage device, and are allowed to exchange energy through the smart grid incurring transfer fees. To design the second strategy, we have assumed that all the facilities have shared access to an energy farm where renewable power is harvested and stored. We have also assumed that the participating facilities can draw renewable energy from the farm at no cost. We have then compared the two approaches and found the conditions under which they achieve similar performance. Through simulations, we have also shown that the model with distributed harvesting and storage outperforms the centralized model when the renewable energy arrivals are independent across different locations. The two strategies have similar performance when the renewable energy arrivals are statistically identical, and battery parameters are chosen adequately.

For the case in which the participating facilities have shared access to a renewable energy farm, we have provided further insights by studying the problem in continuous time. We have specifically designed the optimal access policy, and the optimal energy consumption rate over time. To this end, we have solved a rather challenging optimization problem, which cannot be attacked by using conventional methods. We have therefore combined several optimization techniques to obtain an approximate solution. We have specifically used methods such as partitioning, decomposition, calculus of variations, and Lagrange multipliers. The first two techniques have allowed us to break the problem into smaller sub-problems. We have also introduced artificial variables to cast the mathematical problem into a separable optimization problem. We have then

obtained an approximate solution by determining the optimal trajectories (power consumption profiles) in terms of the auxiliary variables, which have been later optimized by solving a simpler mathematical problem.

We have also proposed a strategy that does not require exact knowledge of future renewable energy arrivals, and is based on continuous-time dynamic programming. To design the proposed online strategy, we have used a model based on stochastic differential equations to depict the random process governing the behaviour over time of the renewable energy available at the central storage. This model ensures that the random process only takes on non-negative values, has continuous sample paths, and is non-stationary.

We have presented numerical results to confirm the rationality of the results obtained, and draw the following insights:

- Renewable energy sharing should be enabled when the participants' conditions differ in at least one of the following aspects:

    1. Pricing signals: A strong motivation to enable energy sharing is to leverage price differences across locations.

    2. Renewable energy arrivals: Even with the same pricing conditions, participants with differences in their local generation can reduce their collective expenditure by sharing renewable energy.

    3. Load demands: Even with the same pricing conditions, and local generation, participants with different load requirements resort to renewable energy sharing to minimize their collective expenditure. This result follows because our strategy seeks to maximize the consumption of renewable energy within the planning horizon. Hence, if a participating facility is unable to consume its own

renewable energy, then it must transfer its excess power to facilities with higher energy demands.

4. Energy initially available: If $J_1(0) \neq J_2(0) \neq \ldots \neq J_{\mathsf{M}}(0)$, then the power sharing strategy is implemented to optimally allocate the total renewable energy available among all the participants.

- There are some conditions under which the distributed and centralized harvesting/storage architectures lead to a similar performance. Specifically, if the renewable energy generation is statistically identical, and if the storage devices are such that their operation leads to the same losses in both models, then the two architectures have similar performance. We have encountered differences in performance when the spatial diversity is accounted for in the distributed model. In such a situation, we have shown that the distributed model outperforms the centralized architecture. A result which follows from the assumed independence of the renewable energy arrivals across different locations, and the increased[9] variance of the renewable energy arrivals in the centralized architecture.

- For $\mathscr{G}(x) = Q_{\mathsf{No}} \left(\frac{x}{Q_{\mathsf{No}}}\right)^{\frac{1}{\kappa}}$ with $Q_{\mathsf{No}} > 0$ and $\kappa > 1$, we have obtained the following insights from the strategy based on continuous-time dynamic programming:

  – If the electricity prices are constant over time, and the renewable energy has zero expected growth/contraction rate, then the optimal energy consumption rate increases linearly with σ, which determines the level of uncertainty in the amount of renewable energy available over time.

  – Let $\tilde{D}(t)$ and $J(t)$ denote respectively the power drawn from, and the energy available at the farm over time. Then, the optimal $\frac{\tilde{D}(t)}{J(t)}$ remains constant when the rel-

[9] We have specifically considered renewable energy arrivals drawn from a uniform distribution. Hence larger generation capacity results in an increased variance for $R(t)$.

ative harvesting/self-discharging rate $\mu(t)$ and the pricing function $P(t)$ are such that $\mu(t) - \kappa\frac{P'(t)}{P(t)}$ is constant over time.

– If Peukert's exponent is close to 1, then we can design the optimal energy consumption rate by assuming that the renewable energy reserve evolves according to a deterministic differential equation.

Chapter 5

Energy Management with Nonlinear Electricity Pricing

Assuming a non-linear pricing scheme, in this chapter we propose strategies to minimize the energy bill incurred by a non-deferrable load over a finite planning horizon. We specifically consider dynamic block pricing, which combines pricing schemes such as time-of-use and consumption-based block pricing. We assume a facility equipped with a renewable energy harvester and a storage device, and propose two genie-aided strategies to minimize its expenditure over a finite planning horizon. The first strategy is obtained by solving a constrained optimization problem through linearisation and discretisation in time (LDT). The second strategy is obtained by solving the same optimization problem in continuous time after introducing appropriate simplifying approximations. In this chapter we also examine the relationship between the cost function and the total amount of energy shifted in time[1] over a single pair of consecutive charging and discharging periods. We then use this analysis to estimate the energy storage capacity required to minimize the expenditure over the planning horizon in consideration.

5.1 Contributions

The main contributions of this chapter are the following:

- Considering dynamic block pricing, we propose strategies to minimize the energy bill incurred by a non-deferrable load facility over a finite planning horizon. We assume

[1] In a single pair of consecutive charging and discharging operations, the energy shifted in time is the total amount of grid-energy charged into the battery and which is later drawn from the battery to (partially) satisfy the load over the discharging period.

that the facility is equipped with a renewable energy harvester and a rechargeable device. We then formulate a constrained optimization problem, and obtain the solution by using different methods. The first method is linearisation and discretisation in time, which allows us to obtain a precision-adjustable solution. The second method is based on calculus of variations (CoV), and delivers an approximate solution in analytic form when the discharging model is Peukert's.

- Assuming a discharging model based on Peukert's Law, we analyse the cost function in terms of the total energy shifted in time within a single pair of consecutive charging and discharging operations. We specifically show that the optimal energy bill is convex in Θ, the total energy shifted in time during the period in consideration. Moreover, after introducing some simplifications we obtain an analytical expression for Θ^*, which is the value of Θ that minimizes the cost function. The obtained expression for Θ^* can be used to determine the storage capacity, which is required to handle the shifting in time of Θ^* energy units, and store the amount of renewable energy generated within the same planning horizon.

5.2 System Model

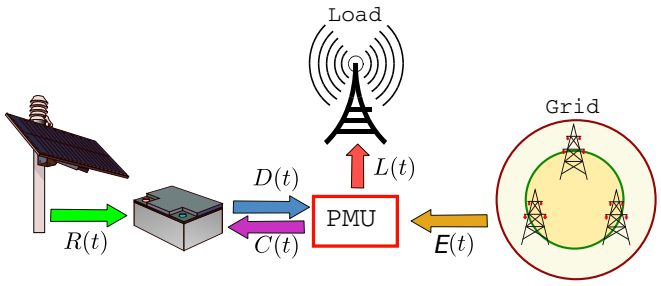

Figure 5.1: System model. The load is represented by a base station. PMU stands for power management unit.

5.2.1 General Setup

Fig. 5.1 shows the principal elements of the system of interest. The non-deferrable load facility is represented by a base station, and is equipped with a renewable energy harvester and a storage device. The facility is permanently connected to the power grid through the power management unit. The power management unit controls the power flow between the grid and the load, and schedules the charging and discharging operations of the battery system. As shown in Fig. 5.1, the facility can be powered directly from the grid, and also from the storage device, which stores locally harvested renewable energy and also energy from the grid.

We consider a finite planning horizon of H time units, where H is such that the components of the system retain their physical properties in $[0,H]$. The load $L(t)$ is assumed to vary as a function of time $t \in [0,H]$. The power drawn from the grid to charge the storage device is denoted by $C(t) \geq 0$, and the effective power discharged is denoted by $D(t) \geq 0$. Note that $D(t) \leq L(t)\ \forall\, t$, and the power drawn from the grid is thus

$$E(t) = L(t) + C(t) - D(t). \tag{5.1}$$

Since the energy available in the storage device comes from both the renewable energy harvester and the grid, in this chapter we restrict $D(t)$ to satisfy $D(t) \leq L(t)\ \forall\, t$. And hence, no energy is returned to the grid.[2]

5.2.2 Electricity Pricing Scheme

In this section we describe the dynamic block pricing model, a combination of time-of-use and consumption-based block pricing schemes. In dynamic block pricing, the

[2] As the battery system stores both renewable and on-grid energy, we find it sensible to enforce $D(t) \leq L(t)\ \forall\, t$. Without such a restriction, the consumers can profit from trading non-renewable energy with the utility, which may not be practical.

relationship between the final cost and the quantity of energy consumed is non-linear. We present two mathematical models to describe this pricing scheme. The first model is continuous-time block pricing, and uses the concept of "chargeable power" function, which takes on the actual power consumed and outputs the effective amount of power based on which the bill is computed. The second model does not employ the "chargeable power" function, but describes the block pricing scheme through a bivariate function, whose inputs are time of the day and energy consumed within a given time interval, and whose output is the cost incurred. The first model is more suitable for a problem formulation in continuous time, whereas the second model is defined in the discrete domain. As we will show, the model in continuous time generalizes the pricing model in the discrete domain, which is the one most often used in the literature.

Continuous-Time Block Pricing

Continuous-time block pricing establishes an energy tariff that depends on both the time of the day, and the amount of energy consumed. In continuous-time block pricing the cost of the energy drawn from the grid in the period $[0,H]$ is computed as follows:

$$\chi = \int_0^H P(t)F\left[E(t)\right]dt, \tag{5.2}$$

where $P(t) > 0 \; \forall \; t$ represents the pricing function, and $F(\cdot)$ is the block tariffing function, defined as follows:

$$F\left[E(t)\right] = \begin{cases} a_1 E(t) & E(t) \leq \Pi_1 \\ a_2 E(t) - b_2 & \Pi_1 < E(t) \leq \Pi_2 \\ & \vdots \\ a_B E(t) - b_B & \Pi_{B-1} < E(t), \end{cases} \tag{5.3}$$

where B is the number of block tariffs, $0 < a_1 < a_2 < \cdots < a_B$ are the penalty factors, $0 < \Pi_1 < \Pi_2 < \cdots < \Pi_{B-1}$ are the pre-defined power thresholds, and $b_j > 0$ are chosen to ensure that $F(\cdot)$ is a continuous function, e.g. $b_2 = (a_2 - a_1)\Pi_1$. The units for $F[E(t)]$, $E(t)$ and b_j are all power units. $P(t)$ is specified in monetary units per unit of energy, and $P(t)F[E(t)]\,dt$ is therefore the tariff charged to the consumer in the interval $[t, t+dt]$ when $dt \to 0$. Clearly, $F(\cdot)$ defines a "chargeable power" function, whose input is the amount of power consumed, and whose output is the quantity based on which the final tariff is computed. Note that $F(\cdot)$ can be written as:

$$F[E(t)] = \max_j \{a_j E(t) - b_j\}, \tag{5.4}$$

with $1 \leq j \leq B$, and $b_1 = 0$. This identity is illustrated in Fig. 5.2.

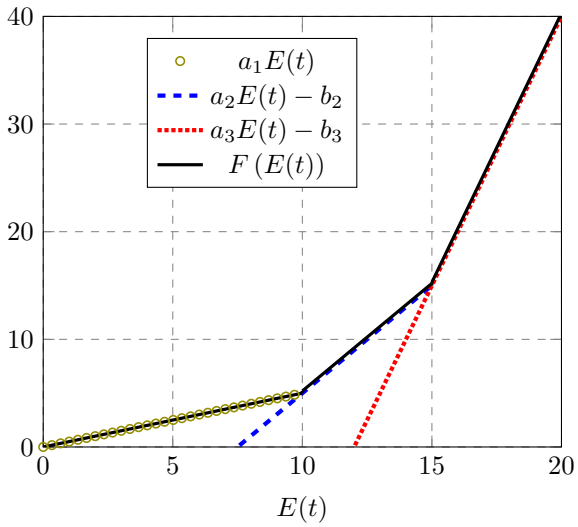

Figure 5.2: Piecewise linear "chargeable power" function.

Discrete-Time Block Pricing

Consider a planning period of N slots, each one of them of length Δt. Then, the energy drawn from the grid $\mathbf{e}_G \in \mathbb{R}_+^N$ in the kth time slot is:

$$e_G(k) = \int_{(k-1)\Delta t}^{k\Delta t} E(t)dt. \tag{5.5}$$

We can also model the dynamic block pricing scheme in terms of $\mathbf{e}_G$ by defining the following bivariate function:

$$\Gamma[k, e_G(k)] = \begin{cases} a_1 P(k\Delta t)e_G(k) & 0 \leq e_G(k) \leq \Delta t \Pi_1 \\ a_2 P(k\Delta t)e_G(k) - \Delta t b_2 & \Delta t \Pi_1 < e_G(k) \leq \Delta t \Pi_2 \\ & \vdots \\ a_B P(k\Delta t)e_G(k) - \Delta t b_B & \Delta t \Pi_{B-1} < e_G(k) \end{cases}, \tag{5.6}$$

where $k \in \{1, \ldots, N\}$ is a time slot in the planning horizon. The definition of $\Gamma[k, e_G(k)]$ can also be written as follows:

$$\Gamma[k, e_G(k)] = \max_j \left\{ a_j P(t) e_G(k) - \Delta t b_j \right\}, \tag{5.7}$$

where, again, $b_1 = 0$. The total energy cost incurred over N time slots can be estimated by using $\Gamma[k, e_G(k)]$ as follows:

$$\chi \approx \sum_{k=1}^{N} \Gamma[k, e_G(k)],$$

where the approximation follows because of the discretisation introduced. The two models are equivalent when $N \to \infty$, and the limit exists. The following are three differences between the functions $F[E(t)]$ and $\Gamma[k, e_G(k)]$:

- Given the power consumed at any time t, the function $F[E(t)]$ returns the "chargeable power" based on which the final bill is computed through integration. In contrast,

$\Gamma[k, e_G(k)]$ directly returns the cost of consuming $e_G(k)$ in the kth time slot.

- The continuous-time block pricing model allows for a closer monitoring of the power consumed by the user. With this scheme the utility can penalize spikes in the load demand. Moreover, this model can depict the more conventional time-varying block pricing schemes simply by defining $P(t)$ as a linear combination of step functions. In contrast, the discrete-time model is based on the energy consumed during a given time slot, and hence may ignore load spikes, especially when the length of the time slot is large.

- By using the continuous-time block pricing model we can obtain a more insightful analytical solution to the cost minimization problem because it allows us to use continuous-time optimization tools such as calculus of variations.

5.2.3 Energy Storage Device

The energy storage device has a limited capacity denoted by $\Psi > 0$. To model the non-linearity of the discharging operation, we introduce $\tilde{D}(t)$, which denotes the power drawn from the storage device to effectively deliver $D(t)$ to the load. Then, the energy $J(t)$ available in the storage system at time $t \geq 0$, can be written as follows:

$$J(t) = J(0) + \int_0^t \varsigma[R(x) + C(x)] - \tilde{D}(x)dx, \tag{5.8}$$

where $0 \leq \varsigma \leq 1$ is the charging efficiency rate, $R(t)$ is the power harvested from the renewable source. As explained in Sec. 1.2.2, we model the relationship between $D(t)$ and $\tilde{D}(t)$ by using an arbitrary function $\mathscr{F} : [0,\infty) \to [0,\infty)$, which is assumed continuous, convex, and strictly increasing. Hence,

$$\tilde{D}(t) = \mathscr{F}[D(t)]. \tag{5.9}$$

The maximum charging power allowed at any time t is denoted by $C_{\max}$, and the maximum discharging rate is $\tilde{D}_{\max}$. That is, $C(t) \leq C_{\max}$, and $\tilde{D}(t) \leq \tilde{D}_{\max}\ \forall\, t$.

5.3 Problem Formulation

In this section, we formulate a constrained optimization problem to minimize the energy bill incurred by the non-deferrable load facility in $[0, H]$.

5.3.1 Continuous-Time Formulation

Assuming that the pricing functions $P(\cdot)$ and $F(\cdot)$ are made known to the consumer in advance, the energy-cost minimization problem can be cast as follows:

$$\text{P5.0:} \quad \min_{C(t),D(t)} \quad \int_0^H P(t)F\left[L(t)+C(t)-D(t)\right]dt$$

subject to the following constraints:

$$0 \leq J(t) \leq \Psi, \tag{5.10a}$$

$$C(t)D(t) = 0, \tag{5.10b}$$

$$C(t) \leq C_{\max}, \tag{5.10c}$$

$$\tilde{D}(t) \leq \tilde{D}_{\max}, \tag{5.10d}$$

$$D(t) \leq L(t), \tag{5.10e}$$

$$C(t) \geq 0,\ D(t) \geq 0\ \forall\, t\ \in\ [0, H]. \tag{5.10f}$$

The quantities $J(t)$ and $\tilde{D}(t)$ are related by (5.8), and $\tilde{D}(t)$ and $D(t)$ are related by (5.9). The constraint (5.10b) ensures that the charging and discharging operations do not take place at the same instant[3] of time. The constraints (5.10c) and (5.10d) ensure that the amount of power injected to, or drawn from the storage device at any time t is within limits. The constraint (5.10e) upper bounds $D(t)$ by the load $L(t)$. Finally, the constraint

[3]Renewable energy arrivals can occur during discharging periods, as we have assumed that the storage device can handle both operations simultaneously.

(5.10f) is introduced to ensure that all the power quantities involved are non-negative.

5.3.2 Discrete-Time Formulation

In this section we propose an alternative problem formulation, which uses the definition of the function $\Gamma[k, e_G(k)]$, introduced in Sec. 5.2.2. We divide the planning horizon into N time slots of length Δt each. Let $\mathbf{e}_C \in \mathbb{R}_+^N$ denote the grid-energy charged into the storage device over the N-slot period, an let $\mathbf{e}_D \in \mathbb{R}_+^N$ denote the energy drawn from the storage device over the same period. Similarly let $\mathbf{e}_R \in \mathbb{R}_+^N$ denote the renewable energy harvested over the N time slots. Finally, let $\mathbf{e}_L \in \mathbb{R}_+^N$ denote the energy requirements of the facility over the N-slot planning horizon. All these energy vectors can be obtained from the respective continuous-time power signals through integration:

$$e_{\mathcal{Z}}(k) = \int_{(k-1)\Delta t}^{k\Delta t} \mathcal{Z}(t)dt,\ \mathcal{Z} \in \{\text{“}C\text{”},\text{“}D\text{”},\text{“}\tilde{D}\text{”},\text{“}L\text{”},\text{“}R\text{”}\}. \tag{5.11}$$

With these definitions, the mathematical problem to minimize χ by designing $\mathbf{e}_C$ and $\mathbf{e}_D$ can be cast as follows:

$$\text{DP5.0:} \quad \min_{\mathbf{e}_C, \mathbf{e}_D} \quad \sum_{k=1}^{N} \Gamma[k, e_G(k)]$$

subject to the following constraints:

$$0 \leq J(k\Delta t) \leq \Psi, \tag{5.12a}$$

$$e_C(k)e_D(k) = 0, \tag{5.12b}$$

$$e_C(k) \leq \Delta t C_{\max}, \tag{5.12c}$$

$$e_{\tilde{D}}(k) \leq \Delta t \tilde{D}_{\max}, \tag{5.12d}$$

$$e_D(k) \leq e_L(k), \tag{5.12e}$$

$$e_D(k) = \min_i \{\alpha_i e_{\tilde{D}}(k) - \Delta t \beta_i\},\ \forall\ k \in \{1, \ldots, N\}. \tag{5.12f}$$

The last constraint (5.12f) follows from the linearisation of (5.9), explained in Sec. 2.4.1, and hence $i \in \{1,2,\ldots,M\}$. The equation (2.12), establishes the relationship between the power quantities $\tilde{d}(k)$ and $d(k)$. To obtain the relationship between $e_D(k)$ and $e_{\tilde{D}}(k)$, we need to integrate with respect to time on both sides of (2.12).

5.4 Proposed Solutions

In this section we discuss how to solve DP5.0, and then propose two strategies to design $C(t)$ and $D(t)$. To solve DP5.0 we need to write the constraint (5.12a) by using the definition of $J(t)$ in (5.8) as follows:

$$0 \leq J(0) + \sum_{i=1}^{k} \varsigma \left[e_R(k) + e_C(k)\right] - e_{\tilde{D}}(k) \leq \Psi, \tag{5.13}$$

and substitute (5.12f) with a set of linear inequalities as explained in Sec. 2.4.1. Then, the problem can be cast as a linear program by ignoring the constraint (5.12b). The strategy obtained after solving the resulting linear program automatically satisfies the constraint (5.12b), as we show in Lemma 5.4.1.

By solving DP5.0 we can obtain the optimal energy management strategy in terms of $\mathbf{e}_C$ and $\mathbf{e}_D$. For small Δt, the signals $C(t)$ and $D(t)$ can then be obtained by assuming that the power charged into, or drawn from the storage device is constant within each time slot, i.e.:

$$C(t) = \frac{e_C(k)}{\Delta t}, \quad D(t) = \frac{e_D(k)}{\Delta t}, \qquad (k-1)\Delta t \leq t < k\Delta t, \ \forall\, k. \tag{5.14}$$

This assumption works well for small Δt. But in other cases, we need to further optimize $C(t)$ and $D(t)$. Hence, in the following we propose two strategies to design $C(t)$ and $D(t)$. The first strategy seeks to optimize $C(t)$ and $D(t)$ directly by introducing discretisation in time in P5.0. The second strategy uses calculus of variations to optimize $C(t)$ and $D(t)$ in continuous time.

5.4.1 Solution by Linearisation and Discretisation in Time (LDT)

We can design $C(t)$ and $D(t)$ by introducing time discretisation in P5.0. For ease of notation, we again consider N time slots in the planning horizon $[0,H]$, each one of duration Δt. Let $\mathbf{c} \in \mathbb{R}_+^N$ represent the grid power charged into the storage device over N time slots, and let $\tilde{\mathbf{d}} \in \mathbb{R}_+^N$ denote the power drawn (before losses) from the device over the same period. The power vectors used in this formulation are obtained by uniformly sampling the corresponding continuous-time functions at a rate of $1/\Delta t$ samples per unit of time, i.e.,

$$\begin{gathered} c(k) = C(k\Delta t),\ d(k) = D(k\Delta t),\ \tilde{d}(k) = \tilde{D}(k\Delta t), \\ r(k) = R(k\Delta t),\ \ell(k) = L(k\Delta t),\ \forall\, k. \end{gathered} \tag{5.15}$$

Let $\mathbf{d} \in \mathbb{R}_+^N$ represent the power effectively delivered to the load when $\tilde{\mathbf{d}}$ is drawn from the storage device, then we can approximate (5.9) by using a concave piecewise linear function as explained in Sec. 2.4.1. For convenience we reproduce Eq. (2.12):

$$G\left[\tilde{d}(k)\right] = \min_i \{\alpha_i \tilde{d}(k) - \beta_i\}, \tag{5.16}$$

with $1 \leq i \leq M$. Therefore, an approximate solution to P5.0, based on linearisation and discretisation in time (LDT), can be obtained by working out the following optimization problem:

$$\text{DP5.1:} \quad \min_{\mathbf{c},\mathbf{d}} \quad \Delta t \sum_{k=1}^{N} p(k) F\left[\ell(k) + c(k) - d(k)\right]$$

s.t. (5.12a) and:

$$c(k)d(k) = 0, \tag{5.17a}$$

$$c(k) \leq C_{\max}, \tag{5.17b}$$

$$\tilde{d}(k) \leq \tilde{D}_{\max}, \tag{5.17c}$$

$$d(k) \leq \ell(k), \tag{5.17d}$$

$$d(k) = G\left[\tilde{d}(k)\right], \ \forall\, k \in \{1,\ldots,N\}. \tag{5.17e}$$

Substituting $F(\cdot)$ according to (5.4) in DP5.1 yields the following optimization problem:

$$\text{DP5.2:} \quad \min_{\mathbf{c},\mathbf{d}} \quad \Delta t \sum_{k=1}^{N} p(k) \max_{j} \{a_j\left[\ell(k) + c(k) - d(k)\right] + b_j\}$$

s.t. (5.12a), (5.17a)–(5.17e). Moreover, introducing the auxiliary variable $\mathbf{z} \in \mathbb{R}_+^N$, which satisfies the following constraint:

$$z(k) \geq a_j\left[\ell(k) + c(k) - d(k)\right] + b_j, \ \forall\, k, \ \forall\ j, \tag{5.18}$$

and by using the definition of $G(\cdot)$, DP5.2 can be written as:

$$\text{DP5.3:} \quad \min_{\mathbf{z},\mathbf{c},\mathbf{d}} \quad \Delta t \sum_{k=1}^{N} p(k) z(k)$$

s.t. (5.12a), (5.17a)–(5.17d), (5.18), and

$$d(k) \leq \alpha_i \tilde{d}(k) - \beta_i, i \ \in \{1,\ldots,M\}, \ k \ \in \ \{1,\ldots,N\}. \tag{5.19}$$

The constraint (5.18) ensures that $z(k) \geq \max_j\{a_j[\ell(k) + c(k) - d(k)] - b_j\}\ \forall\, k$, and the constraint (5.19) follows from (5.17e).

Using matrices, and in particular the lower triangular matrix $\mathbf{A}$ defined in Sec. 2.4.1, DP5.3 can be cast into the following optimization problem:

$$\text{DP5.4:} \quad \min_{\mathbf{c},\mathbf{d},\mathbf{z},\tilde{\mathbf{d}}} \quad \Delta t \mathbf{p}^{\mathrm{T}} \mathbf{z}$$

s.t. (5.17a), (5.17b), (5.17c), and:

$$\begin{pmatrix} a_1\mathbf{I} & -a_1\mathbf{I} & -\mathbf{I} & \mathbf{0} \\ a_2\mathbf{I} & -a_2\mathbf{I} & -\mathbf{I} & \mathbf{0} \\ \vdots & \vdots & \vdots & \vdots \\ a_B\mathbf{I} & -a_B\mathbf{I} & -\mathbf{I} & \mathbf{0} \\ \mathbf{0} & \mathbf{I} & \mathbf{0} & -\alpha_1\mathbf{I} \\ \mathbf{0} & \mathbf{I} & \mathbf{0} & -\alpha_2\mathbf{I} \\ \vdots & \vdots & \vdots & \vdots \\ \mathbf{0} & \mathbf{I} & \mathbf{0} & -\alpha_M\mathbf{I} \\ \varsigma\Delta t\mathbf{A} & \mathbf{0} & \mathbf{0} & -\Delta t\mathbf{A} \\ -\varsigma\Delta t\mathbf{A} & \mathbf{0} & \mathbf{0} & \Delta t\mathbf{A} \end{pmatrix} \begin{pmatrix} \mathbf{c} \\ \mathbf{d} \\ \mathbf{z} \\ \tilde{\mathbf{d}} \end{pmatrix} \preceq \begin{pmatrix} -a_1\boldsymbol{\ell} - \mathbf{1}b_1 \\ -a_2\boldsymbol{\ell} - \mathbf{1}b_2 \\ \vdots \\ -a_B\boldsymbol{\ell} - \mathbf{1}b_B \\ -\beta_1\mathbf{1} \\ -\beta_2\mathbf{1} \\ \vdots \\ -\beta_M\mathbf{1} \\ [\Psi - J(0)]\mathbf{1} - \Delta t\mathbf{A}[\varsigma\mathbf{r}] \\ J(0)\mathbf{1} + \Delta t\mathbf{A}[\varsigma\mathbf{r}] \end{pmatrix} \tag{5.20}$$

The constraints stated in the penultimate and ultimate rows are respectively $J(k\Delta t) \leq \Psi$ and $J(k\Delta t) \geq 0 \ \forall \ k$. If the constraint (5.17a) is ignored, then DP5.4 becomes a linear programming problem, which we term LP5.1. Remarkably, the constraint (5.17a) is automatically satisfied by solving LP5.1, as stated in the following lemma:

Lemma 5.4.1. *Let* $\mathbf{c}^*$ *and* $\tilde{\mathbf{d}}^*$ *denote the solution to LP5.1. Then* $c^*(k)\tilde{d}^*(k) = 0 \ \forall \ k$.

Proof. Let $\tilde{\mathbf{c}}^* = \varsigma\mathbf{c}^*$, and let $\tilde{c}^*(k) - \tilde{d}^*(k) = \Delta J$, where ΔJ is the change in the battery level. Now assume $\tilde{c}^*(k)\tilde{d}^*(k) \neq 0$, which results in losses given by $(1-\varsigma)c(k) + \tilde{d}(k) - d(k)$. If $\Delta J > 0$, then this loss can be reduced[4] to $(1-\varsigma)c(k)$ with a new $c(k) = \frac{\Delta J}{\varsigma}$, and a null discharging operation, i.e. $d(k) = 0$. If $\Delta J < 0$ then this loss can be reduced[5] to $\tilde{d}(k) - d(k)$ with a new $\tilde{d}(k) = \Delta J$, which requires $c(k) = 0$. Reducing power loss results in performance improvement, hence, if $\mathbf{c}^*$, $\tilde{\mathbf{d}}^*$ solve LP5.1, then they must ensure minimum losses, which requires $c^*(k)\tilde{d}^*(k) = 0 \ \forall \ k$. ■

As expected, the computational complexity of DP5.4 increases as N grows. In particular, the number of variables involved in the problem is directly proportional to the number of samples considered in $[0, H]$. Moreover, a new constraint is introduced

[4] To see this, notice that $\Delta J \leq \tilde{c}^*(k)$.
[5] To see this, notice that $|\Delta J| \leq \tilde{d}^*(k)$.

for each linear segment that is added to the definition of $G(\cdot)$ to approximate (5.9). This motivates us to find an alternative approach to solve the problem in continuous time.

5.4.2 Solution by Calculus of Variations (CoV)

Motivated by the computational complexity incurred by the approaches in the discrete domain, we use calculus of variations to obtain further insights and reduce complexity by deriving analytical solutions in continuous time. To use this approach we will assume the following:

1. The planning horizon $[0,H]$ is divided into subintervals, such that in each subinterval either $C(t) \neq 0$ or $D(t) \neq 0$. If $C(t) \neq 0 \; \forall \; t \; \in \; [\delta_i, \zeta_i]$, we refer to $[\delta_i, \zeta_i]$ as the ith charging period. Similarly, if $D(t) \neq 0 \; \forall \; t \; \in \; [\eta_j, \rho_j]$, we refer to $[\eta_j, \rho_j]$ as the jth discharging period. If there are adjacent charging (discharging) periods, they are merged into a single charging (discharging) subinterval. We assume that there are N_C charging periods and N_D discharging periods.

2. We assume perfect knowledge of $\delta_i, \; \zeta_i, \; \eta_j, \; \rho_j, \; J(\delta_i), \; J(\zeta_i), \; J(\eta_j)$, and $J(\rho_j) \; \forall \; i \; \forall \; j$.

The information listed in items 1 and 2 can be obtained by solving DP5.0 at a low[6] sampling rate. Since $J(\delta_i), \; J(\zeta_i), \; J(\eta_j)$ and $J(\rho_j)$ are obtained by solving DP5.0, they satisfy the constraint (5.10a) for all $\; i \in \; \{1, \ldots, N_C\}, \; j \in \; \{1, \ldots, N_D\}$. Moreover, since $C(t)$ and $D(t)$ cannot be non-zero at the same time, they can be designed separately, as we propose next.

[6]The sampling rate need not be high because all that is required is the partition and the value of $J(t)$ at each element of the partitioning sequence.

Charging Operation

Without loss of generality we assume N_C charging periods in $[0,H]$. Let $[\delta_i,\zeta_i]$, with $0 \leq \delta_i < \zeta_i \leq H$ be the ith charging period, hence $D(t) = 0 \; \forall \; t \; \in [\delta_i,\zeta_i]$, and $E(t) = L(t)+C(t)$. For ease of notation, we define $\mathcal{Y}_{C,i}[C(t)] \triangleq \int_{\delta_i}^{\zeta_i} P(t)F\left[L(t)+C(t)\right]dt$, hence the charging operation can be optimized by solving the following optimization problem:

$$\text{P5.1:} \quad \min_{C(t)} \quad \sum_{i=1}^{N_C} \mathcal{Y}_{C,i}[C(t)]$$

subject to the following constraints:

$$J(\delta_i) + \int_{\delta_i}^{t} \varsigma[C(x)+R(x)]dx \geq 0, \tag{5.21a}$$

$$J(\delta_i) + \int_{\delta_i}^{t} \varsigma[C(x)+R(x)]dx \leq \Psi, \tag{5.21b}$$

$$C(t) \leq C_{\max}, \; \forall \; t \in \; [\delta_i,\zeta_i], \tag{5.21c}$$

$$J(\delta_i) + \int_{\delta_i}^{\zeta_i} \varsigma[C(x)+R(x)]dx = J(\zeta_i), \; \forall \; i \; \in \; \{1,\ldots,N_C\}, \tag{5.21d}$$

where we have split the constraint (5.10a) into (5.21a) and (5.21b) for convenience. P5.1 is obtained from P5.0 by setting $D(t) = 0 \; \forall \; t \; \in [\delta_i,\zeta_i]$.

Since $J(\delta_i) \geq 0$ and $C(t) \geq 0$, the constraint (5.21a) can be ignored. Moreover, the quantity $\int_{\delta_i}^{t} \varsigma[C(x)+R(x)]dx$ is a non-decreasing function of t. Hence, the constraint (5.21b) is satisfied if and only if:

$$J(\delta_i) + \int_{\delta_i}^{\zeta_i} \varsigma[C(x)+R(x)]dx \leq \Psi. \tag{5.22}$$

Because $J(\zeta_i) \leq \Psi$, the constraint (5.22) is satisfied if (5.21d) is satisfied. Therefore, to solve P5.1 we only need to consider the constraints (5.21c) and (5.21d). Moreover, for tractability we can relax the constraint (5.21c) as follows:

$$\int_{\delta_i}^{\zeta_i} C(t)dt \leq Q_{C,i}, \; \forall \; i \; \in \{1,\ldots,N_C\}, \tag{5.23}$$

where $Q_{C,i} = C_{\max}(\zeta_i - \delta_i)$. And for ease of notation we define:

$$\overline{\mathsf{R}}_i = \int_{\delta_i}^{\zeta_i} \varsigma R(x)dx. \tag{5.24}$$

Lemma 5.4.2. *P5.1 is infeasible if* $Q_{C,i} < \frac{1}{\varsigma}\left[J(\zeta_i) - J(\delta_i) - \overline{\mathsf{R}}_i\right]$, *for any* $i \in \{1,\ldots,N_C\}$.

Proof. The proof is immediate from inspecting (5.21d) and (5.23). ■

In the remainder of this chapter, we assume $Q_{C,i} \geq \frac{1}{\varsigma}\left[J(\zeta_i) - J(\delta_i) - \overline{\mathsf{R}}_i\right]$, $\forall\ i \in \{1,\ldots,N_C\}$. Moreover, given the objective function and the constraints in P5.1, the optimization problem is separable into N_C independent problems [188].

Before describing the strategy proposed to solve P5.1, we present a discussion regarding the "chargeable power" function $F(\cdot)$. Given its definition as a piece-wise linear function, $F(\cdot)$ makes the continuous-time treatment of the problem more challenging. Hence, it is of interest to determine approximating functions to $F(\cdot)$, which can have more desirable properties such as differentiability. Therefore, in the following we describe a procedure to obtain a differentiable approximation of $F(\cdot)$.

Let $\check{F} : \mathbb{R} \to \mathbb{R}$, be a function which approximates $F(\cdot)$ in a finite interval $[x_{\mathsf{min}}, x_{\mathsf{max}}]$. Moreover, let $\boldsymbol{\theta}$ denote a set of parameters which uniquely specify $\check{F}(\cdot)$. Then, in order to obtain a *good* approximation of $F(\cdot)$, the parameters $\boldsymbol{\theta}$ can be chosen as the argument of the following optimization problem:

$$\text{P5.A:} \quad \min_{\boldsymbol{\theta}} \quad \int_{x_{\mathsf{min}}}^{x_{\mathsf{max}}} \left[\check{F}(x;\boldsymbol{\theta}) - F(x)\right]^2 dx,$$

which can be solved numerically. A simple approximating function can be a single term posynomial,[7] i.e. $\check{F}(x) = \mathsf{A}x^r$. Then A and r can be tuned to minimize the approximation error, as defined in the objective function of P5.A. As we will see in Theorem 5.4.1, this

[7] A single-term posynomial is also referred to as a monomial. However, to emphasize the fact that its power does not necessarily have an integer exponent, we call it a single-term posynomial.

single-term posynomial approximation will allow us to find a more insightful expression for the optimal charging schedule.

Now we proceed to describe the strategy proposed to solve P5.1, and for ease of notation we define

$$\overline{\mathsf{L}}_i = \int_{\delta_i}^{\zeta_i} L(t)dt. \tag{5.25}$$

Then we enunciate the following theorem:

Theorem 5.4.1. *Subject to (5.21d), a necessary condition to minimize the functional* $\mathcal{Y}_{C,i}[C(t)]$ *is:*

$$P(t)\frac{\partial}{\partial C}F\left[C(t)+L(t)\right] = \mathsf{K}_i, \tag{5.26}$$

where $\mathsf{K}_i \in \mathbb{R}$ *are constants that can be chosen to comply with the constraints (5.21d). Moreover, if* $F(x) = \mathsf{A}x^r$*, with* $\mathsf{A} > 0$*, and* $r > 1$*, then (5.26) yields:*

$$C(t) = C^*(t) \triangleq \left(\left[\frac{\mathsf{K}_i}{r\mathsf{A}P(t)}\right]^{\frac{1}{r-1}} - L(t)\right)^+, \ \forall\, t \in [\delta_i, \zeta_i], \tag{5.27}$$

where $(x)^+ = \max(0,x)$*, and* $\mathsf{K}_i \in \mathbb{R}$ *is chosen to comply with the constraint (5.21d), i.e.*

$$\mathsf{K}_i = r\mathsf{A}\left[\frac{\frac{1}{\varsigma}\left[J(\zeta_i) - J(\delta_i) - \overline{\mathsf{R}}_i\right] + \overline{\mathsf{L}}_i}{\displaystyle\int_{\delta_i}^{\zeta_i}\left[\frac{1}{P(t)}\right]^{\frac{1}{r-1}} dt}\right]^{r-1}. \tag{5.28}$$

Proof. See Appendix B.9. ■

Let $E^*(t) \triangleq C^*(t) + L(t)$, then as stated in (5.27), to minimize costs, $E^*(t)$ should be proportional to $\left[\frac{1}{P(t)}\right]^{\frac{1}{r-1}}$. Hence, the grid-energy consumption increases when $r \to 1^+$ and $P(t) \to 0$. These observations allow us to verify the rationality of this result. For a formal proof, readers are referred to Appendix B.9.

Discharging Operation

Consider N_D discharging periods in $[0,H]$ and let $[\eta_j,\rho_j]$ with $0 \leq \eta_j \leq \rho_j \leq H$ be the jth discharging period in $[0,H]$. With $C(t) = 0 \; \forall \; t \; \in [\eta_j,\rho_j]$, P5.0 simplifies to:

$$\text{P5.2:} \quad \min_{D(t)} \quad \sum_{j=1}^{N_D} \int_{\eta_j}^{\rho_j} P(t)F\left[L(t)-D(t)\right]dt$$

subject to the following constraints:

$$J(\eta_j) + \int_{\eta_j}^{t} \varsigma R(x) - \tilde{D}(x)dx \leq \Psi, \tag{5.29a}$$

$$J(\eta_j) + \int_{\eta_j}^{t} \varsigma R(x) - \tilde{D}(x)dx \geq 0, \tag{5.29b}$$

$$D(t) \leq L(t), \tag{5.29c}$$

$$\tilde{D}(t) \leq \tilde{D}_{\max}, \forall \; t \in \; [\eta_j,\rho_j], \tag{5.29d}$$

$$J(\eta_j) + \int_{\eta_j}^{\rho_j} \varsigma R(x) - \tilde{D}(x)dx = J(\rho_j), \; \forall \; j \; \in \; \{1,\ldots,N_D\}, \tag{5.29e}$$

where we have split the constraint (5.10a) into (5.29a) and (5.29b) for convenience. Since $[\eta_j,\rho_j]$ is a discharging period, we will assume that $D(t) \geq R(t) \; \forall \; t \; \in \; [\eta_j,\rho_j]$. Hence, the constraint (5.29a) holds true regardless of $D(t)$ because $J(\eta_j) \leq \Psi$ and $D(t) - R(t) > 0 \; \forall \; t$. If the constraint (5.29e) holds, then so does the constraint (5.29b), because $J(\rho_j) \geq 0$. Therefore, to solve the problem we only need to consider the constraints (5.29d) and (5.29e). Moreover, for tractability we can relax the constraint (5.29d) as follows:

$$\int_{\eta_j}^{\rho_j} \tilde{D}(t)dt \leq Q_{D,j}, \; \forall \; j \; \in \; \{1,\ldots,N_D\}, \tag{5.30}$$

where $Q_{D,j} = \tilde{D}_{\max}\left(\rho_j - \eta_j\right)$. For ease of notation, we introduce the following definition:

$$\overline{\mathsf{R}}_j = \int_{\eta_j}^{\rho_j} \varsigma R(x)dx. \tag{5.31}$$

Then, we enunciate Lemma 5.4.3:

Lemma 5.4.3. *P5.2 is infeasible if* $Q_{D,j} < J(\eta_j) - J(\rho_j) + \overline{\mathsf{R}}_j$, *for any* $j \in \{1,\ldots,N_D\}$.

Proof. The proof is immediate from inspecting (5.29e) and (5.30). ■

Following Lemma 5.4.3, in the remainder of this chapter we will assume $Q_{D,j} \geq J(\eta_j) - J(\rho_j) + \overline{\mathsf{R}}_j,\ \forall\ j \in \{1,\ldots,N_D\}$, hence the constraint (5.29d) can be ignored. Moreover, for concreteness we will consider $F(x) = \mathsf{A}x^r$, and $\tilde{D}(t) = Q_{\mathrm{No}}\left[\frac{D(t)}{Q_{\mathrm{No}}}\right]^{\kappa}$, then we can obtain candidate solutions by solving the following non-linear equation:

$$\lambda_{D,j}\kappa\left[\frac{D(t)}{Q_{\mathsf{No}}}\right]^{\kappa-1} = r\mathsf{A}P(t)\left[L(t)-D(t)\right]^{r-1}\ \forall\, t \in [\eta_j,\rho_j], \tag{5.32}$$

where $\lambda_{D,j}$ is a constant chosen to satisfy (5.29e).

In general, we cannot solve (5.32) in closed form. However, if we make further simplifications, we can obtain some insightful expressions. Therefore, we consider two cases:

- $r \gg \kappa$: In this case, the block-pricing effect dominates[8] over Peukert's effect, thus solving (5.32) yields:

$$D^*(t) = L(t) - \left(\frac{\mathsf{K}_j}{r\mathsf{A}P(t)}\right)^{\frac{1}{r-1}},\ \forall\, t \in [\eta_j,\rho_j], \tag{5.33}$$

  where K_j is a constant chosen to satisfy (5.29e) with $\kappa = 1$. The proof is similar to the proof of Theorem 5.4.1, presented in Appendix B.9. If $\kappa = 1$, then the optimization problem P5.2 takes the form of P5.1, so their solutions have clear similarities.

- $\kappa > r$ or $\Pi_1 > L(t)\ \forall\, t$: In this case, we can disregard the block-pricing effect and obtain the optimal discharging operation by assuming $r = 1$. Similarly, if we assume a sufficiently large local demand $L(t)$, then we can disregard the constraint (5.29c),

[8] This means that the losses incurred from Peukert's effect are negligible if compared to the extra costs incurred during the charging operation.

and the optimal discharging profile is:

$$D^*(t) = Q_{\mathsf{No}} \left[\frac{P(t)}{\lambda_{D,j}\kappa} \right]^{\frac{1}{\kappa-1}}, \ \forall\, t \ \in \ [\eta_j, \rho_j], \tag{5.34}$$

where $\lambda_{D,j}$ is a constant chosen to satisfy (5.29e). This result was obtained in Chapter 2, Theorem 2.4.1.

5.5 Convexity of the Cost Function and Optimal Storage Capacity

In this section we investigate the convexity of the cost function in terms of the amount of energy shifted in time. We particularly consider a single pair of consecutive charging and discharging periods, a scenario which may correspond[9] to a day-long planning horizon. By studying the relationship between cost and total energy shifted in time we can determine the storage capacity that could strike a balance between initial investment and potential financial return.

For ease of notation we will assume that $R(t) = 0 \ \forall\, t$, and let Θ denote the total energy charged into the system during the charging period. Then the energy available in the storage device at the beginning of the discharging period is $\Theta + J(0)$. Moreover, we will reasonably[10] assume that $L(t) - D^*(t) \leq \Pi_1 \ \forall\, t$, so that the pricing function is linear during the discharging period. And finally, for concreteness we will let $F(x) = \mathsf{A}x^r$, and $\mathscr{F}[x] = Q_{\mathrm{No}} \left[\frac{x}{Q_{\mathrm{No}}} \right]^{\kappa}$. With these assumptions, the energy expenditure can be computed as follows:

$$\chi_{\mathsf{CoV}} = \mathsf{A} \int_{\delta_1}^{\zeta_1} P(t) \left[L(t) + C^*(t) \right]^r dt + \int_{\eta_1}^{\rho_1} P(t) \left[L(t) - D^*(t) \right] dt + \chi_{\mathsf{IDLE}}, \tag{5.35}$$

[9] Pricing signals may reflect daily patterns, as such they may have a single valley, and a single peak pricing period over a 24-hour period.

[10] During the discharging period, the facility draws less energy from the grid because the load is also powered from the storage device.

where

$$\chi_{\mathsf{IDLE}} = \int_0^{\delta_1} P(t)F\left[L(t)\right]dt + \int_{\zeta_1}^{\eta_1} P(t)F\left[L(t)\right]dt + \int_{\rho_1}^{H} P(t)F\left[L(t)\right]dt$$

is the energy cost incurred when there are no charging/discharging operations scheduled, and $C^*(t)$ and $D^*(t)$ are given by (5.27) and (5.34).

In the following, we formulate an optimization problem to minimize χ_{CoV} in terms of Θ, which will determine the optimal storage capacity that is necessary to implement the proposed energy management strategy. Once Θ is determined, the storage capacity must satisfy $\Psi \geq J(0) + \Theta$. For simplicity we have assumed $R(t) = 0 \ \ \forall\, t$, if this assumption does not hold, then, a more accurate bound for the storage capacity would be $\Psi \geq J(0) + \Theta + \int_0^H \varsigma R(t)dt$.

$$\text{P5.3:} \quad \min_{\Theta} \quad \chi_{\mathsf{CoV}}$$

The optimal charging profile can be written in terms of Θ from (5.27) as:

$$C^*(t) = \left[\frac{\Theta + \overline{\mathsf{L}}_1}{\displaystyle\int_{\delta_1}^{\zeta_1} \left[\frac{1}{P(t)}\right]^{\frac{1}{r-1}} dt}\right] \left[\frac{1}{P(t)}\right]^{\frac{1}{r-1}} - L(t), \quad t \in [\delta_1, \zeta_1], \tag{5.36}$$

and $C^*(t) = 0 \ \forall\, t \notin [\delta_1, \zeta_1]$.

Since we assume that the pricing function is linear during the discharging operation, the optimal discharging profile can be written in terms of Θ and $J(0)$ as follows:

$$D^*(t) = Q_{\mathsf{No}} \left(\frac{J(0) + \Theta}{Q_{\mathsf{No}} \displaystyle\int_{\eta_1}^{\rho_1} P(t)^{\frac{\kappa}{\kappa-1}} dt}\right)^{\frac{1}{\kappa}} \left[P(t)\right]^{\frac{1}{\kappa-1}}, \quad t \in [\eta_1, \rho_1], \tag{5.37}$$

and $D^*(t) = 0 \ \forall\, t \notin [\eta_1, \rho_1]$. In (5.37) we have assumed that during the discharging operation the storage device has to deliver its entire charge, which includes $J(0)$, the energy initially available. This assumption follows because the energy left unused at

the end of the optimization horizon has zero value.

If we replace $C^*(t)$ and $D^*(t)$ into (5.35) we obtain:

$$\begin{aligned}\chi_{\mathsf{CoV}} = \mathsf{A}\int_{\delta_1}^{\zeta_1} P(t)\left[\left[\frac{\Theta+\overline{\mathsf{L}}_1}{\overline{Pr}}\right]\left(\frac{1}{P(t)}\right)^{\frac{1}{r-1}}\right]^r dt \\ + \int_{\eta_1}^{\rho_1} P(t)\left[L(t) - Q_{\mathsf{No}}\left(\frac{J(0)+\Theta}{Q_{\mathsf{No}}\overline{P\kappa}}\right)^{\frac{1}{\kappa}}[P(t)]^{\frac{1}{\kappa-1}}\right]dt \\ + \chi_{\mathsf{IDLE}},\end{aligned} \tag{5.38}$$

where

$$\overline{Pr} = \int_{\delta_1}^{\zeta_1}\left(\frac{1}{P(t)}\right)^{\frac{1}{r-1}} dt = \int_{\delta_1}^{\zeta_1}[P(t)]^{\frac{1}{1-r}}\,dt,$$

and

$$\overline{P\kappa} = \int_{\eta_1}^{\rho_1} P(t)^{\frac{\kappa}{\kappa-1}} dt.$$

Lemma 5.5.1. *If* $\mathsf{A} > 0$, $r > 1$, $Q_{\mathsf{No}} > 0$ *and* $\kappa > 1$, *then* χ_{CoV} *is convex in* Θ.

Proof. χ_{CoV} is the sum of two convex functions of Θ, hence is convex. By replacing $\overline{Pr}$ with its definition, the first term can be simplified as follows:

$$\mathsf{A}\int_{\delta_1}^{\zeta_1} P(t)\left[\left[\frac{\Theta+\overline{\mathsf{L}}_1}{\overline{Pr}}\right]\left(\frac{1}{P(t)}\right)^{\frac{1}{r-1}}\right]^r dt = \mathsf{A}\left[\Theta+\overline{\mathsf{L}}_1\right]^r\left[\int_{\delta_1}^{\zeta_1}[P(t)]^{\frac{1}{1-r}}\,dt\right]^{1-r},$$

which is convex in Θ if $\mathsf{A} > 0$ and $r > 1$. Similarly, by using the definition of $\overline{P\kappa}$, the second term can be written as:

$$\begin{aligned}\int_{\eta_1}^{\rho_1} P(t)\left[L(t) - Q_{\mathsf{No}}\left(\frac{J(0)+\Theta}{Q_{\mathsf{No}}\overline{P\kappa}}\right)^{\frac{1}{\kappa}}[P(t)]^{\frac{1}{\kappa-1}}\right]dt = \int_{\eta_1}^{\rho_1} P(t)L(t)dt \\ - [J(0)+\Theta]^{\frac{1}{\kappa}}\left(Q_{\mathsf{No}}\int_{\eta_1}^{\rho_1}[P(t)]^{\frac{\kappa}{\kappa-1}}\,dt\right)^{\frac{\kappa-1}{\kappa}},\end{aligned}$$

which is convex in Θ if $\kappa > 1$ and $Q_{\mathsf{No}} > 0$. ■

Following Lemma 5.5.1, there is an optimal Θ, denoted by Θ^*, which minimizes the cost χ_{CoV}. Θ^* should be large enough to ensure that $C^*(t) \geq 0\ \forall\ t$ in (5.36). This consideration can be disregarded if the load demand is negligible during the charging

period, i.e. $L(t) \ll C^*(t)$.

Since χ_{CoV} is convex in Θ, we find Θ^* by solving:

$$\begin{aligned}\frac{d}{d\Theta}\chi_{\mathsf{CoV}} = &\left[\int_{\delta_1}^{\zeta_1} [P(t)]^{\frac{1}{1-r}}\, dt\right]^{1-r} \frac{d}{d\Theta}\mathsf{A}\left[\Theta+\bar{\mathsf{L}}_1\right]^r \\ &- \left(Q_{\mathsf{No}}\int_{\eta_1}^{\rho_1} [P(t)]^{\frac{\kappa}{\kappa-1}}\, dt\right)^{\frac{\kappa-1}{\kappa}} \frac{d}{d\Theta}\left[J(0)+\Theta\right]^{\frac{1}{\kappa}} = 0,\end{aligned} \tag{5.39}$$

which leads to:

$$\left[\int_{\delta_1}^{\zeta_1} [P(t)]^{\frac{1}{1-r}}\, dt\right]^{1-r} \mathsf{A}r\left[\Theta+\bar{\mathsf{L}}_1\right]^{r-1} = \left(Q_{\mathsf{No}}\int_{\eta_1}^{\rho_1} [P(t)]^{\frac{\kappa}{\kappa-1}}\, dt\right)^{\frac{\kappa-1}{\kappa}} \frac{1}{\kappa}\left[J(0)+\Theta\right]^{\frac{1-\kappa}{\kappa}}.$$

We can obtain a solution to this equation through numerical methods. However, if $J(0) = 0$ and $\bar{\mathsf{L}}_1 = 0$, then the solution is:

$$\Theta^* = \left(\frac{\left(Q_{\mathsf{No}}\int_{\eta_1}^{\rho_1} [P(t)]^{\frac{\kappa}{\kappa-1}}\, dt\right)^{\frac{\kappa-1}{\kappa}}}{\kappa\mathsf{A}r\left[\int_{\delta_1}^{\zeta_1} [P(t)]^{\frac{1}{1-r}}\, dt\right]^{1-r}}\right)^{\frac{\kappa}{r\kappa-1}}. \tag{5.40}$$

5.6 Numerical Results and Discussion

In this section we present numerical results to validate the analysis developed throughout the chapter. Unless otherwise stated, in this section we consider the simulation parameters shown in Table 5.1. We assume that $\mathscr{F}(\cdot)$ is given as in (2.4) and evaluate the solutions obtained by assuming the simplified version of $\mathscr{F}(\cdot)$ defined in (2.5). The linear inequalities that we use to approximate Peukert's Law are obtained by using the procedure explained in Appendix A.1, i.e. formulas (A.2) and (A.3), with the partition's midpoints $\{x_2, x_3, \ldots, x_{10}\}$ defined as follows:

$$x_i = (0.4i + 0.6)\, Q_{\mathsf{No}},\ i \in \{2, \ldots, 10\}.$$

We also consider the following "chargeable power" function, which applies during

Table 5.1: Simulation parameters (energy management with non-linear pricing).

H	1
Δt	0.02
δ_1	0
δ_2	0.5
ρ_1	0.5
ρ_2	1
$P(t)$	$-50\sin(2\pi t)+150$
$L(t)$	$\begin{cases} 0 & 0 \le t \le 0.5 \\ 50 & 0.5 < t \le 1 \end{cases}$
ς	1
κ	1.2
Q_{No}	20
$J(0)$	0
$\tilde{D}_{\max}$	$6Q_{\mathsf{No}}$
M	10

the charging period, i.e. when $t \le 0.5$:

$$F[E(t)] = \begin{cases} E(t) & E(t) \le 10 \\ 1.05E(t) - 10 & 10 < E(t) \le 20 \\ 1.1E(t) - 20 & 20 < E(t) \le 30 \\ 1.15E(t) - 35 & 30 < E(t) \le 40 \\ 1.2E(t) - 55 & 40 < E(t) \le 50 \\ 1.25E(t) - 80 & 50 < E(t) \le 60 \\ 1.3E(t) - 110 & 60 < E(t) \le 70 \\ 1.35E(t) - 145 & 70 < E(t) \le 80 \\ 1.4E(t) - 185 & 80 < E(t) \le 90 \\ 1.45E(t) - 230 & 90 < E(t) \le 100 \end{cases} \tag{5.41}$$

For $t > 0.5$ the "chargeable power" function is linear, i.e. $F[E(t)] = E(t)$. Hence, the

cost incurred by the facility in this scenario is:

$$\chi_{\mathsf{sim}} = \int_0^{0.5} P(t)F\left[E(t)\right]dt + \int_{0.5}^{1} P(t)\left[L(t) - D(t)\right]dt. \tag{5.42}$$

The posynomial approximation for $F[E(t)]$, as defined in (5.41), is $\check{F}[E(t)] = 0.6743207[E(t)]^{1.1274085}$, which was obtained by solving P5.A numerically. The piecewise linear function (5.41) and its approximation $\check{F}[E(t)]$ are plotted in Fig. 5.3. As seen, for this particular piecewise linear function, the posynomial approximation is remarkably close. This result follows because the thresholds $\Pi_1, \ldots, \Pi_B$ are equally spaced, and the increments in the penalties are consistent, i.e. the consumed power is charged at a rate 5% higher when the thresholds are breached in all the blocks.

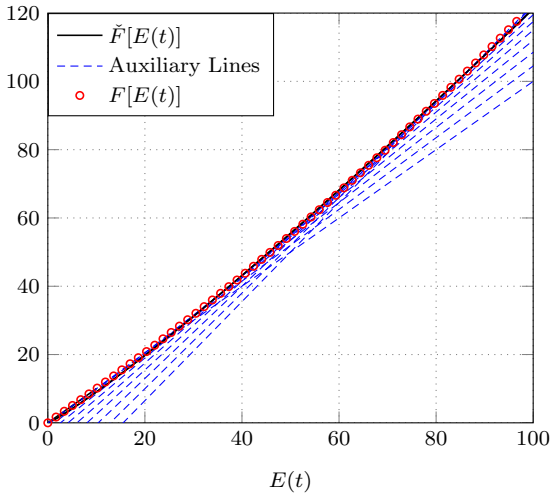

Figure 5.3: Piecewise linear "chargeable power" function and its posynomial approximation.

5.6.1 Proposed Charging and Discharging Operations

We consider the simulation parameters shown in Table 5.1, and the "chargeable power" function defined in (5.41). Then, in Fig. 5.4 we plot the discharging schedule, and the power drawn from the grid during the charging period obtained by using the strategies based on discretisation in time and calculus of variations. In Fig. 5.4, the symbol

$\mathbf{e} = \mathbf{l} + \mathbf{c} - \mathbf{d}$ represents the power drawn from the grid over the N-slot optimization period, and obtained by solving DP5.1. The similarities between the results obtained by using the two approaches follow because of the agreement between the approximating function $\check{F}(x) = \mathsf{A}x^r$, and the piecewise linear function $F(\cdot)$. Moreover, a sufficient number of linear inequalities has been considered to linearise Peukert's Law.

In Fig. 5.4 it is observed that the discharging trajectory obtained through calculus of variations $D(t)$ exceeds the load $L(t)$ in the interval $[0.7, 0.8]$. It should be noted that the trajectory $D(t)$ plotted in Fig. 5.4 was obtained by assuming a large load demand, so as to disregard the constraint $D(t) \leq L(t)$. If the load demand is not large enough, then $D(t)$ needs to satisfy $D(t) = \min\{L(t), D^*(t)\}$, where $D^*(t)$ is the optimal trajectory obtained in Sec. 5.4.2.

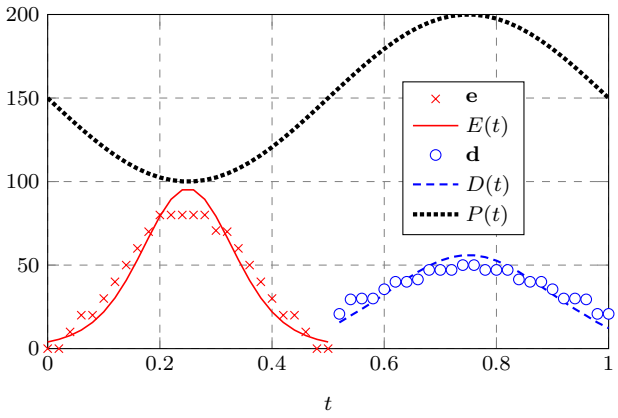

Figure 5.4: Charging and discharging profiles obtained by using the strategies based on discretisation and calculus of variations.

5.6.2 Comparison between the Strategies based on LDT and CoV

We compare the performance of the strategies based on calculus of variations and linearisation and discretisation in time. To ensure a fair comparison, we force $D(t)$ to satisfy $D(t) = \min\{L(t), D^*(t)\}$. We consider the simulation parameters shown in Table 5.1, and the "chargeable power" function defined in (5.41), while letting $\kappa \in \{1.2, 1.4\}$.

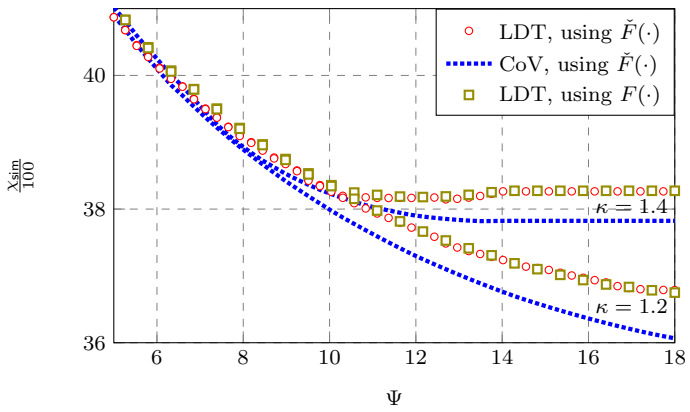

Figure 5.5: Energy cost as a function of the storage capacity. Comparison between the strategies based on LDT and CoV.

In Fig. 5.5 we plot the energy cost incurred with both strategies while varying the storage capacity from 5 to 18 energy units. As shown, the closer is κ to 1^+, the lower is the energy cost incurred, a result that follows because smaller Peukert exponents lead to reduced power loss. Although in this scenario we see a performance gap[11] between the two strategies, we cannot state that one strategy outperforms the other because both approaches are meant to solve the same optimization problem. It is also observed that the energy cost incurred can be computed either by using $F(\cdot)$ or its approximating function $\check{F}(\cdot)$ without introducing significant errors. This follows because the block pricing function was chosen to have small and consistent penalty factors for equally-spaced power thresholds, as seen in Eq. (5.41). Finally, as shown in Fig. 5.5, there is a storage capacity above which no further cost reduction can be achieved. We refer to this quantity as the *critical storage capacity*, and, as observed, it increases as $\kappa \to 1^+$.

In the following, we let $Q_{\mathsf{No}} \in \{20, 30\}$ and $\kappa = 1.4$, and set the other simulation parameters as shown in Table 5.1. We let the storage capacity vary from 5 to 18 energy units, and plot the energy cost incurred by using the proposed strategies in Fig. 5.6. As

[11]The performance gap between the two strategies may indicate an inaccurate representation of the problem in the discrete domain.

seen in Fig. 5.6, incrementing Q_{No} increases the value of the critical storage capacity above which no further cost reduction can be achieved. Moreover, the larger Q_{No}, the smaller the energy expenditure, especially if the storage capacity is above the critical value. This result follows because a large nominal output power results in a wider linear region of operation, which in turn reduces losses derived from Peukert's effect.

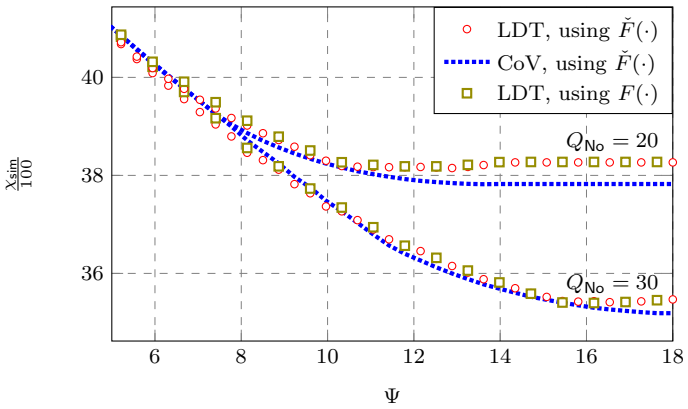

Figure 5.6: Energy cost as a function of the storage capacity. Comparison between the strategies based on LDT and CoV.

5.6.3 Convexity of the Cost Function and Optimal Storage Capacity

To evaluate the accuracy of the expression (5.40), we consider zero load demand throughout the entire planning horizon, but disregard the constraint $D(t) \leq L(t)\ \forall\ t$ by assuming that the energy discharged from the battery can be sold to the utility at retail value. Then, the cost incurred by the facility will be negative, i.e. a profit can be made by exploiting price differences during charging and discharging periods. In the following, we examine the achievable profit as a function of the total amount of energy traded over a single pair of consecutive charging and discharging periods. This will help us to verify the analysis presented in Sec. 5.5, by examining the accuracy of the expression (5.40), which estimates Θ^*, the optimal amount of energy to be shifted in time in a single pair of consecutive charging and discharging operations.

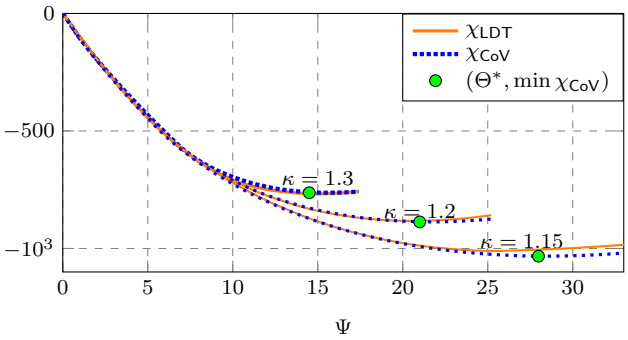

Figure 5.7: Energy cost as a function of the total energy shifted in time. The optimal amount of energy to be shifted in time is denoted by Θ^*.

Again, we consider the planning horizon $[0,1]$, the "chargeable power" function defined in (5.41), the load function $L(t) = 0 \; \forall \, t$, $\kappa \in \{1.15, 1.2, 1.3\}$, and other simulation parameters as in Table 5.1. In Fig. 5.7 we plot χ_{LDT} and χ_{CoV}, which denote the energy cost incurred by using the strategies based on LDT and CoV, respectively. As observed in Fig. 5.7, there is agreement between the value of Θ which minimizes the cost function, and the estimation given in (5.40). Moreover, remarkable similarities are observed between the results obtained through calculus of variations and linearisation and discretisation in time.

Finally, we consider the simulation parameters shown in Table 5.1, and let Q_{No} take on three different values: 10, 20, and 30. We maintain $\hat{D}_{\max} = 6Q_{\mathsf{No}}$ and set $L(t) = 0 \; \forall \, t$. The results are shown in Fig. 5.8. We observe again an agreement between the value of Θ which minimizes the cost function, and the estimate given in (5.40). Similar results are obtained through calculus of variations and linearisation and discretisation in time.

5.7 Summary

Assuming dynamic block pricing, we have proposed strategies to minimize the energy bill incurred by a non-deferrable load facility over a finite planning horizon. We have assumed that the facility is equipped with a renewable energy harvester and a storage

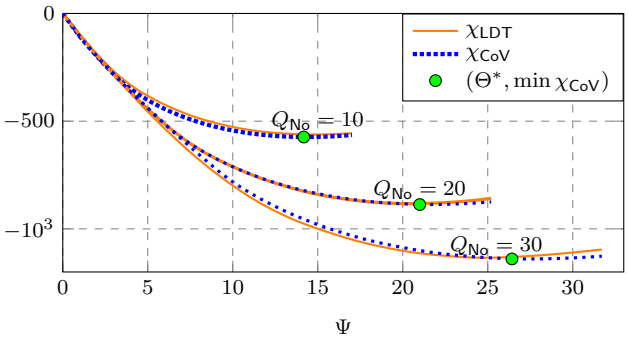

Figure 5.8: Energy cost as a function of energy shifted in time Θ. Optimal Θ is Θ^*.

device. We have then presented two different problem formulations, and worked out two solutions by using different approaches. One way to formulate the problem is by using power signals, either in discrete or continuous time. An alternative formulation can be obtained by using energy signals in discrete time.

We have also analysed the cost function in terms of Θ, the energy shifted in time through a single pair of consecutive charging and discharging operations. Furthermore, after introducing some simplifications we have shown that the cost function is convex in Θ, and have determined the value of Θ that minimizes the energy bill.

The analytical and numerical results presented in this chapter have allowed us to draw the following conclusions:

- The energy bill minimization problem involving dynamic block pricing can be formulated by using either continuous or discrete signals. In the former case, we have derived analytical expressions to estimate the optimal charging and discharging operations. These expressions provide valuable insights, as they can be used to determine the relationship between the achievable cost savings and different storage parameters.

- For the situations in which relaxations cannot be afforded, the formulation using discrete signals may result more appropriate. The advantage of such an approach is

that the sampling frequency can be chosen within the available computational capacity, and different levels of accuracy can be attained as a result. In this respect, we have shown that introducing multiple linear inequalities can be an effective method to handle non-linear constraints.

- Both the analytical and numerical results have shown that there is a critical storage capacity, above which no further cost reduction can be achieved. Therefore, increasing the storage capacity does not necessarily decrease the energy cost. This follows from considerations such as the increasing block electricity rates, and the non-linear discharging model, which penalize charging and discharging operations in proportion to the energy quantities involved.

Chapter 6

Conclusions & Future Research

6.1 Conclusions

We have proposed several strategies to minimize the energy expenditure incurred by non-deferrable load facilities over a finite planning horizon. We have assumed dynamic electricity prices, and facilities equipped with renewable energy harvesters and storage devices. The following are the main contributions of this thesis:

- We have proposed a mathematical framework to design energy-bill minimization strategies for non-deferrable loads with renewable energy harvesting and storage capabilities. Unlike the existing proposals in the literature, this framework incorporates models for the energy storage device, the renewable energy arrivals, and the pricing and incentives schemes.

- We have proposed three genie-aided strategies, which use different optimization approaches, and hence have different computational requirements. To devise the first strategy we have used linearisation, discretisation in time, and linear programming. The second and third strategies have been designed by using evolutionary algorithms and calculus of variations. The strategy based on calculus of variations has allowed us to obtain simpler and more insightful results when the discharging operation is modelled after Peukert's Law.

- We have also proposed two online energy management strategies. The first strategy

uses statistical forecasting methods to estimate future renewable energy arrivals and load requirements. The second proposed strategy is model-independent, and does not rely on forecasting techniques.

- We have proposed two genie-aided strategies to minimize the energy bill incurred by a set of facilities over a finite planning horizon. The facilities are equipped with renewable energy harvesters and storage devices, and their power consumption is non-deferrable. Moreover, they are enabled to share renewable energy either through the smart grid (incurring a transfer fee), or a dedicated connexion (free of charge). To design the first strategy, we have assumed that all the facilities are equipped with their own renewable energy harvester and storage device, and are allowed to exchange renewable energy through the smart grid incurring a transfer fee. To design the second strategy, we have assumed that all the facilities have free access to a shared renewable energy farm. In this context, we have also proposed an online strategy, for which we have used a model based on stochastic differential equations to depict the stochastic process governing the amount of renewable energy available over time.

- Assuming dynamic block pricing, we have proposed two genie-aided strategies to minimize the energy bill incurred by a non-deferrable load facility over a finite planning horizon. The first strategy has been designed by using linearisation and discretisation in time, and the second strategy has been obtained by using calculus of variations.

Our research has resulted in the following discoveries and insights:

- Continuous-time optimization techniques can be used to find approximate solutions to the mathematical problems formulated in this thesis. The results obtained through continuous-time models are explicit, and hence can be used to reduce the complexity

of algorithms designed to run in real time. Specifically, continuous-time optimization techniques can lead to results in analytic form, potentially eliminating the need for iterative routines, such as the ones required to solve a linear programming problem. Continuous-time optimization techniques can be used in conjunction with discrete-time methods to fine tune initial solutions thus increasing their accuracy without incurring a significant number of additional operations.

- Significant problem simplification can be achieved if the total energy demand is considerably much larger than the local (renewable) energy generation, or if the energy locally generated can be sold to the utility at retail value. If the local generation is considerably smaller than the local demand at all times, then we can design the optimal energy management strategy without much concern about excess generation. Hence, exact information about the load at any point in time is not relevant. All that is required to know is that the load is large enough to be above the designed optimal consumption of renewable power at all times. The same conclusion follows if the consumers are allowed to inject renewable energy into the grid at retail value, e.g. following a net metering policy.

- The forecasting error of renewable energy arrivals is less critical when a large storage capacity is considered. Moreover, knowledge of future renewable energy arrivals is less relevant when we know the bequest value of the energy remaining in the battery at the end of the planning period. The first result follows because a large storage capacity offers more freedom to schedule consumption. In contrast, a limited storage capacity requires more accurate information to decide on whether to carry out discharging operations so as to secure space for future renewable energy arrivals. The second result can be counter-intuitive, but follows from optimization principles, and

is obtained after introducing the substitutions and relaxations explained in Chapter 3.

- An ingenious strategy to handle the causality constraint is to set the power discharged to be proportional to the amount of energy stored in the system at all times. That is, if $J(t)$ and $\tilde{D}(t)$ denote respectively the amount of energy stored and the power drawn from the storage device at time t, then, we can let $\tilde{D}(t) = \theta(t)J(t),\ J(t) \geq 0\ \forall\ t$, and design $\tilde{D}(t)$ by optimizing $\theta(t)$, which we assume non-negative at all times. Posing the problem in terms of $\theta(t)$ will allow us to disregard the causality constraint because $J(t) \to 0$ implies $\tilde{D}(t) \to 0$. This strategy is more beneficial in scenarios in which the causality constraint is difficult to handle, e.g. when $J(t)$ is a random variable.

- In Chapter 4, we have proposed two strategies to minimize the energy bill incurred by a set of facilities enabled to share renewable energy. We have considered two arrangements: one in which each facility is equipped with its own renewable energy harvester and storage device, and a second arrangement, in which all of them share access to a renewable energy farm. We have compared the two approaches and found the conditions under which they achieve similar performance. Through simulations, we have also shown that the approach with distributed generation outperforms the centralized arrangement when the renewable energy arrivals are independent across different locations. The two strategies have a similar performance if their renewable generation is statistically identical, and their storage devices have similar[1] characteristics, e.g. size and efficiency.

- A strategy to solve complex optimization problems, such as the one posed in Sec. 4.4.1, is to combine optimization techniques such as partitioning, decomposition, calculus of variations, and Lagrange multipliers. The partitioning and decomposition

[1]The storage parameters are such that the same discharging operation incurs the same power loss in both arrangements.

methods can be used to break the problem into smaller sub-problems. Moreover, artificial variables can be introduced to transform the mathematical problem into a separable optimization problem. The problem can then be solved in two steps: in the first step, the trajectories can be optimized in terms of the artificial variables, and in the second step, the artificial variables can be optimized by solving a simpler mathematical problem. In our particular case, the first problem has been solved by using calculus of variations, whereas the second problem has been tackled through Lagrange multipliers. Thus, the combination of these methods has allowed us to tackle a problem, which is otherwise intractable.

6.2 Future Research

Four interesting problems are suggested for further investigation:

1. The first research problem is to design renewable energy management strategies by using models that take into account the geographic variations that characterize distributed generation. To that end, weather forecasts, and irradiance and wind flow maps can be incorporated into the strategies. It is therefore of interest to investigate the trade-off between the computational complexity incurred by processing large amounts of data, and the monetary savings derived from the resulting strategies.

2. The second problem is to design renewable energy management strategies considering random, market-driven electricity prices. When large consumers opt to bid directly in the wholesale electricity market, they need to adopt strategies to manage their exposure and minimize their expenditures. This research problem is challenging because it involves modelling renewable energy arrivals, electricity prices, and power requirements. While different statistical forecasting approaches

can be considered, the question of which techniques are the most cost effective, and computationally efficient, remains unsolved.

3. Given the continuous improvements in energy storage technologies, it is of interest to understand the trade-off between the capital expenditures and the achievable cost savings. Capital expenditures are incurred to purchase required equipment such as batteries, renewable energy harvesters, or power converters. The available choices of devices may offer distinctive advantages, e.g. some storage technologies may be more efficient, but also cost more, some devices may require replacements more often than others, etc. To evaluate their effective financial benefits, it is necessary to consider their initial cost and lifetime degradation. This poses several challenges, especially in modeling, e.g. how can the lifetime degradation be included in the formulation? What utility functions are appropriate to model environmentally friendly, yet more expensive alternatives?

4. In regards to the role of renewable energy in communication technologies, it is of interest to design strategies that allow base stations to properly operate in stand-alone mode. Most of the existing works have assumed a base station that is permanently connected to the grid, which allows the designer to focus on issues such as minimizing monetary expending. However, in areas without reliable power delivery services, the base stations may need to operate in off-grid mode, at least for some period of time. In stand-alone mode the priority is to satisfy the requests made by the mobile users and guarantee an acceptable quality-of-service. The challenge is thus to cope with the uncertainty of the renewable energy arrivals, and be able to deliver an acceptable service within the periods of grid disruption. Moreover, for base stations in grid-connected mode, a holistic profit maximiza-

tion scheme can be devised by jointly designing energy management strategies, and data pricing programs. The first strategies are meant to reduce operational expenditure, whereas the data pricing programs are designed to increase revenue. To this end, the variations in energy prices and mobile traffic can be exploited to make cellular operators more profitable while maintaining their standard quality-of-service.

Appendix A

Additional Results

A.1 Method to Solve P2.A

An approximate solution to P2.A can be obtained if we let $f_i(x) = \alpha_i x - \beta_i$ be a tangent line to the curve $\mathscr{F}^{-1}(x)$, which touches it at equally[1] spaced points x_i's. For example, if $\mathscr{F}^{-1}(\cdot)$ is modelled after Peukert's Law, i.e. if

$$\mathscr{F}^{-1}(x) = \min\left\{ Q_{\text{No}}\left[\frac{x}{Q_{\text{No}}}\right]^{\frac{1}{\kappa}}, x \right\}, \tag{A.1}$$

then for[2] $i > 1$, we have:

$$\alpha_i = \frac{1}{\kappa}\left(\frac{x_i}{Q_{\text{No}}}\right)^{\frac{1-\kappa}{\kappa}}, \tag{A.2}$$

and

$$\beta_i = -\frac{\kappa - 1}{\kappa} Q_{\text{No}}^{\frac{\kappa-1}{\kappa}} x_i^{\frac{1}{\kappa}}. \tag{A.3}$$

Therefore, if the discharging model assumed is Peukert's, then we can use (A.2) and (A.3) to replace (2.10) with the following set of linear inequality constraints:

$$d(k) \leq \frac{1}{\kappa}\left(\frac{x_i}{Q_{\text{No}}}\right)^{\frac{1-\kappa}{\kappa}} \tilde{d}(k) + \frac{\kappa - 1}{\kappa} Q_{\text{No}}^{\frac{\kappa-1}{\kappa}} x_i^{\frac{1}{\kappa}}, \tag{A.4}$$

for any equally-spaced points $x_i > 0$, $i \in \{2, \ldots, M\}$. Note that if $\mathscr{F}^{-1}(\cdot)$ is defined according to (A.1), and the first segment is chosen to approximate $\mathscr{F}^{-1}(\cdot)$ in $[0, Q_{\text{No}}]$, then $\alpha_1 = 1$ and $\beta_1 = 0$.

[1] The x_i's can be chosen as the midpoints of the intervals $[\Phi_i, \Phi_{i+1}]$, $i \in \{2, \ldots, M-2\}$. While x_1 and x_{M-1} can be respectively the midpoints of $[0, \Phi_1]$ and $[\Phi_{M-1}, \tilde{D}_{\max}]$.

[2] If $\mathscr{F}^{-1}()$ is defined according to Peukert's model, then $\mathscr{F}^{-1}()$ is linear in $[0, \Phi_1]$.

A.2 Number of Realisations Numerical Results Chapter 3

The ten thousand realisations figure was determined empirically. The same number of independent runs was considered for each of the battery size values. Then, this number was progressively increased until the result was a smooth and consistent cost savings curve. The cost savings curve is non-decreasing with respect to the battery size. Therefore, a smooth and consistent curve can be seen as a sign of convergence. Note that this would not be possible if the experiments were not independent across battery size values. Fig. A.1, which shows the performance of the ARIMA-based online algorithm, illustrates this idea. For consistency, the same figure (ten thousand) was maintained for evaluating algorithms based on other forecasting techniques, even if their performance variability across runs was lower.

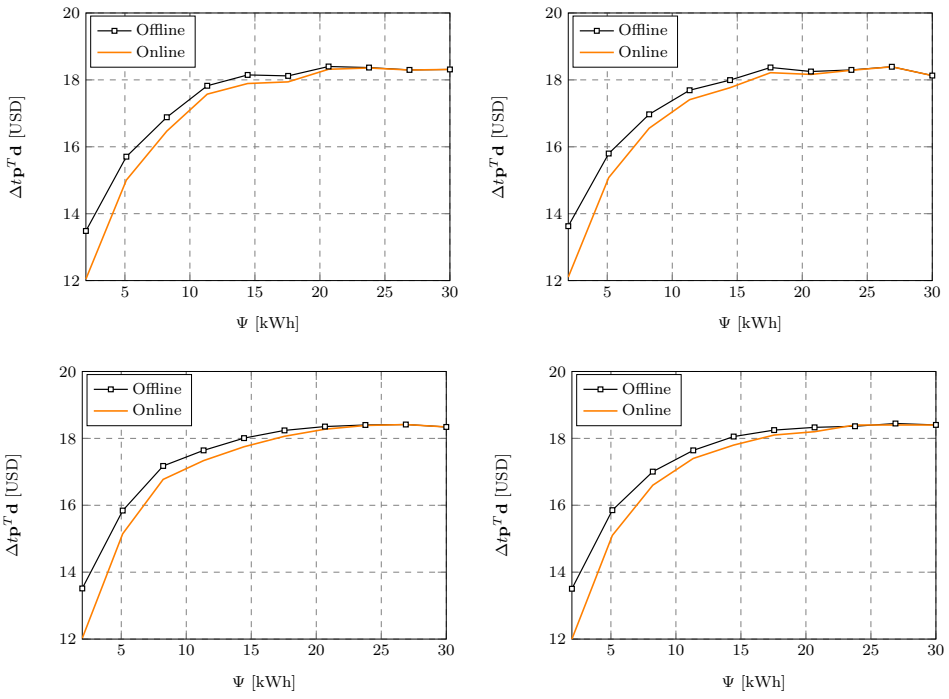

Figure A.1: ARIMA-based online algorithm. Average performance for different number of runs: 500 (top left), 1000 (top right), 2000 (bottom left), 10000 (bottom right).

A.3 Transition Probabilities Time-Inhomogeneous Markov Chain

Table A.1: Transition probabilities, Markov chain model.

Transition time (hour)	Source	Destination				
		E_1	E_2	E_3	E_4	E_5
6 to 7	E_1	0.54	0.40	0.06	0.00	0.00
7 to 8	E_1	0.36	0.41	0.22	0.01	0.00
	E_2	0.02	0.06	0.82	0.10	0.00
	E_3	0.00	0.00	0.17	0.83	0.00
8 to 9	E_1	0.35	0.46	0.11	0.08	0.00
	E_2	0.01	0.10	0.56	0.32	0.01
	E_3	0.00	0.01	0.13	0.84	0.02
	E_4	0.00	0.03	0.00	0.60	0.37
9 to 10	E_1	0.37	0.48	0.11	0.04	0.00
	E_2	0.09	0.29	0.27	0.33	0.02
	E_3	0.01	0.04	0.18	0.62	0.15
	E_4	0.00	0.01	0.02	0.20	0.77
	E_5	0.00	0.00	0.06	0.05	0.89
10 to 11	E_1	0.27	0.27	0.20	0.20	0.06
	E_2	0.06	0.52	0.16	0.16	0.10
	E_3	0.06	0.18	0.18	0.36	0.21
	E_4	0.00	0.04	0.05	0.53	0.38
	E_5	0.00	0.00	0.00	0.03	0.97
11 to 12	E_1	0.50	0.25	0.00	0.12	0.12
	E_2	0.00	0.44	0.23	0.30	0.03
	E_3	0.05	0.26	0.26	0.11	0.31
	E_4	0.01	0.04	0.08	0.72	0.15
	E_5	0.00	0.00	0.04	0.06	0.90
12 to 13	E_1	0.33	0.66	0.00	0.00	0.00
	E_2	0.21	0.42	0.25	0.08	0.04
	E_3	0.19	0.22	0.19	0.33	0.07
	E_4	0.01	0.07	0.14	0.76	0.01
	E_5	0.00	0.00	0.02	0.28	0.70
13 to 14	E_1	0.71	0.07	0.14	0.07	0.00
	E_2	0.31	0.50	0.15	0.04	0.00
	E_3	0.11	0.32	0.50	0.07	0.00
	E_4	0.02	0.06	0.58	0.34	0.00
	E_5	0.00	0.01	0.05	0.94	0.00
14 to 15	E_1	0.52	0.39	0.08	0.00	0.00
	E_2	0.21	0.66	0.12	0.00	0.00
	E_3	0.04	0.77	0.18	0.00	0.00
	E_4	0.02	0.06	0.92	0.00	0.00
15 to 16	E_1	0.89	0.11	0.00	0.00	0.00
	E_2	0.88	0.12	0.00	0.00	0.00
	E_3	0.08	0.92	0.00	0.00	0.00
16 to 17	E_1	1.00	0.00	0.00	0.00	0.00
	E_2	1.00	0.00	0.00	0.00	0.00

Appendix B

Various Proofs

B.1 Proof of Proposition 2.4.1

Proof. Since $\tilde{D}(t) \geq 0 \; \forall \, t$, we have:

$$\varsigma \int_0^H R(x)dx + \int_0^t [\varsigma R(x) - \tilde{D}(x)]dx \geq \varsigma \int_0^H R(x)dx + \int_0^t [\varsigma R(x)]dx - \int_0^H \tilde{D}(x)dx \; \forall \, t.$$

Moreover, substituting $\int_0^H \tilde{D}(t)dt = \varsigma \int_0^H R(t)dt$ yields:

$$\varsigma \int_0^H R(x)dx + \int_0^t [\varsigma R(x) - \tilde{D}(x)]dx \geq \varsigma \int_0^H R(x)dx + \int_0^t [\varsigma R(x)]dx - \varsigma \int_0^H R(x)dx \; \forall \, t,$$

which implies:

$$\varsigma \int_0^H R(x)dx + \int_0^t [\varsigma R(x) - \tilde{D}(x)]dx \geq \int_0^t [\varsigma R(x)]dx \; \forall \, t.$$

Since $J(0) = \varsigma \int_0^H R(x)dx$ and $\int_0^t [\varsigma R(x)]dx \geq 0$ the proof is complete. ■

B.2 Proof of Proposition 2.4.2

Proof. Since $\tilde{D}(t) \geq 0 \; \forall \, t$, we have:

$$\varsigma \int_0^H R(x)dx + \int_0^t [\varsigma R(x) - \tilde{D}(x)]dx \leq \varsigma \int_0^H R(x)dx + \int_0^t \varsigma R(x)dx \leq 2\varsigma \int_0^H R(x)dx.$$

Hence, if $\Psi \geq 2\varsigma \int_0^H R(x)dx$, then $J(t) \leq \Psi \; \forall \, t$. ■

B.3 Proof of Theorem 2.4.1

Proof. To solve this optimization problem we use the Lagrange multipliers rule for calculus of variations [24]. Hence, we consider the following Lagrangian:

$$\mathscr{L}(\lambda, D) = \int_0^H -P(t)D(t) + \lambda \mathscr{F}[D(t)]\, dt - \lambda J(0).$$

By applying the Euler-Lagrange optimality condition we obtain:

$$-P(t) + \lambda \mathscr{F}'[D(t)] = 0, \tag{B.1}$$

where $\mathscr{F}'(x) = \frac{d}{dx}\mathscr{F}(x)$. If $\mathscr{F}(x) = Q_{\mathsf{No}}\left[\frac{x}{Q_{\mathsf{No}}}\right]^{\kappa}$, with $Q_{\mathsf{No}} > 0$ and $\kappa > 1$, then the Euler-Lagrange optimality condition implies that the optimal discharging profile, denoted by $D^*(t)$ has the form:

$$D^*(t) = Q_{\mathsf{No}}\left[\frac{P(t)}{\lambda\kappa}\right]^{\frac{1}{\kappa-1}}.$$

The constant λ can be obtained by replacing $D^*(t)$ into the constraint:

$$\int_0^H Q_{\mathrm{No}}\left[\frac{D^*(t)}{Q_{\mathrm{No}}}\right]^{\kappa} dt = J(0),$$

which leads to:

$$\lambda = \frac{1}{\kappa\left(\dfrac{J(0)}{Q_{\mathrm{No}}\displaystyle\int_0^H P(t)^{\frac{\kappa}{\kappa-1}}\, dt}\right)^{\frac{\kappa-1}{\kappa}}}.$$

■

B.4 Proof of Theorem 3.6.1

Proof. Following the Proposition 3.6.2, if $\Psi \geq \varsigma \int_0^H R(t)dt + J(0)$, then the constraint (3.4) can be disregarded because the battery is large enough to avert wastage of renewable energy. To find optimal $\theta(t)$ we use Pontryagin's Maximum Principle as fol-

lows. Let $\mathscr{H}(J,\theta,t)$ denote the Hamiltonian of the dynamic system with state variable $J(t)$, which evolves according to $dJ(t) = \varsigma R(t) - \theta(t)J(t)dt$, and cost function $\int_0^H P(t)\mathscr{G}[\theta(t)J(t)]\,dt + KJ(H)$, then $\mathscr{H}(J,\theta,t)$ can be written as:

$$\mathscr{H}(J,\theta,t) = P(t)\mathscr{G}[\theta(t)J(t)] + \lambda(t)[\varsigma R(t) - \theta(t)J(t)], \tag{B.2}$$

where $\lambda(t)$ is the time-varying Lagrange multiplier [25]. The costate equation $\frac{d\lambda}{dt} = -\frac{\partial \mathscr{H}}{\partial J}$ yields:

$$\frac{d\lambda}{dt} = \lambda(t)\theta(t) - P(t)\frac{\partial}{\partial J}\mathscr{G}[\theta(t)J(t)]. \tag{B.3}$$

The stationary condition requires:

$$0 = \frac{\partial \mathscr{H}}{\partial \theta} = P(t)\frac{\partial}{\partial \theta}\mathscr{G}[\theta(t)J(t)] - \lambda(t)J(t). \tag{B.4}$$

If $J(t) > 0\ \forall\ t$, conditions (B.3) and (B.4) imply[1] $\frac{d\lambda}{dt} = 0$. Hence $\lambda(t)$ is a constant, which can be determined from the boundary condition [26]:

$$\lambda(H) = \frac{d}{dJ}KJ\bigg|_{t=H} = K. \tag{B.5}$$

Therefore, from (B.4) we can obtain the following condition for optimal $\theta^*(t)$:

$$P(t)\frac{\partial}{\partial \theta}\mathscr{G}[\theta(t)J(t)] = KJ(t). \tag{B.6}$$

We can obtain a closed-form solution if we let $\mathscr{G}[\theta(t)J(t)] = Q_{\mathsf{No}}\left(\frac{\theta(t)J(t)}{Q_{\mathsf{No}}}\right)^{\frac{1}{\kappa}}$:

$$\theta(t) = \frac{Q_{\mathsf{No}}}{J(t)}\left[\frac{P(t)}{\kappa K}\right]^{\frac{\kappa}{\kappa-1}},\ J(0) > 0. \tag{B.7}$$

Note that Proposition 3.6.1 states that if $J(0) > 0$, then $J(t) > 0\ \forall\ t$.

■

[1] To see it note that for any differentiable function $\mathscr{G}:\mathbb{R}\to\mathbb{R}$, we have $\theta\frac{\partial}{\partial\theta}\mathscr{G}(\theta J) = J\frac{\partial}{\partial J}\mathscr{G}(\theta J)$.

B.5 Proof of Proposition 3.4.1

Proof. For ease of notation, let $r_k := r(k)$, and note that $\mathbb{E}\left[(r_k - \hat{r}_k)^2 \mid s(k-1) = E_x\right]$ is convex in $\hat{r}_k$. Thus, we can minimize $\mathbb{E}\left[(r_k - \hat{r}_k)^2 \mid s(k-1) = E_x\right]$ by differentiating with respect to $\hat{r}_k$. The first-order condition $\frac{d}{d\hat{r}_k}\mathbb{E}\left[(r_k - \hat{r}_k)^2 \mid s(k-1) = E_x\right] = 0$ leads to $\hat{r}_k = \mathbb{E}[r_k \mid s(k-1) = E_x]$. Moreover,

$$\begin{aligned}\mathbb{E}[r_k \mid s(k-1) = E_x] = \frac{\Lambda}{2|\mathcal{S}|}P(s(k) = E_1 \mid s(k-1) = E_x) \\ + \frac{3\Lambda}{2|\mathcal{S}|}P(s(k) = E_2 \mid s(k-1) = E_x) \\ + \ldots + \frac{(2|\mathcal{S}|-1)\Lambda}{2|\mathcal{S}|}P\left(s(k) = E_{|\mathcal{S}|} \mid s(k-1) = E_x\right),\end{aligned} \tag{B.8}$$

which can be written compactly as $\mathbb{E}[r_k \mid s(k-1) = E_x] = \frac{\Lambda}{2|\mathcal{S}|}\sum_{i=1}^{|\mathcal{S}|}(2i - 1)P(s(k) = E_i \mid s(k-1) = E_x)$. ■

B.6 Proof of Theorem 4.4.1

Proof. Following Lemma 4.4.1, we can ignore the constraint (4.15) because $J(0) \geq \zeta$. Moreover, since $J(H) = J(0) - \sum_{j=1}^{N}\gamma_j + \int_0^H \varsigma R(t)dt$, and does not depend[2] on the optimization variables $D_1(t), \ldots, D_{\mathsf{M}}(t)$, we can remove $P(H)J(H)$ from the objective function in P4.B2.

The objective in P4.B2 is a sum of functionals of $D_i(t), i \in \{1, \ldots, \mathsf{M}\}$ for $t \in [t_{j-1}, t_j]$. Moreover, P4.B2 is a separable optimization problem [188], and we can determine candidate solutions $D_i(t),\ i \in \{1, \ldots, \mathsf{M}\}$ for each interval $[t_{j-1}, t_j]$, by using the Lagrange multipliers rule for calculus of variations [24]. Specifically, we write the following Lagrangian in terms of the optimization variables $D_1(t), \ldots, D_{\mathsf{M}}(t)$:

$$\mathscr{L}(D_1, \ldots, D_{\mathsf{M}}; \lambda_j) = -\int_{t_{j-1}}^{t_j}\left[\sum_{i=1}^{\mathsf{M}} P_i(t)D_i(t)\right]dt + \lambda_j\left(\int_{t_{j-1}}^{t_j}\mathscr{F}[D_1(t) + \ldots + D_{\mathsf{M}}(t)]\,dt - \gamma_j\right).$$

[2] If $\gamma_1, \ldots, \gamma_N$ are given, then so is $J(H)$.

The conditions for optimality $\frac{\partial}{\partial D_i}\mathscr{L}(D_1,\ldots,D_{\mathsf{M}};\lambda_j)=0\ \forall\ i$, cannot be all satisfied at the same time, unless all prices $P_i(t)$ are equal, i.e. $P_i(t)=P_1(t)\ \forall\ i,\ \forall\ t\ \in\ [t_{j-1},t_j]$. In fact, the objective in P4.B2 attains its maximum when in each subinterval $[t_{j-1},t_j]$ either $D_i(t)=0\ \forall\ t\ \in\ [t_{j-1},t_j]$, or is such that:

$$\int_{t_{j-1}}^{t_j}\mathscr{F}\left[D_i(t)\right]dt=\gamma_j. \tag{B.9}$$

Following the constraint (4.17), if $D_i(t)$ satisfies (B.9), then for all $n\neq i$: $D_n(t)=0\ \forall\ t\ \in\ [t_{j-1},t_j]$. That is, if[3] $\gamma_j>0$, then in each subinterval $[t_{j-1},t_j]$ there is a single $D_i(t)$ which is not identically 0 in $[t_{j-1},t_j]$. Therefore, for each time slot $[t_{j-1},t_j]$, there are M possibilities, and each of them can be denoted by a number i which refers to the single $D_i(t)$ that is *not* identically 0 in $[t_{j-1},t_j]$.

Let $s_j\in\ \{1,2,\ldots,\mathsf{M}\}$, denote the selected possibility in $[t_{j-1},t_j]$, then:

$$\int_{t_{j-1}}^{t_j}\left[\sum_{i=1}^{\mathsf{M}}P_i(t)D_i(t)\right]dt=\int_{t_{j-1}}^{t_j}P_{s_j}(t)D_{s_j}(t)dt. \tag{B.10}$$

Since $P_{k_j}(t)\geq P_i(t)\ \forall\ t\ \in\ [t_{j-1},t_j]$, the functional $\int_{t_{j-1}}^{t_j}P_{s_j}(t)D_{s_j}(t)dt$ attains its maximum when $s_j=k_j$. Moreover, the k_jth possibility is such that for all $n\neq k_j$, $D_n(t)=0\ \forall\ t\ [t_{j-1},t_j]$, and $D_{k_j}(t)$ is chosen to satisfy the constraint (4.17), i.e.:

$$\int_{t_{j-1}}^{t_j}\mathscr{F}\left[D_{k_j}(t)\right]dt=\gamma_j. \tag{B.11}$$

Therefore, the optimal $D_{k_j}(t)$ in $[t_{j-1},t_j]$ can be obtained by solving the following optimization problem:

$$\max_{D_{k_j}}.\quad\int_{t_{j-1}}^{t_j}\left[P_{k_j}(t)D_{k_j}(t)\right]dt$$

s.t. (B.11). To use the Lagrange multipliers rule for calculus of variations [24], we

[3]The case $\gamma_j=0$ is trivial as $D_i(t)=0\ \forall\ t\in[t_{j-1},t_j]$ and for all $i\in\{1,\ldots,\mathsf{M}\}$.

define:

$$\mathscr{L}\left(D_{k_j},\lambda\right) = -\int_{t_{j-1}}^{t_j} P_{k_j}(t)D_{k_j}(t)dt + \lambda\left[\int_{t_{j-1}}^{t_j} \mathscr{F}\left[D_{k_j}(t)\right]dt - \gamma_j\right]. \tag{B.12}$$

The optimality condition $\frac{\partial}{\partial D_{k_j}}\mathscr{L}\left(D_{k_j},\lambda\right) = 0$ yields (4.22). Moreover, if $\mathscr{F}(x) = Q_{\mathsf{No}}\left(\frac{x}{Q_{\mathsf{No}}}\right)^{\kappa}$, with $Q_{\mathsf{No}} > 0$ and $\kappa > 1$, then (4.22) yields:

$$D_{k_j}(t) = \mathscr{K}_j\left[P_{k_j}(t)\right]^{\frac{1}{\kappa-1}}, \tag{B.13}$$

where $\mathscr{K}_j$ is a constant chosen to satisfy (B.11). By replacing (B.13) into (B.11), we obtain $\mathscr{K}_j$ as follows:

$$\mathscr{K}_j = \left(\frac{\gamma_j {Q_{\mathsf{No}}}^{\kappa-1}}{\int_{t_{j-1}}^{t_j} P_{k_j}(\tau)^{\frac{\kappa}{\kappa-1}}d\tau}\right)^{\frac{1}{\kappa}}. \tag{B.14}$$

■

B.7 Proof of Lemmas 4.4.2 and 4.4.3

From (B.13) and (B.14) we see that

$$\int_{t_{j-1}}^{t_j} P_{k_j}(t)D^*_{k_j}(t)dt = \mathscr{K}_j\int_{t_{j-1}}^{t_j}\left[P_{k_j}(t)\right]^{\frac{\kappa}{\kappa-1}}dt = \gamma_j^{\frac{1}{\kappa}}\left(Q_{\mathsf{No}}\Omega_j\right)^{\frac{\kappa-1}{\kappa}}, \tag{B.15}$$

where

$$\Omega_j = \int_{t_{j-1}}^{t_j} P_{k_j}(\tau)^{\frac{\kappa}{\kappa-1}}d\tau,\ j\ \in\ \{1,2,\ldots,N\}.$$

By using (B.15) we can simplify ρ as follows:

$$\rho = \sum_{j=1}^{N}\left(Q_{\mathsf{No}}\Omega_j\right)^{\frac{\kappa-1}{\kappa}}\gamma_j^{\frac{1}{\kappa}} + P(H)\left[Z - \sum_{j=1}^{N}\gamma_j\right], \tag{B.16}$$

where $Z = J(0) + \int_0^H \varsigma R(t)dt$.

Proof of Lemma 4.4.2:

Proof. Since $\sum_{j=1}^{N}\left(Q_{\mathsf{No}}\Omega_j\right)^{\frac{\kappa-1}{\kappa}}\gamma_j^{\frac{1}{\kappa}} + P(H)\left[Z - \sum_{j=1}^{N}\gamma_j\right]$ is concave in γ_j for $\kappa > 1$ and

$Q_{\mathsf{No}} > 0$, the condition for optimality is:

$$\frac{\partial}{\partial \gamma_j}\left[\sum_{j=1}^{N}\left(Q_{\mathsf{No}}\Omega_j\right)^{\frac{\kappa-1}{\kappa}}\gamma_j^{\frac{1}{\kappa}} + P(H)\left(Z-\sum_{j=1}^{N}\gamma_j\right)\right] = 0, \tag{B.17}$$

which yields the result in (4.26). Note that the result in (4.26) is such that $\left(Z-\sum_{j=1}^{N}\gamma_j\right) \geq 0$. To see this, recall that $Z = J(0) + \int_0^H \varsigma R(t)dt$, and $J(0) \geq \sum_{j=1}^{N}\gamma_j,\ 0 \leq t \leq H$, which yields $\left(Z-\sum_{j=1}^{N}\gamma_j\right) \geq 0$ since $\int_0^H \varsigma R(\tau)d\tau \geq 0$. ■

Proof of Lemma 4.4.3:

Proof. If $P(H) = 0$, then it is optimal to set $J(H) = 0$ because the energy left unused at $t = H$ has zero unit-price. Moreover, since $R(t) = 0\ \forall\, t$, from (4.21) we have:

$$\sum_{j=1}^{N}\gamma_j = J(0). \tag{B.18}$$

With $P(H) = 0$, we have $\rho = \sum_{j=1}^{N}\left(Q_{\mathsf{No}}\Omega_j\right)^{\frac{\kappa-1}{\kappa}}\gamma_j^{\frac{1}{\kappa}}$. Hence, to derive the optimal $\gamma_1,\ldots,\gamma_N$ that maximize ρ subject to (B.18), we write the following Lagrangian:

$$\mathscr{L}(\gamma_1,\ldots,\gamma_N,\lambda) = \sum_{j=1}^{N}\left(Q_{\mathsf{No}}\Omega_j\right)^{\frac{\kappa-1}{\kappa}}\gamma_j^{\frac{1}{\kappa}} - \lambda\left[\sum_{i=1}^{N}\gamma_i - J(0)\right]. \tag{B.19}$$

The conditions for optimality $\frac{\partial}{\partial \gamma_j}\mathscr{L}(\gamma_1,\ldots,\gamma_N,\lambda) = 0$ yield:

$$\Omega_j\gamma_i = \Omega_i\gamma_j,\ \forall\, i \neq j. \tag{B.20}$$

Thus, (4.27) can be obtained by replacing (B.20) into the constraint (B.18). ■

B.8 Proof of Theorem 4.4.2

Proof. Because $J(t) > 0, \forall\, t$, define $f(J) = \log(J)$ and use Ito's lemma to write the stochastic differential equation for $f(J)$:

$$df = \left(\frac{\partial f}{\partial t} + [\mu-\theta]J\frac{\partial f}{\partial J} + \frac{1}{2}\sigma^2J^2\frac{\partial^2 f}{\partial J^2}\right)dt + \sigma J\frac{\partial f}{\partial J}d\mathscr{W}, \tag{B.21}$$

where the time index (t) has been removed for brevity. After replacing $f[J(t)] = \log[J(t)]$ in (B.21), we obtain:

$$df = \left(\mu(t) - \theta(t) - \frac{1}{2}\sigma^2\right)dt + \sigma d\mathscr{W}. \tag{B.22}$$

Recall Ito's integral definition for real-valued deterministic integrands [33]: Let $g : \mathbb{R} \to \mathbb{R}$ be a square-integrable function in $[a,b]$, then:

$$\int_a^b g(t)d\mathscr{W} \triangleq \lim_{\Delta t \to 0} \sum_i g(t_i)\left[\mathscr{W}(t_{i+1}) - \mathscr{W}(t_i)\right], \tag{B.23}$$

where $\Delta t = t_{i+1} - t_i$. By using Ito's integral definition in (B.22), we obtain:

$$J(t) = J(0)\exp\left[\int_0^t \left(\mu(\tau) - \theta(\tau) - \frac{1}{2}\sigma^2\right)d\tau + \sigma\mathscr{W}(t)\right]. \tag{B.24}$$

Comparing (B.24) and (4.32), we obtain (4.33). ■

B.9 Proof of Theorem 5.4.1

Proof. We define the following Lagrangian to find necessary conditions to minimize each $\mathcal{Y}_{C,i}[C(t)]$, under the constraint (5.21d):

$$\mathscr{L}(C(t),\lambda_{C,i}) = \int_{\delta_i}^{\zeta_i} \left[P(t)F\left[C(t)+L(t)\right] + \lambda_{C,i}C(t)\right]dt - \lambda_{C,i}\frac{1}{\varsigma}\left[J(\zeta_i) - J(\delta_i) - \overline{\mathsf{R}}_i\right].$$

Hence, from the Euler-Lagrange equation, $C(t)$ must satisfy the following condition to minimize/maximize $\mathcal{Y}_{C,i}[C(t)]$ under the constraint (5.21d):

$$\frac{d}{dt}\left(\frac{\partial}{\partial C'}[P(t)F\left[C(t)+L(t)\right] + \lambda_{C,i}C(t)]\right) = \frac{\partial}{\partial C}[P(t)F\left[C(t)+L(t)\right] + \lambda_{C,i}C(t)],$$

which simplifies to:

$$\frac{\partial}{\partial C}[P(t)F\left[C(t)+L(t)\right] + \lambda_{C,i}C(t)] = 0,$$

and can be re-arranged to yield (5.26).

■

Bibliography

[1] International Energy Agency, *Electricity Information 2015*, ser. IEA Statistics, 2015, Accessed: June 2016. [Online]. Available: https://www.iea.org/bookshop/666-Electricity_Information_2015

[2] ——, *Renewables Information 2014*, ser. IEA Statistics, 2014, Accessed: June 2016. [Online]. Available: http://www.oecd-ilibrary.org/energy/renewables-information-2014_renew-2014-en

[3] United Nations, *Adoption of the Paris agreement: Proposal by the president*, 2015, Framework convention on climate change. Accessed: June 2016. [Online]. Available: https://unfccc.int/resource/docs/2015/cop21/eng/l09.pdf

[4] L. Bird, M. Milligan, and D. Lew, *Integrating Variable Renewable Energy: Challenges and Solutions*. National Renewable Energy Laboratory, 2013, Accessed: June 2016. [Online]. Available: www.nrel.gov/docs/fy13osti/60451.pdf

[5] B. B. McKeon, J. Furukawa, and S. Fenstermacher, "Advanced lead acid batteries and the development of grid scale energy storage systems," *Proceedings of the IEEE*, vol. 102, no. 6, pp. 951–963, June 2014.

[6] D. Linden and T. Reddy, *Handbook of Batteries*, 3rd ed., ser. McGraw-Hill Handbooks. McGraw-Hill Education, 2002.

[7] J. M. Griffin and S. L. Puller, *Electricity deregulation: choices and challenges*. Chicago: University of Chicago Press, 2005, vol. 4.

[8] P. Palensky and D. Dietrich, "Demand side management: Demand response, intelligent energy systems, and smart loads," *IEEE Transactions on Industrial Informatics*, vol. 7, no. 3, pp. 381–388, Aug 2011.

[9] Southern California Edision, *Schedule TOU-GS-2-RTP General Service - Medium Real Time Pricing*, December 2015, Accessed: June 2016. [Online]. Available: https://www.sce.com/NR/sc3/tm2/pdf/CE331.pdf

[10] S. Borenstein, "The redistributional impact of non-linear electricity pricing," National Bureau of Economic Research, Tech. Rep., 2010, Accessed: June 2016. [Online]. Available: http://www.nber.org/papers/w15822

[11] "IEEE Adoption of Smart Energy Profile 2.0 Application Protocol Standard," *IEEE Std 2030.5-2013*, pp. 1–348, Nov 2013.

[12] Pacific Gas and Electric Company, *Tiered Base Plan (E1)*, 2016, Accessed: June 2016. [Online]. Available: http://www.pge.com/en/myhome/saveenergymoney/plans/tiers/index.page

[13] U.S. Department of Energy, "Benefits of demand response in electricity markets and recommendations for achieving them," 2006, Report to U.S. Congress pursuant to section 1252 of the Energy Policy Act of 2005. Accessed: June 2016. [Online]. Available: http://eetd.lbl.gov/sites/all/files/publications/report-lbnl-1252d.pdf

[14] Federal Energy Regulatory Commission, "Assessment of demand response and advanced metering," no. AD-06-2-00, Dec. 2012, Staff report. Accessed: June 2016. [Online]. Available: www.ferc.gov/legal/staff-reports/12-20-12-demand-response.pdf

[15] M. H. Albadi and E. F. El-Saadany, "Demand response in electricity markets: An overview," in *Power Engineering Society General Meeting, 2007. IEEE*, June 2007, pp. 1–5.

[16] United States Congress, "Energy policy act," pp. 962–963, August 2005, Public Law 109-58. Accessed: June 2016. [Online]. Available: https://www.gpo.gov/fdsys/pkg/PLAW-109publ58/pdf/PLAW-109publ58.pdf

[17] S. E. I. Association, "Net metering facts," May 2016, Accessed Dec. 2016. [Online]. Available: http://www.seia.org/sites/default/files/resources/NEM%20TP%27s%206-2-16.pdf

[18] Database of State Incentives for Renewables & Efficiency (DSIRE), "Customer credits for monthly net excess generation (neg) under net metering," January 2016, US. Department of Energy. Accessed: June 2016. [Online]. Available: http://ncsolarcen-prod.s3.amazonaws.com/wp-content/uploads/2016/01/NEG-1.2016.pdf

[19] U.S. Department of Energy, "Electric power annual 2014," Tech. Rep., February 2016, Accessed: June 2016. [Online]. Available: https://www.eia.gov/electricity/annual/pdf/epa.pdf

[20] T. Couture and Y. Gagnon, "An analysis of feed-in tariff remuneration models: Implications for renewable energy investment," *Energy Policy*, vol. 38, no. 2, pp. 955 – 965, 2010.

[21] A. Poullikkas, "A comparative assessment of net metering and feed in tariff schemes for residential PV systems," *Sustainable Energy Technologies and Assessments*, vol. 3, pp. 1 – 8, 2013, Accessed: June 2016. [Online]. Available: http://www.sciencedirect.com/science/article/pii/S2213138813000313

[22] E.ON UK, *Feed-in-tariffs factsheet*, 2014, Accessed: June 2016. [Online]. Available: https://www.eonenergy.com

[23] D. Doerffel and S. A. Sharkh, "A critical review of using the peukert equation for determining the remaining capacity of lead-acid and lithium-ion batteries," *Journal of Power Sources*, vol. 155, no. 2, pp. 395–400, 2006.

[24] M. Giaquinta and S. Hildebrandt, *Calculus of Variations I*. Berlin, Heidelberg: Springer Berlin Heidelberg, 2004.

[25] S. P. Sethi and G. Thompson, *Optimal Control Theory*, 2nd ed. Springer US, 2000.

[26] F. L. Lewis, D. L. Vrabie, and V. L. Syrmos, *Optimal Control*. Hoboken : John Wiley & Sons, 2012.

[27] S. Boyd and L. Vandenberghe, *Convex Optimization*. New York, NY, USA: Cambridge University Press, 2004.

[28] R. J. Vanderbei, *Linear programming: foundations and extensions*, 4th ed. New York: Springer, 2014, vol. 196.

[29] T. Jansen, *Analyzing evolutionary algorithms: the computer science perspective*. New York; Berlin;: Springer, 2013.

[30] R. Durrett, *Probability: Theory and Examples*. Cambridge: Cambridge University Press, 2010.

[31] H. Kobayashi, B. L. Mark, and W. Turin, *Probability, random processes, and statistical analysis*. Cambridge; New York: Cambridge University Press, 2012.

[32] S. E. Shreve, *Stochastic calculus for finance*. New York: Springer, 2004, vol. 2.

[33] B. Øksendal, *Stochastic Differential Equations: An Introduction with Applications*, 5th ed. Berlin, Heidelberg: Springer Berlin Heidelberg, 1998.

[34] R. H. Shumway and D. S. Stoffer, *Time Series Analysis and Its Applications*. New York, NY: Springer New York, 2000.

[35] J. Byun, I. Hong, and S. Park, "Intelligent cloud home energy management system using household appliance priority based scheduling based on prediction of renewable energy capability," *IEEE Transactions on Consumer Electronics*, vol. 58, no. 4, pp. 1194–1201, 2012.

[36] M. Pipattanasomporn, M. Kuzlu, and S. Rahman, "An algorithm for intelligent home energy management and demand response analysis," *IEEE Transactions on Smart Grid*, vol. 3, no. 4, pp. 2166–2173, Dec 2012.

[37] M. Collotta and G. Pau, "A novel energy management approach for smart homes using bluetooth low energy," *IEEE Journal on Selected Areas in Communications*, vol. 33, no. 12, pp. 2988–2996, Dec 2015.

[38] M. Erol-Kantarci and H. T. Mouftah, "TOU-aware energy management and wireless sensor networks for reducing peak load in smart grids," in *Vehicular Technology Conference Fall (VTC 2010-Fall), 2010 IEEE 72nd*, Sept 2010, pp. 1–5.

[39] M. Jaradat, M. Jarrah, Y. Jararweh, M. Al-Ayyoub, and A. Bousselham, "Integration of renewable energy in demand-side management for home appliances," in *2014 International Renewable and Sustainable Energy Conference (IRSEC)*, Oct 2014, pp. 571–576.

[40] Y. Guo, M. Pan, and Y. Fang, "Optimal power management of residential customers in the smart grid," *IEEE Transactions on Parallel and Distributed Systems*, vol. 23, no. 9, pp. 1593–1606, Sept 2012.

[41] R. Urgaonkar, B. Urgaonkar, M. Neely, and A. Sivasubramaniam, "Optimal power cost management using stored energy in data centers," *ACM SIGMETRICS Performance Evaluation Review*, vol. 39, no. 1, pp. 181–192, 2011.

[42] Y. Wang, X. Lin, and M. Pedram, "Adaptive control for energy storage systems in households with photovoltaic modules," *IEEE Transactions on Smart Grid*, vol. 5, no. 2, pp. 992–1001, March 2014.

[43] A. H. Mohsenian-Rad, V. W. S. Wong, J. Jatskevich, R. Schober, and A. Leon-Garcia, "Autonomous demand-side management based on game-theoretic energy consumption scheduling for the future smart grid," *IEEE Transactions on Smart Grid*, vol. 1, no. 3, pp. 320–331, Dec 2010.

[44] A. H. Mohsenian-Rad and A. Leon-Garcia, "Optimal residential load control with price prediction in real-time electricity pricing environments," *IEEE Transactions on Smart Grid*, vol. 1, no. 2, pp. 120–133, Sept 2010.

[45] S. Althaher, P. Mancarella, and J. Mutale, "Automated demand response from home energy management system under dynamic pricing and power and comfort constraints," *IEEE Transactions on Smart Grid*, vol. 6, no. 4, pp. 1874–1883, July 2015.

[46] H. T. Nguyen, D. T. Nguyen, and L. B. Le, "Energy management for households with solar assisted thermal load considering renewable energy and price uncertainty," *IEEE Transactions on Smart Grid*, vol. 6, no. 1, pp. 301–314, 2015.

[47] Y. Liu, N. U. Hassan, S. Huang, and C. Yuen, "Electricity cost minimization for a residential smart grid with distributed generation and bidirectional power transactions," in *2013 IEEE PES Innovative Smart Grid Technologies Conference (ISGT)*. IEEE, 2013, pp. 1–6.

[48] M. Muratori and G. Rizzoni, "Residential demand response: Dynamic energy management and time-varying electricity pricing," *IEEE Transactions on Power Systems*, vol. 31, no. 2, pp. 1108–1117, March 2016.

[49] Z. Chen, L. Wu, and Y. Fu, "Real-time price-based demand response management for residential appliances via stochastic optimization and robust optimization," *IEEE Transactions on Smart Grid*, vol. 3, no. 4, pp. 1822–1831, Dec 2012.

[50] C. O. Adika and L. Wang, "Autonomous appliance scheduling for household energy management," *IEEE Transactions on Smart Grid*, vol. 5, no. 2, pp. 673–682, 2014.

[51] Z. Wu, S. Zhou, J. Li, and X. P. Zhang, "Real-time scheduling of residential appliances via conditional risk-at-value," *IEEE Transactions on Smart Grid*, vol. 5, no. 3, pp. 1282–1291, May 2014.

[52] I. Georgievski, V. Degeler, G. A. Pagani, T. A. Nguyen, A. Lazovik, and M. Aiello, "Optimizing energy costs for offices connected to the smart grid," *IEEE Transactions on Smart Grid*, vol. 3, no. 4, pp. 2273–2285, 2012.

[53] S. Lee, B. Kwon, and S. Lee, "Joint energy management system of electric supply and demand in houses and buildings," *IEEE Transactions on Power Systems*, vol. 29, no. 6, pp. 2804–2812, Nov 2014.

[54] S. Chen, N. B. Shroff, and P. Sinha, "Heterogeneous delay tolerant task scheduling and energy management in the smart grid with renewable energy," *IEEE Journal on Selected Areas in Communications*, vol. 31, no. 7, pp. 1258–1267, July 2013.

[55] P. M. van de Ven, N. Hegde, L. Massoulié, and T. Salonidis, "Optimal control of end-user energy storage," *IEEE Transactions on Smart Grid*, vol. 4, no. 2, pp. 789–797, June 2013.

[56] C. Vivekananthan, Y. Mishra, and F. Li, "Real-time price based home energy management scheduler," *IEEE Transactions on Power Systems*, vol. 30, no. 4, pp. 2149–2159, July 2015.

[57] D. M. Han and J. H. Lim, "Smart home energy management system using IEEE 802.15.4 and ZigBee," *IEEE Transactions on Consumer Electronics*, vol. 56, no. 3, pp. 1403–1410, Aug 2010.

[58] M. Liu, F. L. Quilumba, and W. J. Lee, "A collaborative design of aggregated residential appliances and renewable energy for demand response participation," *IEEE Transactions on Industry Applications*, vol. 51, no. 5, pp. 3561–3569, Sept 2015.

[59] Z. Wang, C. Gu, F. Li, P. Bale, and H. Sun, "Active demand response using shared energy storage for household energy management," *IEEE Transactions on Smart Grid*, vol. 4, no. 4, pp. 1888–1897, Dec 2013.

[60] T. Li and M. Dong, "Real-time energy storage management with renewable integration: Finite-time horizon approach," *IEEE Journal on Selected Areas in Communications*, vol. 33, no. 12, pp. 2524–2539, 2015.

[61] T. Erseghe, A. Zanella, and C. G. Codemo, "Optimal and compact control policies for energy storage units with single and multiple batteries," *IEEE Transactions on Smart Grid*, vol. 5, no. 3, pp. 1308–1317, May 2014.

[62] C. G. Codemo, T. Erseghe, and A. Zanella, "Energy storage optimization strategies for smart grids," in *2013 IEEE International Conference on Communications (ICC)*, June 2013, pp. 4089–4093.

[63] L. Zhang and Y. Li, "Optimal energy management of wind-battery hybrid power system with two-scale dynamic programming," *IEEE Transactions on Sustainable Energy*, vol. 4, no. 3, pp. 765–773, July 2013.

[64] T. Li and M. Dong, "Online control for energy storage management with renewable energy integration," in *2013 IEEE International Conference on Acoustics, Speech and Signal Processing*, May 2013, pp. 5248–5252.

[65] A. J. Conejo, J. M. Morales, and L. Baringo, "Real-time demand response model," *IEEE Transactions on Smart Grid*, vol. 1, no. 3, pp. 236–242, Dec 2010.

[66] Z. Wang and Y. He, "Two-stage optimal demand response with battery energy storage systems," *IET Generation, Transmission Distribution*, vol. 10, no. 5, pp. 1286–1293, 2016.

[67] L. Huang, J. Walrand, and K. Ramchandran, "Optimal demand response with energy storage management," in *Smart Grid Communications (SmartGridComm), 2012 IEEE Third International Conference on*, Nov 2012, pp. 61–66.

[68] P. Harsha and M. Dahleh, "Optimal management and sizing of energy storage under dynamic pricing for the efficient integration of renewable energy," *IEEE Transactions on Power Systems*, vol. 30, no. 3, pp. 1164–1181, May 2015.

[69] Z. Xu, X. Guan, Q. S. Jia, J. Wu, D. Wang, and S. Chen, "Performance analysis and comparison on energy storage devices for smart building energy management," *IEEE Transactions on Smart Grid*, vol. 3, no. 4, pp. 2136–2147, Dec 2012.

[70] Y. Wu, V. K. N. Lau, D. H. K. Tsang, L. P. Qian, and L. Meng, "Optimal energy scheduling for residential smart grid with centralized renewable energy source," *IEEE Systems Journal*, vol. 8, no. 2, pp. 562–576, June 2014.

[71] M. Rastegar, M. Fotuhi-Firuzabad, H. Zareipour, and M. Moeini-Aghtaie, "A probabilistic energy management scheme for renewable-based residential energy hubs," *IEEE Transactions on Smart Grid*, vol. PP, no. 99, pp. 1–11, 2016.

[72] M. Cabras, V. Pilloni, and L. Atzori, "A novel smart home energy management system: Cooperative neighbourhood and adaptive renewable energy usage," in *2015 IEEE International Conference on Communications (ICC)*, June 2015, pp. 716–721.

[73] C. Molitor, A. Benigni, A. Helmedag, K. Chen, D. Cali, P. Jahangiri, D. Muller, and A. Monti, "Multiphysics test bed for renewable energy systems in smart homes," *IEEE Transactions on Industrial Electronics*, vol. 60, no. 3, pp. 1235–1248, March 2013.

[74] X. Liu, L. Ivanescu, R. Kang, and M. Maier, "Real-time household load priority scheduling algorithm based on prediction of renewable source availability," *IEEE Transactions on Consumer Electronics*, vol. 58, no. 2, pp. 318–326, May 2012.

[75] A. Mishra, D. Irwin, P. Shenoy, J. Kurose, and T. Zhu, "Greencharge: Managing renewable energy in smart buildings," *IEEE Journal on Selected Areas in Communications*, vol. 31, no. 7, pp. 1281–1293, July 2013.

[76] K. Mackey, R. McCann, K. Rahman, and R. Winkelman, "Evaluation of a battery energy storage system for coordination of demand response and renewable energy resources," in *2013 4th IEEE International Symposium on Power Electronics for Distributed Generation Systems (PEDG)*, July 2013, pp. 1–8.

[77] F. Xiong, *Digital modulation techniques*, 2nd ed. Boston, MA: Artech House, 2006.

[78] A. Goldsmith, *Wireless Communications*. Cambridge: Cambridge University Press, 2005.

[79] D. Valerdi, Q. Zhu, K. Exadaktylos, S. Xia, M. Arranz, R. Liu, and D. Xu, "Intelligent energy managed service for green base stations," in *2010 IEEE Globecom Workshops*, 2010, pp. 1453–1457.

[80] Z. Hasan, H. Boostanimehr, and V. K. Bhargava, "Green cellular networks: A survey, some research issues and challenges," *IEEE Communications Surveys Tutorials*, vol. 13, no. 4, pp. 524–540, Fourth 2011.

[81] A. P. Bianzino, C. Chaudet, D. Rossi, and J. L. Rougier, "A survey of green networking research," *IEEE Communications Surveys Tutorials*, vol. 14, no. 1, pp. 3–20, First 2012.

[82] H. A. H. Hassan, A. Pelov, and L. Nuaymi, "Integrating cellular networks, smart grid, and renewable energy: Analysis, architecture, and challenges," *IEEE Access*, vol. 3, pp. 2755–2770, 2015.

[83] A. Kwasinski and A. Kwasinski, "Increasing sustainability and resiliency of cellular network infrastructure by harvesting renewable energy," *IEEE Communications Magazine*, vol. 53, no. 4, pp. 110–116, April 2015.

[84] V. Chamola and B. Sikdar, "Solar powered cellular base stations: current scenario, issues and proposed solutions," *IEEE Communications Magazine*, vol. 54, no. 5, pp. 108–114, May 2016.

[85] S. Ulukus, A. Yener, E. Erkip, O. Simeone, M. Zorzi, P. Grover, and K. Huang, "Energy harvesting wireless communications: A review of recent advances," *IEEE Journal on Selected Areas in Communications*, vol. 33, no. 3, pp. 360–381, March 2015.

[86] V. Mancuso and S. Alouf, "Reducing costs and pollution in cellular networks," *IEEE Communications Magazine*, vol. 49, no. 8, pp. 63–71, August 2011.

[87] Y. Mao, G. Yu, and C. Zhong, "Energy consumption analysis of energy harvesting systems with power grid," *IEEE Wireless Communications Letters*, vol. 2, no. 6, pp. 611–614, December 2013.

[88] Y. Mao, J. Zhang, and K. B. Letaief, "A Lyapunov Optimization Approach for Green Cellular Networks With Hybrid Energy Supplies," *IEEE Journal on Selected Areas in Communications*, vol. 33, no. 12, pp. 2463–2477, Dec 2015.

[89] R. Vaze, R. Garg, and N. Pathak, "Dynamic power allocation for maximizing throughput in energy-harvesting communication system," *IEEE/ACM Transactions on Networking*, vol. 22, no. 5, pp. 1621–1630, Oct 2014.

[90] B. Gurakan, O. Ozel, J. Yang, and S. Ulukus, "Energy cooperation in energy harvesting communications," *IEEE Transactions on Communications*, vol. 61, no. 12, pp. 4884–4898, December 2013.

[91] K. Tutuncuoglu, A. Yener, and S. Ulukus, "Optimum policies for an energy harvesting transmitter under energy storage losses," *IEEE Journal on Selected Areas in Communications*, vol. 33, no. 3, pp. 467–481, March 2015.

[92] C. Hu, J. Gong, X. Wang, S. Zhou, and Z. Niu, "Optimal green energy utilization in MIMO systems with hybrid energy supplies," *IEEE Transactions on Vehicular Technology*, vol. 64, no. 8, pp. 3675–3688, Aug 2015.

[93] K. Huang, M. Kountouris, and V. O. K. Li, "Renewable powered cellular networks: Energy field modeling and network coverage," *IEEE Transactions on Wireless Communications*, vol. 14, no. 8, pp. 4234–4247, Aug 2015.

[94] O. Orhan, D. Gündüz, and E. Erkip, "Energy harvesting broadband communication systems with processing energy cost," *IEEE Transactions on Wireless Communications*, vol. 13, no. 11, pp. 6095–6107, Nov 2014.

[95] D. Zhai, M. Sheng, X. Wang, and Y. Li, "Leakage-aware dynamic resource allocation in hybrid energy powered cellular networks," *IEEE Transactions on Communications*, vol. 63, no. 11, pp. 4591–4603, Nov 2015.

[96] M. Zhao, J. Zhao, W. Zhou, J. Zhu, and S. Zhang, "Energy efficiency optimization in relay-assisted networks with energy harvesting relay constraints," *China Communications*, vol. 12, no. 2, pp. 84–94, Feb 2015.

[97] T. Zhang, H. Xu, D. Liu, N. C. Beaulieu, and Y. Zhu, "User association for energy-load tradeoffs in HetNets with renewable energy supply," *IEEE Communications Letters*, vol. 19, no. 12, pp. 2214–2217, Dec 2015.

[98] D. W. K. Ng, E. S. Lo, and R. Schober, "Energy-efficient resource allocation in OFDMA systems with hybrid energy harvesting base station," *IEEE Transactions on Wireless Communications*, vol. 12, no. 7, pp. 3412–3427, July 2013.

[99] S. Y. Lee, C. Y. Liu, M. K. Chang, D. N. Yang, and Y. W. P. Hong, "Cooperative multicasting in renewable energy enhanced relay networks - expending more power to save energy," *IEEE Transactions on Wireless Communications*, vol. 15, no. 1, pp. 753–768, Jan 2016.

[100] M. Li, H. Nishiyama, N. Kato, Y. Owada, and K. Hamaguchi, "On the energy-efficient of throughput-based scheme using renewable energy for wireless mesh networks in disaster area," *IEEE Transactions on Emerging Topics in Computing*, vol. 3, no. 3, pp. 420–431, Sept 2015.

[101] J. Gong, J. S. Thompson, S. Zhou, and Z. Niu, "Base station sleeping and resource allocation in renewable energy powered cellular networks," *IEEE Transactions on Communications*, vol. 62, no. 11, pp. 3801–3813, Nov 2014.

[102] D. Li, W. Saad, I. Guvenc, A. Mehbodniya, and F. Adachi, "Decentralized energy allocation for wireless networks with renewable energy powered base stations," *IEEE Transactions on Communications*, vol. 63, no. 6, pp. 2126–2142, June 2015.

[103] B. Devillers and D. Gündüz, "A general framework for the optimization of energy harvesting communication systems with battery imperfections," *Journal of Communications and Networks*, vol. 14, no. 2, pp. 130–139, April 2012.

[104] V. Chamola and B. Sikdar, "Outage estimation for solar powered cellular base stations," in *2015 IEEE International Conference on Communications (ICC)*, June 2015, pp. 172–177.

[105] V. Chamola, B. Krishnamachari, and B. Sikdar, "An energy and delay aware downlink power control strategy for solar powered base stations," *IEEE Communications Letters*, vol. 20, no. 5, pp. 954–957, May 2016.

[106] V. Chamola and B. Sikdar, "Resource provisioning and dimensioning for solar powered cellular base stations," in *2014 IEEE Global Communications Conference*, Dec 2014, pp. 2498–2503.

[107] N. Reyhanian, V. Shah-Mansouri, B. Maham, and C. Yuen, "Renewable energy distribution in cooperative cellular networks with energy harvesting," in *Personal, Indoor, and Mobile Radio Communications (PIMRC), 2015 IEEE 26th Annual International Symposium on*, Aug 2015, pp. 1617–1621.

[108] D. Liu, Y. Chen, K. K. Chai, T. Zhang, and M. Elkashlan, "Two-dimensional optimization on user association and green energy allocation for HetNets with hybrid energy sources," *IEEE Transactions on Communications*, vol. 63, no. 11, pp. 4111–4124, Nov 2015.

[109] J. Xu, L. Duan, and R. Zhang, "Cost-aware green cellular networks with energy and communication cooperation," *IEEE Communications Magazine*, vol. 53, no. 5, pp. 257–263, May 2015.

[110] Y. K. Chia, S. Sun, and R. Zhang, "Energy cooperation in cellular networks with renewable powered base stations," *IEEE Transactions on Wireless Communications*, vol. 13, no. 12, pp. 6996–7010, Dec 2014.

[111] S. Bu, F. R. Yu, Y. Cai, and X. P. Liu, "When the smart grid meets energy-efficient communications: Green wireless cellular networks powered by the smart grid," *IEEE Transactions on Wireless Communications*, vol. 11, no. 8, pp. 3014–3024, 2012.

[112] L. Rao, X. Liu, L. Xie, and W. Liu, "Coordinated energy cost management of distributed internet data centers in smart grid," *IEEE Transactions on Smart Grid*, vol. 3, no. 1, pp. 50–58, 2012.

[113] D. Niyato, X. Lu, and P. Wang, "Adaptive power management for wireless base stations in a smart grid environment," *IEEE Wireless Communications*, vol. 19, no. 6, pp. 44–51, December 2012.

[114] J. Peng, P. Hong, and K. Xue, "Optimal power management under delay constraint in cellular networks with hybrid energy sources," *Computer Networks*, vol. 78, pp. 107–118, Feb. 2015.

[115] C. Liu and B. Natarajan, "Power management in heterogeneous networks with energy harvesting base stations," *Physical Communication*, vol. 16, pp. 14–24, Sept. 2015.

[116] G. Betti, E. Amaldi, A. Capone, and G. Ercolani, "Cost-aware optimization models for communication networks with renewable energy sources," in *INFOCOM, 2013 Proceedings IEEE*, April 2013, pp. 3231–3236.

[117] H. Ghazzai, E. Yaacoub, M. Alouini, and A. Abu-Dayya, "Optimized green operation of LTE networks in the presence of multiple electricity providers," in *2012 IEEE Globecom Workshops*, Dec 2012, pp. 664–669.

[118] ——, "Optimized smart grid energy procurement for LTE networks using evolutionary algorithms," *IEEE Transactions on Vehicular Technology*, vol. 63, no. 9, pp. 4508–4519, Nov 2014.

[119] T. Han and N. Ansari, "On optimizing green energy utilization for cellular networks with hybrid energy supplies," *IEEE Transactions on Wireless Communications*, vol. 12, no. 8, pp. 3872–3882, 2013.

[120] ——, "Smart grid enabled mobile networks: Jointly optimizing BS operation and power distribution," in *2014 IEEE International Conference on Communications (ICC)*, June 2014, pp. 2624–2629.

[121] H. A. H. Hassan, A. Ali, L. Nuaymi, and S. E. Elayoubi, "Renewable energy usage in the context of energy-efficient mobile network," in *2015 IEEE 81st Vehicular Technology Conference (VTC Spring)*, May 2015, pp. 1–7.

[122] N. Abji, A. Tizghadam, and A. Leon-Garcia, "Energy storage management in core networks with renewable energy in time-of-use pricing environments," in *2015 IEEE International Conference on Communications (ICC)*, June 2015, pp. 135–141.

[123] J. Xu and R. Zhang, "Cooperative energy trading in CoMP systems powered by smart grids," *IEEE Transactions on Vehicular Technology*, vol. 65, no. 4, pp. 2142–2153, April 2016.

[124] ——, "CoMP meets smart grid: A new communication and energy cooperation paradigm," *IEEE Transactions on Vehicular Technology*, vol. 64, no. 6, pp. 2476–2488, June 2015.

[125] C. A. Hernandez-Aramburo, T. C. Green, and N. Mugniot, "Fuel consumption minimization of a microgrid," *IEEE Transactions on Industry Applications*, vol. 41, no. 3, pp. 673–681, May 2005.

[126] Q. Jiang, M. Xue, and G. Geng, "Energy management of microgrid in grid-connected and stand-alone modes," *IEEE Transactions on Power Systems*, vol. 28, no. 3, pp. 3380–3389, Aug 2013.

[127] S. Sun, M. Dong, and B. Liang, "Joint supply, demand, and energy storage management towards microgrid cost minimization," in *Smart Grid Communications (SmartGridComm), 2014 IEEE International Conference on*, Nov 2014, pp. 109–114.

[128] K. Rahbar, J. Xu, and R. Zhang, "Real-time energy storage management for renewable integration in microgrid: An off-line optimization approach," *IEEE Transactions on Smart Grid*, vol. 6, no. 1, pp. 124–134, 2015.

[129] P. Yang and A. Nehorai, "Joint optimization of hybrid energy storage and generation capacity with renewable energy," *IEEE Transactions on Smart Grid*, vol. 5, no. 4, pp. 1566–1574, July 2014.

[130] C. Chen, S. Duan, T. Cai, B. Liu, and G. Hu, "Smart energy management system for optimal microgrid economic operation," *IET Renewable Power Generation*, vol. 5, no. 3, pp. 258–267, May 2011.

[131] S. Bahramirad, W. Reder, and A. Khodaei, "Reliability-constrained optimal sizing of energy storage system in a microgrid," *IEEE Transactions on Smart Grid*, vol. 3, no. 4, pp. 2056–2062, Dec 2012.

[132] P. Malysz, S. Sirouspour, and A. Emadi, "An optimal energy storage control strategy for grid-connected microgrids," *IEEE Transactions on Smart Grid*, vol. 5, no. 4, pp. 1785–1796, July 2014.

[133] R. Palma-Behnke, C. Benavides, F. Lanas, B. Severino, L. Reyes, J. Llanos, and D. Sáez, "A microgrid energy management system based on the rolling horizon strategy," *IEEE Transactions on Smart Grid*, vol. 4, no. 2, pp. 996–1006, June 2013.

[134] Y. Zhang, N. Gatsis, and G. B. Giannakis, "Robust energy management for microgrids with high-penetration renewables," *IEEE Transactions on Sustainable Energy*, vol. 4, no. 4, pp. 944–953, Oct 2013.

[135] A. Chaouachi, R. M. Kamel, R. Andoulsi, and K. Nagasaka, "Multiobjective intelligent energy management for a microgrid," *IEEE Transactions on Industrial Electronics*, vol. 60, no. 4, pp. 1688–1699, April 2013.

[136] I. Koutsopoulos and L. Tassiulas, "Optimal control policies for power demand scheduling in the smart grid," *IEEE Journal on Selected Areas in Communications*, vol. 30, no. 6, pp. 1049–1060, July 2012.

[137] A. Parisio and L. Glielmo, "A mixed integer linear formulation for microgrid economic scheduling," in *Smart Grid Communications (SmartGridComm), 2011 IEEE International Conference on*, Oct 2011, pp. 505–510.

[138] M. Fathi and H. Bevrani, "Statistical cooperative power dispatching in interconnected microgrids," *IEEE Transactions on Sustainable Energy*, vol. 4, no. 3, pp. 586–593, July 2013.

[139] Z. Wang, B. Chen, J. Wang, M. M. Begovic, and C. Chen, "Coordinated energy management of networked microgrids in distribution systems," *IEEE Transactions on Smart Grid*, vol. 6, no. 1, pp. 45–53, Jan 2015.

[140] D. T. Nguyen and L. B. Le, "Optimal energy management for cooperative microgrids with renewable energy resources," in *Smart Grid Communications (SmartGridComm), 2013 IEEE International Conference on*, Oct 2013, pp. 678–683.

[141] S. J. Ahn, S. R. Nam, J. H. Choi, and S. I. Moon, "Power scheduling of distributed generators for economic and stable operation of a microgrid," *IEEE Transactions on Smart Grid*, vol. 4, no. 1, pp. 398–405, March 2013.

[142] G. Martinez, N. Gatsis, and G. B. Giannakis, "Stochastic programming for energy planning in microgrids with renewables," in *Computational Advances in Multi-Sensor Adaptive Processing (CAMSAP), 2013 IEEE 5th International Workshop on*, Dec 2013, pp. 472–475.

[143] M. J. Neely, A. S. Tehrani, and A. G. Dimakis, "Efficient algorithms for renewable energy allocation to delay tolerant consumers," in *Smart Grid Communications (SmartGridComm), 2010 First IEEE International Conference on*, Oct 2010, pp. 549–554.

[144] D. E. Olivares, C. A. Cañizares, and M. Kazerani, "A centralized energy management system for isolated microgrids," *IEEE Transactions on Smart Grid*, vol. 5, no. 4, pp. 1864–1875, July 2014.

[145] W. Su, J. Wang, and J. Roh, "Stochastic energy scheduling in microgrids with intermittent renewable energy resources," *IEEE Transactions on Smart Grid*, vol. 5, no. 4, pp. 1876–1883, July 2014.

[146] S. Lakshminarayana, T. Q. S. Quek, and H. V. Poor, "Combining cooperation and storage for the integration of renewable energy in smart grids," in *Computer Communications Workshops (INFOCOM WKSHPS), 2014 IEEE Conference on*, April 2014, pp. 622–627.

[147] S. Grillo, M. Marinelli, S. Massucco, and F. Silvestro, "Optimal management strategy of a battery-based storage system to improve renewable energy integration in distribution networks," *IEEE Transactions on Smart Grid*, vol. 3, no. 2, pp. 950–958, June 2012.

[148] C. Cecati, C. Citro, and P. Siano, "Combined operations of renewable energy systems and responsive demand in a smart grid," *IEEE Transactions on Sustainable Energy*, vol. 2, no. 4, pp. 468–476, Oct 2011.

[149] Y. M. Atwa, E. F. El-Saadany, M. M. A. Salama, and R. Seethapathy, "Optimal renewable resources mix for distribution system energy loss minimization," *IEEE Transactions on Power Systems*, vol. 25, no. 1, pp. 360–370, Feb 2010.

[150] C. Chen, S. Duan, T. Cai, B. Liu, and G. Hu, "Optimal allocation and economic analysis of energy storage system in microgrids," *IEEE Transactions on Power Electronics*, vol. 26, no. 10, pp. 2762–2773, Oct 2011.

[151] H. P. Khomami and M. H. Javidi, "Energy management of smart microgrid in presence of renewable energy sources based on real-time pricing," in *Smart Grid Conference (SGC), 2014*, Dec 2014, pp. 1–6.

[152] Z. Shu and P. Jirutitijaroen, "Optimal operation strategy of energy storage system for grid-connected wind power plants," *IEEE Transactions on Sustainable Energy*, vol. 5, no. 1, pp. 190–199, 2014.

[153] T. Cui, Y. Wang, H. Goudarzi, S. Nazarian, and M. Pedram, "Profit maximization for utility companies in an oligopolistic energy market with dynamic prices," in *Online Conference on Green Communications (GreenCom), 2012 IEEE*, Sept 2012, pp. 86–91.

[154] H. Liu, Y. Shen, Z. B. Zabinsky, C. C. Liu, A. Courts, and S. K. Joo, "Social welfare maximization in transmission enhancement considering network congestion," *IEEE Transactions on Power Systems*, vol. 23, no. 3, pp. 1105–1114, Aug 2008.

[155] L. Jiang and S. Low, "Real-time demand response with uncertain renewable energy in smart grid," in *Communication, Control, and Computing (Allerton), 2011 49th Annual Allerton Conference on*, Sept 2011, pp. 1334–1341.

[156] O. Kilkki, A. Alahäivälä, and I. Seilonen, "Optimized control of price-based demand response with electric storage space heating," *IEEE Transactions on Industrial Informatics*, vol. 11, no. 1, pp. 281–288, Feb 2015.

[157] N. Li, L. Chen, and S. H. Low, "Optimal demand response based on utility maximization in power networks," in *2011 IEEE Power and Energy Society General Meeting*, July 2011, pp. 1–8.

[158] H. S. V. S. K. Nunna and S. Doolla, "Demand response in smart distribution system with multiple microgrids," *IEEE Transactions on Smart Grid*, vol. 3, no. 4, pp. 1641–1649, Dec 2012.

[159] H. M. Soliman and A. Leon-Garcia, "Game-theoretic demand-side management with storage devices for the future smart grid," *IEEE Transactions on Smart Grid*, vol. 5, no. 3, pp. 1475–1485, May 2014.

[160] Q. Dong, L. Yu, W. Z. Song, L. Tong, and S. Tang, "Distributed demand and response algorithm for optimizing social-welfare in smart grid," in *Parallel Distributed Processing Symposium (IPDPS), 2012 IEEE 26th International*, May 2012, pp. 1228–1239.

[161] A. Mnatsakanyan and S. W. Kennedy, "A novel demand response model with an application for a virtual power plant," *IEEE Transactions on Smart Grid*, vol. 6, no. 1, pp. 230–237, Jan 2015.

[162] P. Samadi, H. Mohsenian-Rad, R. Schober, and V. W. S. Wong, "Advanced demand side management for the future smart grid using mechanism design," *IEEE Transactions on Smart Grid*, vol. 3, no. 3, pp. 1170–1180, Sept 2012.

[163] L. Jia and L. Tong, "Renewables and storage in distribution systems: Centralized vs. decentralized integration," *IEEE Journal on Selected Areas in Communications*, vol. 34, no. 3, pp. 665–674, March 2016.

[164] W. Zhang, Y. Xu, W. Liu, C. Zang, and H. Yu, "Distributed online optimal energy management for smart grids," *IEEE Transactions on Industrial Informatics*, vol. 11, no. 3, pp. 717–727, June 2015.

[165] Y. Wu, X. Tan, L. Qian, D. H. K. Tsang, W. Z. Song, and L. Yu, "Optimal pricing and energy scheduling for hybrid energy trading market in future smart grid," *IEEE Transactions on Industrial Informatics*, vol. 11, no. 6, pp. 1585–1596, Dec 2015.

[166] B. G. Kim, S. Ren, M. van der Schaar, and J. W. Lee, "Bidirectional energy trading for residential load scheduling and electric vehicles," in *INFOCOM, 2013 Proceedings IEEE*, April 2013, pp. 595–599.

[167] H. I. Su and A. E. Gamal, "Modeling and analysis of the role of fast-response energy storage in the smart grid," in *Communication, Control, and Computing (Allerton), 2011 49th Annual Allerton Conference on*, Sept 2011, pp. 719–726.

[168] J. Leithon, S. Sun, and T. J. Lim, "Energy management strategies for base stations powered by the smart grid," in *2013 IEEE Global Communications Conference (GLOBECOM)*, Dec 2013, pp. 2635–2640.

[169] ——, "An evolutionary algorithm for energy management in cellular base stations under time-of-use pricing," in *2015 IEEE International Conference on Communications (ICC)*, June 2015, pp. 215–220.

[170] ——, "Energy management strategies for base stations in a smart grid environment," *Transactions on Emerging Telecommunications Technologies*, 2014, dOI: 10.1002/ett.2861.

[171] J. Leithon, T. J. Lim, and S. Sun, "Battery-aided demand response strategy under continuous-time block pricing," *IEEE Transactions on Signal Processing*, vol. 64, no. 2, pp. 395–405, Jan 2016.

[172] ——, "Online energy management strategies for base stations powered by the smart grid," in *Smart Grid Communications (SmartGridComm), 2013 IEEE International Conference on*, Oct 2013, pp. 199–204.

[173] ——, "Renewable Energy Management in Cellular Networks: An Online Strategy based on ARIMA Forecasting and a Markov Chain Model," in *2016 IEEE Wireless Communications and Networking Conference (WCNC)*, April 2016.

[174] ——, "Energy exchange among base stations in a cellular network through the smart grid," in *2014 IEEE International Conference on Communications (ICC)*, June 2014, pp. 4036–4041.

[175] ——, "Online demand response strategies for non-deferrable loads with renewable energy," *IEEE Transactions on Smart Grid*, 2016, submitted.

[176] ——, "Renewable-powered base stations with time-of-use and consumption-based block pricing," in *2015 IEEE 81st Vehicular Technology Conference (VTC Spring)*, May 2015, pp. 1–5.

[177] J. Nachbar, "Concave and convex functions," 2015, Accessed in Dec. 2016. [Online]. Available: https://pages.wustl.edu/files/pages/imce/nachbar/concavity.pdf

[178] R. Hyndman and G. Athanasopoulos, *Forecasting: principles and practice*. OTexts: Melbourne, Australia, 2013, Accessed: 20 Jun. 2016. [Online]. Available: http://otexts.org/fpp/

[179] R. Hyndman, "Package 'forecast'," April 2016, Accessed Dec. 2016. [Online]. Available: https://cran.r-project.org/web/packages/forecast/forecast.pdf

[180] G. A. Spedicato, T. S. Kang, S. B. Yalamanchi, and D. Yadav, "The markovchain package: A package for easily handling discrete markov chains in r," Accessed Dec. 2016. [Online]. Available: https://cran.r-project.org/web/packages/markovchain/vignettes/an_introduction_to_markovchain_package.pdf

[181] National Renewable Energy Laboratory, PVWatts calculator, Accessed Sept. 2015. [Online]. Available: http://pvwatts.nrel.gov

[182] S. Wilcox and W. Marion, "Users Manual for TMY3 Data Sets," National Renewable Energy Laboratory, Tech. Rep. NREL/TP-581-43156, 2008, Accessed Dec. 2016. [Online]. Available: http://www.nrel.gov/docs/fy08osti/43156.pdf

[183] F.-R. Chang, *Stochastic optimization in continuous time*. Cambridge, UK; New York: Cambridge University Press, 2004.

[184] I. Kannan and C. K. Krueger, *Advanced Analysis: on the Real Line*. New York, NY: Springer New York, 1996.

[185] H. Morimoto, *Stochastic control and mathematical modeling: applications in economics*. Cambridge: Cambridge University Press, 2010, vol. no. 131.

[186] I. Karatzas and S. E. Shreve, *Brownian motion and stochastic calculus*, 2nd ed. New York: Springer, 1996, vol. 113.

[187] W. Fleming and R. Rishel, *Deterministic and Stochastic Optimal Control*. New York, NY: Springer New York, 1975, vol. 1.

[188] S. Boyd, L. Xiao, A. Mutapcic, and J. Mattingley, "Notes on decomposition methods," April 2008, Accessed: June 2016. [Online]. Available: https://see.stanford.edu/materials/lsocoee364b/08-decomposition_notes.pdf

List of Publications

Journals

(J1) Johann Leithon, Sumei Sun, and Teng Joon Lim, "Energy management strategies for base stations in a smart grid environment," *Transactions on Emerging Telecommunications Technologies.* John Wiley & Sons, 2014.

(J2) Johann Leithon, Teng Joon Lim, and Sumei Sun, "Battery-Aided Demand Response Strategy Under Continuous-Time Block Pricing," *IEEE Transactions on Signal Processing*, vol. 64, no. 2, pp. 395-405, Jan. 2016.

(J3) Johann Leithon, Teng Joon Lim, and Sumei Sun, "Online Demand Response Strategies for Non-Deferrable Loads with Renewable Energy," *IEEE Transactions on Smart Grid.* In revision, 2016.

Conferences

(C1) Johann Leithon, Teng Joon Lim, and Sumei Sun, "Online energy management strategies for base stations powered by the smart grid," in *Proceedings of 2013 IEEE International Conference on Smart Grid Communications (SmartGridComm)*, Vancouver, BC, Oct. 2013.

(C2) Johann Leithon, Sumei Sun, and Teng Joon Lim, "Energy management strategies for base stations powered by the smart grid," in *Proceedings of 2013 IEEE Global Communications Conference (GLOBECOM)*, Atlanta, GA, Dec. 2013.

(C3) Johann Leithon, Teng Joon Lim, and Sumei Sun, "Energy exchange among base stations in a Cellular Network through the Smart Grid," in *Proceedings of 2014 IEEE International Conference on Communications (ICC)*, Sydney, NSW, June 2014.

(C4) Johann Leithon, Sumei Sun, and Teng Joon Lim, "An evolutionary algorithm for energy management in cellular base stations under time-of-use pricing," in *Proceedings of 2015 IEEE International Conference on Communications (ICC)*, London, UK, June 2015.

(C5) Johann Leithon, Teng Joon Lim, and Sumei Sun, "Renewable-Powered Base Stations with Time-of-Use and Consumption-Based Block Pricing," in *Proceedings of 2015 IEEE 81st Vehicular Technology Conference (VTC Spring)*, Glasgow, UK, May 2015.

(C6) Johann Leithon, Teng Joon Lim, and Sumei Sun, "Renewable Energy Management in Cellular Networks: An Online Strategy based on ARIMA Forecasting and a Markov Chain Model," in *Proceedings of 2016 IEEE Wireless Communications and Networking Conference (WCNC)*, Doha, Qatar, April 2016.